COLLEGE OF BASIC AND APPLIED SCIENCES

UNIVERSITY OF GHANA

DEVELOPMENT OF NOVEL ELECTROCHEMICAL BIOSENSORS FOR CLINICAL DIAGNOSIS OF INFECTIOUS DISEASES

BY

FRANCIS DZIDEFO KRAMPA

(10363861)

THIS THESIS IS SUBMITTED TO THE SCHOOL OF GRADUATE STUDIES IN PARTIAL FULFILMENT OF THE REQUIREMENT FOR THE AWARD OF DOCTOR OF PHILOSOPHY DEGREE IN MOLECULAR CELL BIOLOGY OF INFECTIOUS DISEASES

DEPARTMENT OF BIOCHEMISTRY, CELL AND MOLECULAR BIOLOGY

JULY 2019

DECLARATION

This thesis titled, "*Development of novel electrochemical biosensors for clinical diagnosis of infectious diseases*", presented for the award of Ph.D comprises the research I performed at the West African Centre for Cell Biology of Infectious Pathogens between March 2016 and April 2019 under the tutelage of Professor Gordon Awandare, Dr Prosper Kanyong, Dr Osbourne Quaye and Dr Jonathan Adjimani. In consonance with good scientific practice, I have duly acknowledged the pre-existing findings reported by other investigators.

Francis D. Krampa (Student)

Professor Gordon Awandare
(Supervisor)

Dr Prosper Kanyong
(Co-supervisor)

Dr Jonathan Adjimani
(Co-supervisor)

Dr Osbourne Quaye
(Co-supervisor)

ABSTRACT

In the field of biomedical diagnostics, rapid and effective monitoring of important analytes is an essential goal, and for this reason, significant progress has been made towards developing high performing analytical tools. Despite these advancements, the majority of the techniques are not suitable for routine uptake in resource-limited regions due to technical and infrastructural challenges. Clinical diagnostics is particularly affected since it is not always available at the point-of-need, notably for infectious diseases which is the key concern to public health in these regions. It is therefore necessary to explore efficient and robust analytical techniques that address the deficiencies of traditional diagnostic methods in preparedness for outbreaks and field-readiness. Electrochemical biosensors provide an attractive means to analyze the content of a biological sample due to the direct conversion of a biological event to an electronic signal. The thesis aimed at applying advances in electrochemical biosensor technologies in the development of diagnostic devices for point-of-care testing of infectious diseases. Given that the transducer is of uttermost importance in electrochemical sensors, the suitability of screen-printed electrodes was assessed for use as base transducers. Following this step, nanocomposites made from conductive polymers; poly(3,4-ethylenedioxythiophene):poly(4-styrenesulfonate) (PEDOT:PSS), 1-ethyl-3-methylimidazolium tetrafluoroborate ([EMIM][BF4]), nafion (Naf) and graphene nanoplatelets (GNPs) were used to modify the electrode surfaces in order to enhance their electrochemical performance. Characterization of screen-printed carbon electrodes (SPCE) modified with IL/PEDOT:PSS and GNPs/Naf showed nano-porous surfaces with enhanced electrocatalytic properties of up to 40-fold compared to the bare unmodified electrodes. The modified surfaces were applied to detect trace levels of electroactive analytes in environmental and biological samples. The PEDOT:PSS/IL

was utilised in conjunction with amperometry towards sensitive detection of catechol and differential pulse voltammetry applied at the GNPs/Naf for simultaneous analysis of dopamine (DA) and N-acetyl-p-aminophenol (APAP) in their binary mixtures. The sensors showed excellent selectivity and sensitivity toward the target analytes, with limit of detection of 23.7 μM for catechol and 0.13 μM and 0.25 μM for DA and APAP, respectively. Subsequently, three strategies for immobilizing antibodies (physisorption, covalent binding and polydopamine assisted binding) on screen-printed micro gold electrode surfaces were evaluated for the development of a malaria immunosensor. A sensitive and efficient biosensor was achieved for *Plasmodium falciparum* histidine-rich protein-II (PfHRP-II), aided by the robust covalent coupling between anti-PfHRP-II antibodies and an amine layer glutaraldehyde crosslinking on a screen-printed gold microelectrode. The sensor which was built on a label-free impedimetric format was highly reproducible with a low detection limit of 38.0 pg/mL. Based on the efficiency of the covalent immobilisation, the method was repurposed to detect surface antigens of hepatitis B virus. The sensor possessed sufficient sensitivity and selectivity for hepatitis B surface antigens in buffer with a low detection limit of 0.7 ng/mL. These findings demonstrate that the novel nanocomposite-modified sensing platforms could be effective conductive supports in enhancing electroanalysis. The impedimetric immunosensors are a promising inexpensive alternative for label-free analyte detection. Together, these strategies could be integrated into high performing portable self-contained instruments for point-of-care diagnostic application in resource-limited settings.

ACKNOWLEDGEMENT

Foremost, I thank Professor Gordon Awandare, Dr Prosper Kanyong, Dr Jonathan Adjimani and Dr Osbourne Quaye who supervised this work. I am deeply indebted to Dr Prosper Kanyong for making this 'relatively new' field an enjoyable journey, turning me from a novice to a more balanced and pragmatic electrochemist within a short time. I acknowledge the indirect inspiration from his recommendation '***Wilful Blindness'*** which I read alongside preliminary work on the malaria biosensor.

I wish to thank The West Africa Centre for Cell Biology of Infectious Pathogens (WACCBIP) who, through funding from the World Bank, sponsored my training and this research work. I owe Professor Awandare a debt of gratitude for starting the collaboration with Dr Kanyong and for grafting the 'Diagnostics Group' into the Cell Biology and Immunology Laboratory of WACCBIP. This research could not have been started or completed successful without his unrelenting financial support for the purchase of very expensive reagents/items.

Many thanks to Dr Yaw Aniweh for lending an intellectual insight into practically anything scientific and to Professor Andrew Anthony Adjei without whose mentorship I would not have reached this point. Special thanks to Professor Lisa Hall of the Cambridge Analytical Biotechnology- Hall Laboratory, Cambridge University who hosted my experiential learning and to Cassie Henderson whom I worked closely with. To my colleagues who have become my dearest friends during this adventurous time, it has been a pleasure.

I am honoured to have a dedicated supportive and encouraging family without whom I could not have come this far.

TABLE OF CONTENT

LIST OF FIGURES

LIST OF TABLES

LIST OF ABBREVIATIONS

AC	Alternating current
Ag/AgCl	Silver-silver chloride
AuNP	Gold nanoparticle
APAP	*N*-acetyl-*p*-aminophenol
BSA	Bovine serum albumin
CE	Counter Electrode
CP	Conductive polymer
DA	Dopamine
DC	Direct current
DPV	Differential pulse voltammetry
EIS	Electrochemical impedance spectroscopy
ELISA	Enzyme linked immunosorbent assay
GCE	Glassy carbon electrode
GO	Graphene oxide
ICT	Immunochromatographic test
LAMP	Loop mediated isothermal amplification
LDH	Lactate dehydrogenase
LoD	Limit of detection

mAb	Monoclonal antibody
PBS	Phosphate buffered saline
PCR	Polymerase chain reaction
PDDA	Poly (allylamine hydrochloride),
PEDOT:PSS	Poly(3,4-ethylenedioxythiophene):poly(4-styrenesulfonate)
*Pf*HRP-II	Plasmodium falciparum histidine rich protein-II
PoC	Point of care
RE	Reference Electrode
RDT	Rapid diagnostic test
RSD	Relative standard deviation
SAM	Self-assembled monolayer
SD	Standard deviation
SEM	Scanning electron microscope
SERS	Surface-enhanced Raman spectroscopy
SPE	Screen Printed electrode
SPCE	Screen Printed carbon electrode
SPGµE	Screen Printed gold microelectrode
WE	Working Electrode
WHO	World Health Organization

LIST OF SYMBOLS

%	Percent
~	Approximately
<	Lesser than
=	Equal to
>	Greater than
≥	Greater than equal to
°C	Degree Celsius
µ	Micro
A	Ampere
F	Faraday constant
fM	Femtomolar
g	Gram
Hz	Hertz
k	Kilo
k_{cat}	Turnover number
Kd	Dissociation constant
K_D	Volmer constant
L	Litre
m	Meter
M	Molarity
n	Number or moles of electrons; Nano

p	Pico
R^2	Regression coefficient
R_{ct} (ΔR_{ct})	Charge transfer resistance (difference in R_{ct})
Rs	Solution resistance
T	Temperature
V	Volt
v/v	Volume/Volume
υ	Scan rate
ω	Angular frequency
w/v	Weight/Volume
Z	Impedance
Zw	Warburg impedance
Ω	Ohm

CHAPTER 1

INTRODUCTION

1.1 Infectious diseases at a glance

The demand for systems that detect pathogens or evidence of their existence spans from medical diagnostics, environmental monitoring, food quality to pharmaceutical and industrial application. Among these, medical diagnostics is of precedence as it implicates the health of the general population (Lee et al., 2010; Mahato et al., 2016; Morrison et al., 2007; Raba et al., 2013).

Infectious diseases of various aetiologies are a leading cause of death worldwide with the biggest burden in low-income countries, predominantly in young children (Figure 1.1). About 230 million cases, excluding HIV/AIDS and tuberculosis, were recorded globally in 2016 as Disability-Adjusted Life Years (DALY). One DALY equalling one lost year of a healthy life.

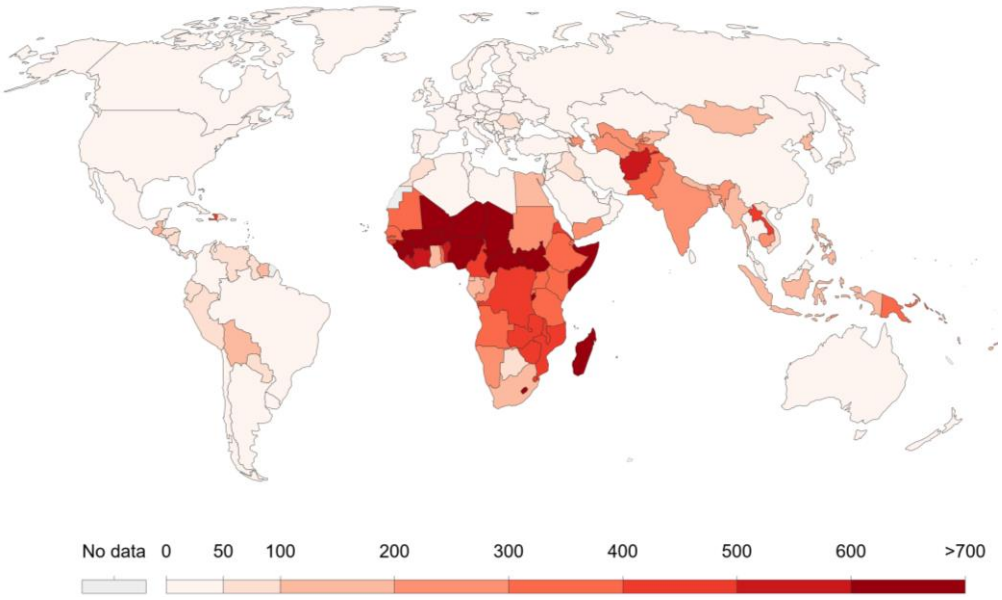

Figure 1. 1 Infectious disease death rates per 100,000 people in 2017
Global Burden of Diseases (https://ourworldindata.org/burden-of-disease).

Intervention and control programs have included mainly vaccination, education and improvements in primary healthcare delivery. However, healthcare systems are still hindered by the appropriate management of patients who report to facilities. Principal among these challenges is the lack of rapid and efficient diagnostics (Blaschke et al., 2015; Caliendo et al., 2013). Consequently, patients are sometimes treated based on clinical presentations, which tends to be ineffective in illnesses such as fevers where clinical features are non-specific. For example, cases of bacterial infections may not be guided by appropriate antibiotic therapy without accurate diagnostic tools. Treating such patients presumptively is susceptible to misdiagnosis, extra cost to patients with overtreatment, or increased potential of antimicrobial resistance. Reports have documented high proportions of bacterial infections in febrile children treated for malaria at a time where guidelines from the World Health Organisation (WHO) recommended presumptive malaria treatment in febrile presentations (Brent et al., 2006; Nadjm et al., 2010).

1.2 Infectious Diseases Diagnostics: The problem of the developing world

The challenges in pathogen detection or relevant biomarkers suggestive of disease is often localised to under-resourced areas (Blaschke et al., 2015). In contrast to the developed countries, there seems to be a lack of clear policy in the healthcare delivery systems of low-middle income countries despite the underlying factor of infectious disease burden. A key area of this neglect is access to diagnostics or diagnostic facilities (Peeling & Mabey, 2010). Allegedly, there is little budget allocated to diagnostics in the general healthcare investments (Kobusingye et al., 2005; Nkengasong et al., 2010). Healthcare facilities are sparsely distributed in sub-Sahara Africa with the majority in

urban areas but ~80% of its population live in rural areas (Alkire et al., 2014). Poorly distributed laboratory facilities may inconvenience patients from rural areas who have to travel several hours and return later (up to weeks) for results. The distance and cost may become a deterrent to compliance or follow-up.

Where laboratories do exist, the accuracy of testing tools and the general turnaround time could be affected by outdated methods that are lacking in robustness or samples requiring storage until adequate numbers are attained before analysis. Considering the pre-existing erratic power outages in these regions, the quality of specimen may be lost during storage. Routine tests lack regulatory standards and may be used without evidence of their effectiveness. Other challenges to laboratories include lack of specialists, inadequate supply-chain management for consumables and reagents, inconsistent water supply, poor laboratory setup or architecture and poor maintenance culture of equipment. It is therefore reasonable to speculate that some clinicians neglect laboratory services and resort to presumptive therapy due to loss of confidence in test results (Peeling & Mabey, 2010; Ronald et al., 2006).

1.3 The need for improved diagnostic tests

Testing tools are indispensable because they are directly implicated in a patient's clinical outcome. Accurate, rapid and affordable diagnostic tests are required to inform suitable therapy, assess prognosis and assist in disease surveillance (Caliendo et al., 2013). It is important for diagnostic tests to remain architecturally and operationally simple, without the need for additional equipment and sample processing. This would facilitate self-testing and enable uptake in underdeveloped areas by community health workers or even pharmacists who administer over-the-counter drugs for treatment.

There are about 1,400 pathogens that infect humans (Taylor et al., 2001), however, most diagnostic tests are specific to a single disease or pathogen. The situation is further complicated by the emergence of new strains and sub-populations which affect the sensitivity of tests. New testing tools capable of multiplexed detection or that discriminate between species diversity are therefore required.

The improved sensitivity offered by molecular testing and the ability to detect multiple-markers in parallel is useful in identifying targets from the diversified pathogen sub-populations. Detection of multiple specific pathogens and drug-resistant markers in parallel would be an immediate breakthrough in guiding informative therapy in critical systemic infections where results from cultures may delay. Yet, most molecular methods in clinical diagnostics still require a level of sophistication that restricts widespread adoption in under-resourced laboratories.

1.4 Point of Care Tests (PoCTs)

To increase access to testing, Point of Care Tests (PoCTs) are needed to replace laborious and sophisticated methods. PoCT is defined as "a medical test that is conducted at or near the site of patient care" (Kost, 2002; Price, 2001). Immunochromatographic lateral flow assays, also called rapid diagnostic tests (RDTs), have transformed the diagnosis of infectious diseases (Koczula & Gallotta, 2016). These portable paper-based devices often embedded in a plastic cassette platform can provide results within 5–30 minutes. Its principle is similar to enzyme-linked immunosorbent assay (ELISA) and involves the use of nitrocellulose paper for capillary suction of biological samples containing a target. Upon addition of a sample, target analytes interact with antibodies conjugated onto colloidal gold prefixed at the sample

chamber. The sample then migrates upstream via the nitrocellulose paper towards a zone where a second antibody specific to the analyte has been immobilised to form an immunocomplex; confirmation of successful formation of the immunocomplex is indicated by the presence of a coloured line. Several commercial RDTs have greatly increased access to screening and testing in developing countries; notably for malaria (Mason et al., 2002), hepatitis B (Pereira et al., 2015), syphilis (Herring et al., 2006), HIV (Bristow et al., 2014) to mention a few. They are simple to perform, do not require instrumentation, disposable, inexpensive and most importantly, fast turnaround time. Yet, despite the obvious attractiveness of the RDTs, the substantial disadvantages of immunoassay constrain the expansion of practical applications of these diagnostic platforms in infectious disease diagnostics (Table 1).

New PoCTs would be particularly useful for diseases such as tuberculosis, where culture methods can take up to six weeks before a complex treatment regime spanning a minimum of 6 months can begin. For diseases that require quantitation of parameters (mostly viral infections; viral titres), PoCTs tend to be lacking or not readily accessible where they are urgently needed to provide better care. The limited availability of PoCTs could be attributed to capital investments required in developing diagnostic tests, where a perceived fear of losses seems to discourage the private sector from committing substantial investments even into products with high commercial prospects (WHO, 2011). All new test devices including PoCTs are required to meet the '***A.S.S.U.R.E.D'*** standards of the WHO (Drain et al., 2014). These set of features symbolise; ***A:*** affordability to persons at risk of infection, ***S:*** sensitivity with minimal false-negatives, ***S:*** specific with minimal few false-positives, ***U:*** User-friendliness and simplicity of testing with minimal training, ***R:*** rapidity of turnaround time to enable treatment at first assessment, ***R:*** robustness without samples requiring storage, ***E:*** equipment-free, and

D: expedited delivered to areas of need. In spite of recent technological reforms and advances in diagnostics, most developing countries where infectious diseases are prevalent are incapable of technology uptake. Untrained personnel, under-resourced facilities, intermittent power supply and limited funding are some underlying factors which could further exacerbate the disease burden. Also noteworthy, some diagnostic tests (test kits) used in developing countries have not been rigorously evaluated (D Bell & Peeling, 2006). Considerable progress has been made towards diagnosing diseases such as malaria with a high degree of reliability (Krampa et al., 2017b). However, several analytical parameters (turnaround time, assay complexity, low throughput) are still unmet, hence these promising diagnostic technologies are unsuitable for uptake particularly in areas where they are most needed. Research has focussed on self-contained, high performing PoCTs using biosensing models. Biosensors have significant advantages of superior diagnostics; cost efficiency and rapid turnaround time as has been reported by growing amounts of published work (Dias et al., 2014; Vigneshvar et al., 2016). These relatively new class of PoCTs have the features required to bridge the gaps and pre-existing limitations in ensuring highly accurate diagnostics (Sampath & Ecker, 2004).

Table 1: Advantages and disadvantages of test-systems based on the lateral flow immunoassay platform [Adopted from (Andryukov et al., 2020)].

Advantages	Disadvantages
− Cheap, rapid, inexpensive, and easy to apply tests.	− Suitable only for primary screening and require confirmation of positive results by independent methods.
− Long shelf-life of test systems	− Special equipment (scanners, reflectometers, CCD cameras) and software are required to obtain quantitative results.
− Test systems do not require special temperature conditions for storage.	− Technological improvement of the method increases cost and duration of the analysis.
− No additional special equipment is required.	− In a competitive format, response negatively correlates with concentration.
− Possibility of multiplexed formats of test systems	− Possible technical errors in application of specimen may affect the accuracy and reproducibility of result.
− They do not need qualified personnel	− Increase in sensitivity of tests is based on the use of gold, silver, or enzyme nanoparticles, which limits shelf-life, increases cost of analysis, and breaks the one-step rule of application.
− They can be used by general practice physicians or patients at home	− Tested specimen must be in the form of a solution. Preliminary dissolution of dry specimens is mandatory.
− Visual result is clear and easily − distinguishable	− When the analyte content in the solution is low, the specimen needs to be concentrated.
− Tests are usually sold as kits with a set of all the items needed to perform the test	

1.5 Biosensors as PoCTs

Biosensors started with Clark's ground-breaking oxygen sensor in 1956 and the amperometric enzyme electrode for glucose later in 1962 (Yoo & Lee, 2010). Today, improvements in its analytical parameters coupled with the capability of miniaturisation and multiplexing have exemplified the modern biosensor as a promising and powerful approach to early disease diagnosis. They are self-contained analytical devices in which a biological component that generates a recognition event is intimately associated with a physical element that transduces the recognition event, and responds selectively to the concentration or activity of a chemical species (Buerk, 1993; Chaubey & Malhotra, 2002). They can be applied to probe analytes qualitatively and quantitatively in complex matrices (blood, urine, saliva, tissue, cell cultures, food and environmental samples) (Zhang & Ning, 2012). The components and classifications of biosensors are detailed in Chapter II (Section 2.2).

Transduction of the target-receptor binding event is translated through an optical, mass or electrochemical readout. An example of optical transduction is the visual immunochromatographic RDT which is interpreted by a colour change. However, optical sensing is associated with poor sensitivity, the need for optically transparent samples/materials and expensive auxiliary equipment. Electrochemical transduction offers better sensitivity, low cost instrumentation and is easily miniaturised which can facilitate translation into PoCTs as achieved by glucometers (Clausmeyer et al., 2014; Lee, 2008; Patel et al., 2016; Stradiotto et al., 2003). Some of its drawbacks include additional instrumentation for readouts and difficult interpretation of results.

1.6 Aim and Objectives

In the pursuit of a PoCT for infectious diseases, we hypothesised that electrochemical biosensors allow for sensitive detection and quantification of analytes. The overall aim was to design a label-free, disposable electrochemical biosensor array, based on nanostructured surfaces, with the capacity for the simultaneous clinical diagnosis of malaria and hepatitis B.

The aim was addressed through four (4) objectives;

Objective 1: Evaluation of the suitability of in-house screen-printed carbon electrodes (SPCE) and screen-printed gold microelectrodes (SPGµE) as a base transducer for electrochemical sensors.

Objective 2: Modification of the surface properties of the SPCE such as the deposition of conductive nanocomposites to enhance its electroanalytical performance characteristics.

Objective 3: Immobilisation of biological components onto the surface of the nanostructured SPCE and SPGµE to develop electrochemical biosensors for malaria and hepatitis B diagnosis.

Objective 4: Optimisation of the assay working conditions and application of the optimised assay for the simultaneous analysis of the biomarkers in clinical samples.

1.7 Scope and organisation of the thesis

The thesis details the research performed towards the development of electrochemical biosensors which are a powerful tool in analytical chemistry. It was based largely on proofs-of-concept using in-house screen-printed macro carbon electrodes and gold microelectrodes for sensitive detection and quantification of analytes. Chapter 2

highlights the basic components of biosensors, the stages of their development and strategies for bioreceptor immobilisation. A theoretical overview of the principles underlying the methods used during this work, such as voltammetry and electrochemical impedance spectroscopy is also presented.

In Chapter 3, the potential applicability of the modified surfaces as electrochemical sensing platforms is demonstrated. Two specific sensors are presented, including the design, fabrication and characterisation of the base transducers and their subsequent use for the analysis of catechol, a priority pollutant in water, as well as the simultaneous analyses of dopamine and acetaminophen in urine. These organic compounds are easily oxidizable and reducible and electrochemical detection provides an easy procedure for direct and selective detection.

Chapters 4 and 5 describe the development of a label-free impedimetric biosensor for malaria and hepatitis B respectively. Markers for malaria and hepatitis B; *Plasmodium falciparum* histidine-rich protein-II (*Pf*HRP-II) and hepatitis B surface antigens (HBsAg) were selected as a proxy for infectious disease immunosensors and to demonstrate multi-parallel analyte detection. These diseases were selected because, despite the introduction of several intervention strategies including an effective hepatitis B vaccination, the estimated overall burden of both diseases remain in sub-Saharan Africa. In order to maintain the orientation and functionality of bioreceptor molecules, different methods of controlled immobilisation of antibodies were evaluated. The capacity of the sensor for multiplexed detection of malaria and hepatitis B was also demonstrated.

Finally, an overview of findings and conclusions that provide suggestions for future work are detailed in Chapter 6.

CHAPTER 2

LITERATURE REVIEW

2.1 Introduction to biosensors

Any device with the ability to translate measurable signals to the desired outcome falls within the category of a sensor. This begins with the five senses of the human body. Selected servants were also required to taste the food served to kings in order to detect poisoning and caged canaries were deployed into coal mine shafts as audible warning systems to alert miners of toxic gases. Prior to the breakthrough in laboratory testing for diabetes, ants were used as sensors for diabetic urine and even before that, physicians and nurses had to taste urine from their patients for traces of sugar.

Sensors measure a variety of physical (temperature, mass, pressure or distance) and chemical (pH) parameters while biosensors are chemical sensors in which a biological element is used to generate a biochemical mechanism (Thévenot et al., 2001; Turner et al., 1987). These properties have been applied to biological and non-biological matrices with a focus on medical diagnostics.

Owing to the demand for rapid testing and personalised healthcare, the global market for biosensors is forecasted to grow from the current $19.2 billion to $31.5 billion by 2024 (Figure 2.1), the largest market share being for PoC devices.

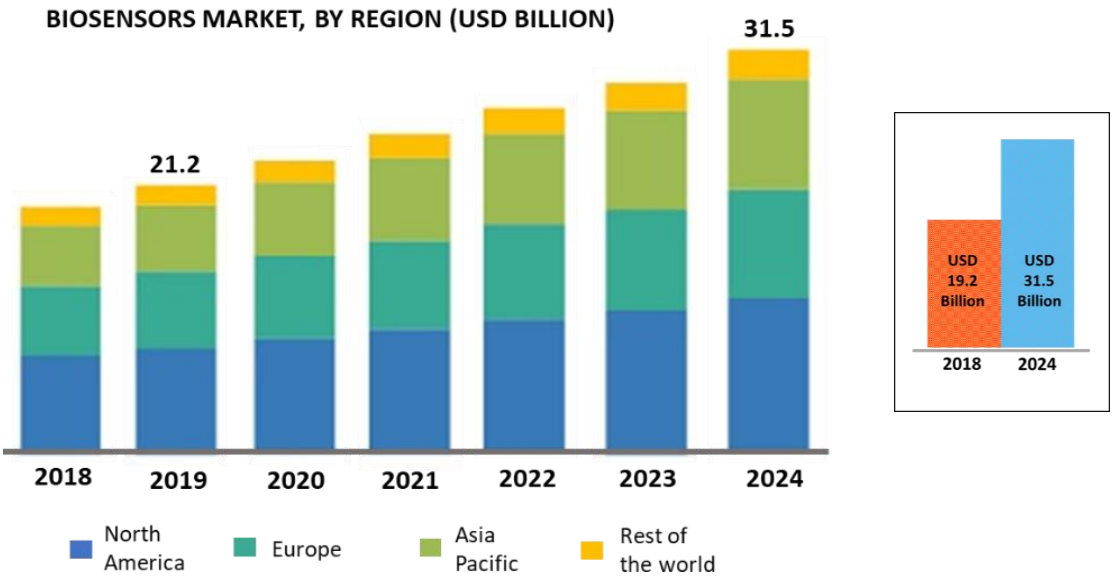

Figure 2. 1 Forecasted growth and demand for biosensors
The global biosensors market by type, product, technology, application and geography forecasted to 2024.
https://www.marketsandmarkets.com/Market-Reports/biosensors-market-798.html

2.2 Components of a biosensor

The core components of a biosensor are the bioreceptor or biorecognition molecule, transducer and a signal analysis system (Morrison et al., 2007; Perumal & Hashim, 2014). Biosensors can be classified either according to the mechanisms of biorecognition or by the mode of signal transduction employed. A general layout and classifications are outlined in Figure 2.2.

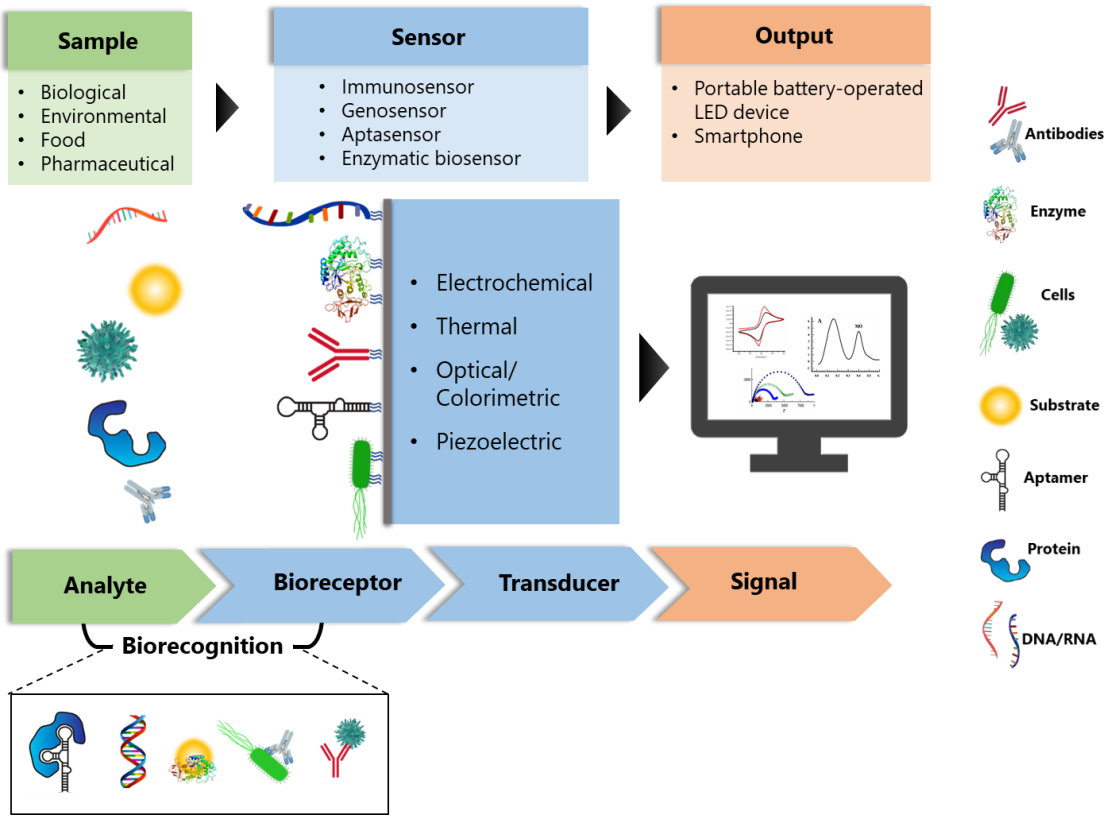

Figure 2. 2 Schematic representation of a biosensor.

Biosensors vary based on their transducers and bioreceptors. The interaction of analytes with bioreceptor components (antibody, aptamer, nucleic acid and antigen) in different biosensors is converted to quantifiable signals through the transducer and then analysed in a system.

2.2.1 The bioreceptor

Biosensors differ from chemical sensors because they incorporate biological molecules capable of recognising an analyte. The bioreceptors are placed in close association with the transducer where after interaction with an analyte, produces a desired signal. The biological component can be antibodies, proteins (peptides, enzymes or antigens),

aptamers, nucleic acids (DNA or RNA), phages, cells or cellular components (receptors, organelles) and/or tissues (Figure 2.2). The bioreceptor confers specificity and selectivity to the biosensor given that they select for specific analytes and thus, can prevent interference of other materials in the complex sample matrix. Biosensors can also be classified based on the bio-recognition process. For example, biosensors based on immuno-diagnostic methods are called immunosensors. They employ either an antibody as capture for antigens or vice versa. Where aptamers are used as the bioreceptor, the biosensor is termed an aptasensor and a genosensor where a nucleic acid probe is used to target DNA or RNA. Others include enzymatic biosensors, whole-cell biosensors, phage biosensors, molecularly-imprinted polymer (MIP)-sensors and affibody sensors.

2.2.2 Transducer

The transducer transfers biological recognition events into a quantifiable signal, which could be an electrochemical, optical, thermal or piezoelectric response. A key determining parameter of sensitivity in biosensors is the accurate correlation of any measured signals to the actual quantity of the target. Thus, transducers are vital components of biosensors. A sub-classification of biosensors according to their transduction procedures is illustrated in Figure 2.2. Further discussions pertaining to transducers in this chapter are limited to electrochemical transduction.

2.2.3 Signal analysis or processing unit

After signals in response to the biorecognition event are generated, they are transformed into a desirable output. For example, visual optical indicators based on colour changes have been used in conjunction with enzymatic biosensors where a substrate's transformation is indicative of enzyme catalysis or inhibition (De Carvalho, 2011; Justino et al., 2015). In other setups such as whole-cell biosensors, analytical information can be obtained by evaluating the metabolic status of microbes and tissue-culture cells including; growth inhibition, substrate uptake, bioluminescence, cell viability, cell respiration or specific gases produced (De Carvalho, 2011; Di Gennaro et al., 2011; Wang et al., 2014).

Portable, digital battery-operated devices are attractive digital readouts, and the popularity of mobile phones has prompted the interest to develop applications and accessory devices for integration of biosensors into smartphones (Gawali & Wadhai, 2018; Ionescu, 2017; Lillehoj et al., 2013; Liu et al., 2014).

2.3 The theoretical background of electrochemical methods in biosensing

Electrochemistry encompasses the study of electron transfer reactions between an electrode in contact with a solution (Fisher, 1996; Manahan, 2010). This differs from chemical reactions where electrons are transferred between molecules within the bulk solution. Electrochemical reactions occur primarily at the electrode-solution interface and require at least two conducting electrodes (working, WE and reference, RE) in contact with electroactive species, making up an electrochemical cell. The desired electrochemical reactions occur at the WE while the indispensable RE monitors current and potential fluctuations of the WE under zero-current (Fisher, 1996). Methods used

in electrochemistry either control (potentiostatic) or measure (potentiometric) the potential in electrochemical systems.

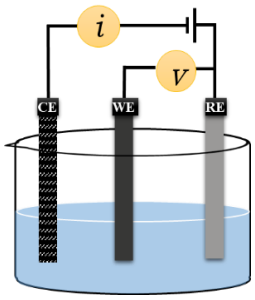

Figure 2. 3 An integrated circuit design of a basic 3 electrode sensing system. The potential of the WE and RE are sustained at the same level by balancing the current at CE (Kellner et al., 2015). The transfer of electrons between electrodes and solution is initiated by application of a potential to the system which will, in turn, produce the current.

2.3.1 Principles of electrochemistry and electrochemical transduction

2.3.1.1 The faradaic and non-faradaic processes

During an electrochemical reaction, the faradaic and non-faradaic processes occur at the electrode surfaces. The faradaic, or charge transfer process involves the movement of electrons between electrode-electrolyte. The non-faradaic process takes into account the occurrences that change the electrical double layer such as adsorption, desorption (or voltammetric stripping), changes in solution composition, biorecognition, or electrode surface area alterations. Non-Faradaic effects, if uncontrolled during experiments can interfere with the charge transfer processes. Formation of an electrical double layer, for example, is characterized by condensation of ions at the electrode-solution interface to compensate for excess charges on the electrode.

2.3.1.2 The Faradaic process

Faradaic processes are monitored through the transfer of electrons during the oxidation-reduction reaction of an analyte, denoted as in equation 1 which occurs under a thermodynamically or kinetically favourable potential region.

$$A + ne^- \rightleftharpoons B \qquad (1)$$

Where *A* is the oxidized species, *n* the moles of electrons, and B for the reduced species.

Redox reactions do not occur spontaneously, thus they require a potential to provide the energy for the Faradaic process, controlled by mass-transport and electron transfer (shown in Fig. 3.2). The Nernst equation describes the relationship between electrochemical potential and the relative activity of chemical species, where E_{cell} is the potential of the process under scrutiny, E^0_{cell} is the standard cell potential, R is the molar gas constant, T is the absolute temperature, n is the number of electrons transferred, F is the Faraday constant, and Q is the ratio of ion concentration at the anode to ion concentration at the cathode (In this case of Eqn. 1, Q= [A]/[B]).

$$E_{cell} = E^0_{cell} - \frac{RT}{nF} lnQ \quad = \quad E^0_{cell} - \frac{0.059}{nF} lnQ \qquad (2)$$

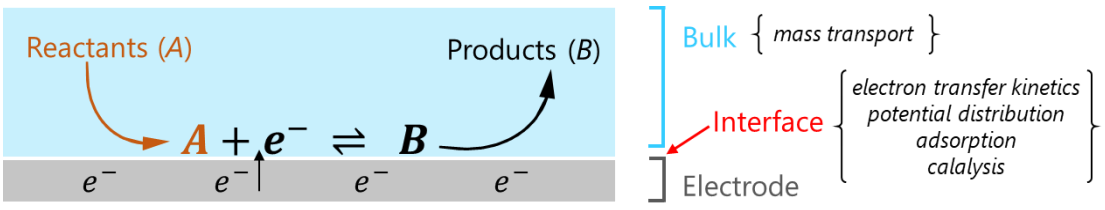

Figure 2. 4 Illustration of the rate-determining steps of a faradaic process
It involves mass transport of electroactive species (A) to the surface of the electrode where it is reduced (B) and transported back into the bulk solution.

2.3.1.3 Mass transport mechanisms

Mass transport is critical to the observable current since it is responsible for conveying molecules to and from the electrode's surface (Kissinger et al., 2019). Factors that influence mass transport of species include diffusion coefficient, concentration gradient, potential gradient, and analyte charges. When diffusion, convection and migration occur concurrently, it complicates the mass-transport process making it difficult to relate the current output to the analyte concentration.

Working within a still undisturbed solution or high scan rates (up to 100 mV/s) may help to minimise the effects of convection on mass transport. Migration can be decreased with concentrated supporting electrolytes to reduce the electrical field of charge; however, high concentrations of supporting electrolyte (often KCl in excess of 0.1M) which is added to annul the effects of migration and potential drop (Compton et al., 2013) could further compound the diffusion.

Diffusion, therefore, becomes the major contributor to mass transport effects. If the reaction is limited by diffusion alone as seen in amperometric systems, the relationship between current and analyte concentration is governed by Cottrell behaviour (equation 3)

$$I = nFADC\sqrt{\frac{D}{\pi t}} \qquad (3)$$

Given; n: number of electrons, F: Faraday's constant, A: electrode area, D: diffusion layer, C; concentration and t: time.

Since diffusion occurs spontaneously from a high to a low concentration, the Stokes-Einstein equation is used to describe the diffusion coefficient (D), relating it to temperature (T), the viscosity (η), and hydrodynamic radius (R) of the diffusive species:

$$D = \frac{kT}{6\pi\eta R} \quad (4)$$

k is the Boltzmann constant.

2.3.1.4 Kinetics of electron transfer

Electrons move across a charge gradient at the electrode-electrolyte interface, the mechanism requires electrons in the valence orbitals of reduced species to have higher energy than electrons at the electrode surface oxidation to occur, and the vice versa for reduction. When mass transport is high, the electrochemical process is controlled by the rate of electron transfer between the electrode and the electroactive species (k_f and k_b for the forward and backward reactions respectively). In a reversible reaction (Eqn. 1), the kinetics of electron transfer is faster than the mass transport rate (ks >> km) hence the electron transfer reaction at the electrode surface, depending on the concentrations of A and B, is rapid and in equilibrium according to Nernst (under STP). Considering that an anodic and cathodic reaction occurs on the same electrode, the electron transfer process controls the relationship between electrode potential and current response.

$$A + ne^- \underset{k_b}{\overset{k_f}{\rightleftharpoons}} B \quad (5)$$

Given the rates of the forward k_f and backward $k_b$reactions are;

$$k_f = k^0 \exp\left(\frac{-\alpha F}{RT}\left[E - E_f^0\right]\right); \quad k_b = k^0 \exp\left(\frac{-(1-\alpha)F}{RT}\left[E - E_f^0\right]\right) \quad (6)$$

k^0 is the overall electron transfer rate constant, E is the cell potential, k_f and kb are the rates of the forward and backward reaction, respectively, E_f^0 and E_b^0 the standard

potentials of the forward and backward reactions, respectively. The combined mass transport coefficients and electron transfer rate constants can be expressed in terms of the overall flux in an electrochemical system, given by the Butler-Volmer equation (Dreyer et al., 2016).

$$j = j_o \cdot \left[\exp\left(\frac{\alpha_a nF}{RT}\eta\right) - \exp\left(-\frac{\alpha_c nF}{RT}\eta\right)\right] \qquad (7)$$

Where; j is the electrode current density, j_o is the current density, η is activation overpotential, a_c and a_a are the cathodic and anodic charge transfer coefficients respectively.

The current-potential relationship within a kinetically controlled experiment differs from diffusion-controlled systems. This is because high mass transports of electroactive species to the electrode are controlled by the rate of electron transfer between the electrode and the electroactive species. When an electrochemical system is reversible, k^0 of both oxidation and reduction is high and the current responses become limited by mass transport ($k^0 > m_t$). Voltammetric experiments involving such systems show two separate waves (oxidation and a reduction wave) in a current-potential plot. In an irreversible reaction, mass transport is sufficiently high so that the current response is limited only by the rate of electron transfer ($m_t > k^0$). This is because the rate of the forward reaction is greater than the product of the mass transport coefficient and the rate of the backwards reaction which slows the kinetics of electron transfer compared with the mass transport rate. In such circumstances, little current flows around the formal potential for the redox couple, therefore large potentials are required at the anode and cathode to drive the electrochemical reaction. Quasi-reversible electrochemical reactions have $m_t \sim k^0$.

2.3.2 Methods in electrochemistry

Electrochemical methods are classified as bulk and interfacial methods. Interfacial methods can occur when no current flows across the cell (static mode) or an under controlled current and potential (dynamic mode). Voltammetry is most frequently used. It is based on voltage, current and time relationships in a three-electrode electrochemical system (Rackus et al., 2015; Trojanowicz et al., 2003; Uslu & Ozkan, 2011). Either under quiescent or hydrodynamic conditions. Hydrodynamic conditions are beneficial to mass transport and improvements in detection limits. Application of injection analysis systems is also beneficial in improving the sensitivity and sample throughput of amperometric methods (Felix & Angnes, 2010; Trojanowicz & Kołacińska, 2016). A classification of electrochemical methods used in sensing is outlined in Figure 2.5.

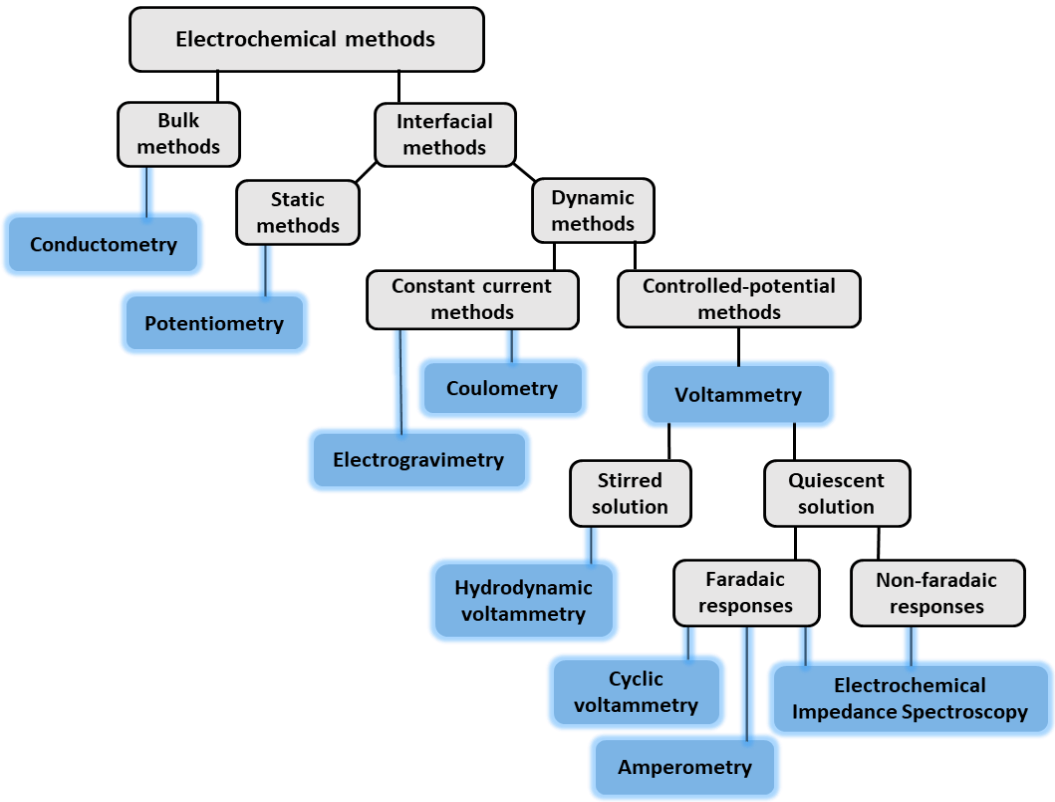

Figure 2. 5 The methods used in electrochemical immunosensor developments.

2.3.2.1 Cyclic Voltammetry

Cyclic voltammetry (CV) provides electrochemical properties of transducer materials, thermodynamic and kinetic information about electroactive species. It involves applying a potential sweep to an electrochemical system and then measuring the resulting current (Compton et al., 2013). An illustration of the CV process and its corresponding cyclic voltammogram of a reversible redox process is illustrated in Figure 2.6. At the start of the potential ramp (t_o) there is no electrode-electrolyte interaction. As the potential of the electrode increases towards the standard potential of the cell half, the faradaic process of the reaction is activated and catalyses an anodic reaction. This is characterised by an increased current in response to electron transfer between the electrode and reactants in the bulk until reactants decrease sufficiently. The peak oxidation current (I_{pc}), is indicative of a build-up of products in the diffusion layer, causing the current response to diminish. At a switching potential ($t_{1/2}$), and the phenomenon is reversed if the reaction is reversible to the stop potential (t_1) where the concentration of the reactants is assumed to be equal to the bulk solution and the concentration of the products is assumed to be nil.

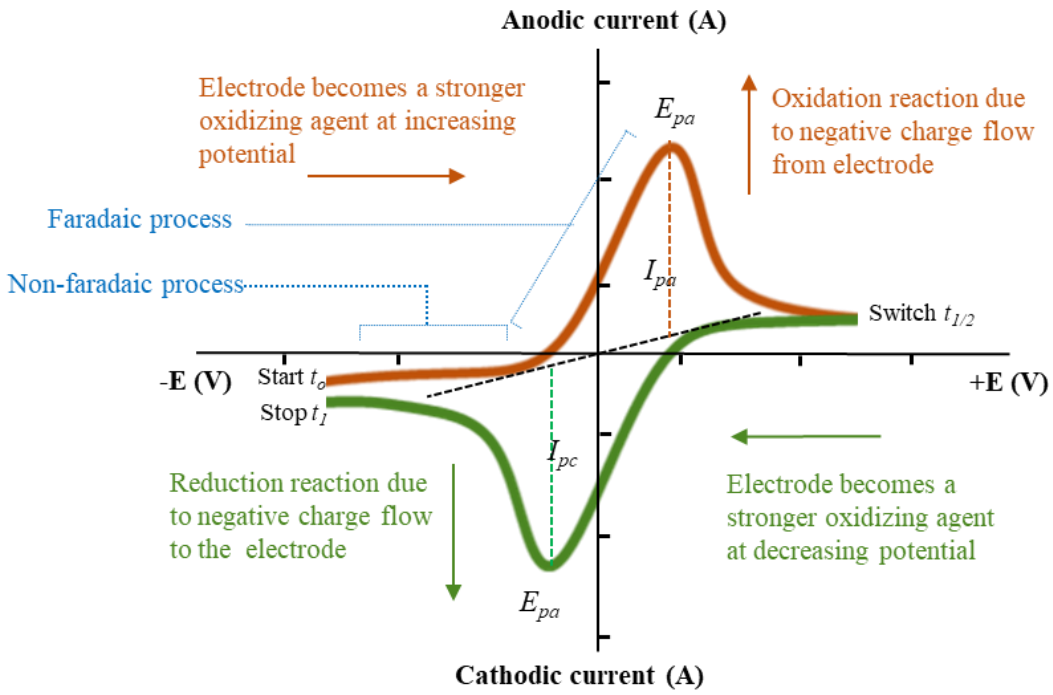

Figure 2. 6 A typical cyclic voltammogram within a reversible redox species. The traces show oxidation and reduction reaction pathways of the electroactive species in an electrochemical cell. The extrapolations represent the peak currents (I_{pa} and I_{pc}) and peak potentials (E_{pa} and E_{pc}) for the anodic/reduction and cathodic/oxidation reactions.

The duration of the scan must be adequate for the redox reaction to occur during CV. The differences between peaks (ΔE_p) identifies the reversibility of a redox couple, independent of the scan rate. Assuming standard conditions, a redox couple produces a theoretical separation of ~57 mV (Eqn. 8) for a one-electron transfer process. Larger ΔE values for voltammograms with distinctive anodic and cathodic peaks are suggestive of quasi-reversible reactions.

$$\Delta E = E_{pa} - E_{pc} = \frac{0.057}{n} \qquad (8)$$

Where n is the number of electrons transferred in the half-reaction.

The formal potential of the cell is found in the middle of E_{pa} and E_{pc}, hence;

$$E^0 = \frac{E_{pa} - E_{pc}}{2} \quad (9)$$

In an ideal reversible reaction, I_{pa} and I_{pc} are similar and defined in by the Randles-Ševćik equation (Ngamchuea et al., 2014), as

$$I_p = \pm 0.4463 nFAC \sqrt{\left(\frac{nFvD}{RT}\right)} \quad (10)$$

Where; I_p is the voltammetric peak current, D is the diffusion coefficient of the analyte, υ is the scan rate, C is the concentration of the analyte.

Convection is the major limitation where at very low scan rates, current response is more attributable to the Brownian movement of electroactive species than mass transport. Using extremely high scan rates also induce a larger Nernst diffusion layer due to an overcharged electrode surface.

2.3.2.2 Electrochemical Impedance Spectroscopy

Electrochemical impedance spectroscopy (EIS) is used in monitoring processes which change the conductivity of an electrochemical system. It can monitor both non-faradaic (capacitive accumulation from charge separation at the electrode interface) and faradaic processes of the charge transfer between the electrode and electroactive species (Prodromidis, 2010). Impedance (Z) is defined as the opposition force to an electrical current in a circuit, thus a measure of the circuit's resistance (R) to electrical current flow. Impedance (Eqn. 11) differs from resistance in that, it applies a small sinusoidal potential (AC potential) of fixed frequency and does not obey the Ohms law (Brockman, 2012; Lasia, 2014).

$$Z_\omega = \frac{E_\omega}{I_\omega} \quad (11)$$

Where; E_ω is the frequency-dependent potential and I_ω the frequency-dependent current. The transformation of angular frequency, ω, to a linear frequency, f (in Hz), is expressed as

$$\omega = 2\pi f \quad (12)$$

Application of EIS in biosensing takes into account resistance (a real component of impedance, Z', Eqn. 13) and capacitance (an imaginary component of impedance Z'', Eqn. 14). The data is often described in Nyquist plots (Z' vs. Z'')

$$Z' = R_s + \frac{R_{CT}}{1 + \omega^2 {R_{ct}}^2 {C_{DL}}^2} \quad (13)$$

$$Z' = R_s + \frac{R_{CT}}{1 + \omega^2 {R_{ct}}^2 {C_{DL}}^2} \quad (14)$$

Where; R_S is the solution resistance, R_{CT} is the charge transfer resistance and C_{DL} is the double-layer capacitance.

The R_{ct} accounts for the resistance impeding the charge transfer when the electrons cross the electrode-electrolyte interface (Preiss et al., 2013). It is determined by the diameter of the semicircle obtained in the Nyquist plot. A R_s occurs between the WE and RE at high frequencies and is dependent on the electrolyte concentration, electrode material and geometry, temperature and geometry of the electrode. The Nyquist plot is fitted into a simplified Randles circuit (Randviir et al., 2012) where the individual components can be extracted (Figure 2.7). The Warburg component (Warburg impedance (*Z*W)) accounts for the diffusion of the ions in the electrochemical reaction (Prodromidis, 2010).

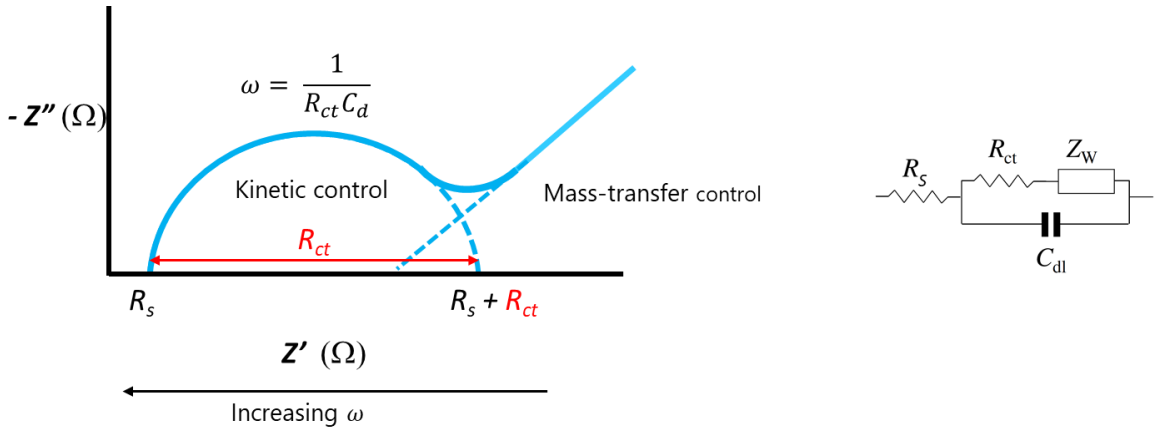

Figure 2. 7 A Nyquist plot of an ideal electrochemical cell.
The plot is represented as real impedance (Z') versus imaginary impedance (–Z'') and an equivalent Randles equivalent circuit used in modelling the data for a reversible redox species consisting resistance of the solution phase (R_s), the capacitance of the double layer (C_{DL}), charge-transfer resistance (R_{CT}) at the electrode surface and Warburg diffusion element (W).

2.4 Physical properties and setup of electrochemical sensing system setup

Electrochemical sensors can employ the concept of a three-electrode system consisting of a working electrode (WE), auxiliary or counter electrode (CE) and a reference electrode (RE); depicted in Figure 2.10.

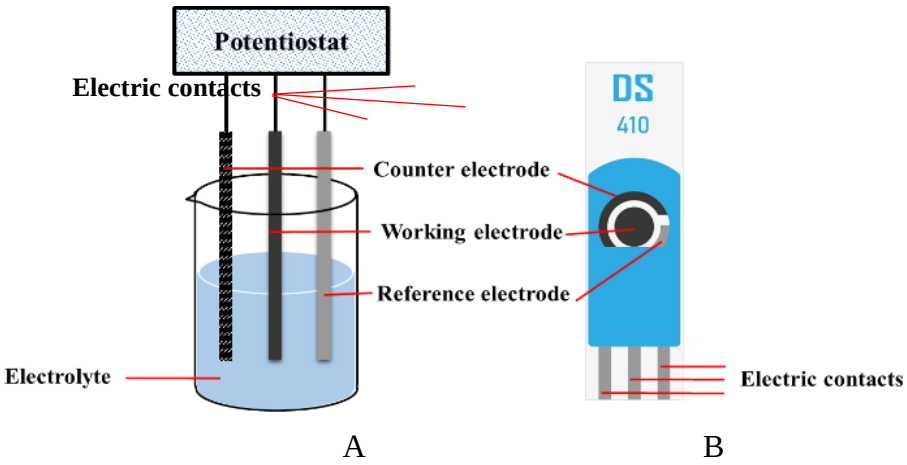

Figure 2. 8 An electrochemical cell and screen-printed electrode.
An electrochemical cell (A) consisting of working, counter and reference electrodes; and a screen-printed carbon electrode (B) with a carbon composite working and counter electrode and an Ag/AgCl reference electrode.

The reaction of interest occurs at the WE while the RE monitors the potential differences generated within the cell. The CE combines to stabilise and facilitate passage of current by adjusting for errors in the potentials resulting from a polarised WE. The RE helps to monitor the potentials generated by the other electrodes and electrolyte (Rani et al., 2018). Electrochemical cells are controlled by a potentiostat and monitored for characteristics such as current potential, impedance, capacitance, to mention a few (Faulkner & Bard, 2002). Not all methods require all three electrodes to be present within the cell. Potentiometric methods can apply only the WE and RE.

2.4.1 Electrode materials

The materials used for a WE depend upon the analyte as it could improve or impede the desired electroanalytical signals. It confers electrochemical characteristics to the sensor since it interacts directly with the reaction. A dropping mercury electrode traced back to Heyrovsky's invention in detecting metallic and organic compounds is probably the first documentation of a WE (Adams, 1958). Mercury's wide cathodic potential range and renewable surface conferred these properties; however, its use was discouraged due to toxicity. Electrodes made from noble, chemically stable, conductive metals such as platinum and gold are the most appropriate for electroanalysis, but expensive to research and mass production.

The need for alternative low budget electrodes has led to the investigation of variant carbon allotropes of graphite and diamond as appropriate electrode materials in classical electrochemical analysis. Examples include glassy carbon electrode (GCE), carbon fibres, highly ordered pyrolytic graphite (HOPG), single and multi-walled carbon nanotubes (SWCNTs and MWCNTs respectively) and boron-doped diamond

electrode (BDDE). Among these, carbon-based electrodes have the additional benefit of having a large potential window, low background current and rich surface chemistry. RE usually consist of silver metal coated with a layer of silver chloride (Ag/AgCl) and suitable materials for CE are platinum or silver.

2.4.2 Electrode designs and modifications

2.4.2.1 Screen-printed electrodes

The concurrent advances in nanotechnology and the quest for portable electrochemical devices have focussed on miniaturised electrochemical transducers, particularly printed electrodes. Screen printing has become the core of portable electrodes which could also be obtained. Fabrication of screen-printed electrodes (SPEs) requires depositing a layer/layers of conductive ink unto an inert surface such as ceramic, glass fibre or polyvinyl chloride (PVC) (Ha et al., 2005). Inexpensive mass production of disposable SPEs is made possible by automated and semi-automated systems (Randviir et al., 2014). Miniaturised electrodes can also be achieved through inkjet printing, gravure and flexography (Österholm et al., 2016; Pudas et al., 2005).

SPEs have revolutionised the integration of transducers into portable diagnostic devices. The commercial success of glucose sensors can be partly linked to advances in printing technology (Newman & Turner, 2005). The advantages of SPEs overcome the drawbacks of conventional electrodes as they are simpler to set-up and allow for independent tests thereby preventing errors related to contamination. Disposability after single usage prevents them from carry-over contaminations from re-usage and miniaturisation offers a distinct functional feature of a small sample and reagent volumes. Furthermore, SPEs can be efficiently printed on inexpensive substrates

according to any design with the possibility of multiple electrodes that allow for multi-parallel testing. These attributes make them potential candidates for cost-efficient portable products. A traditional three-electrode setup and a miniature screen-printed electrode is shown in Figure 2.10.

2.4.2.2 Conductive polymers

In electrochemical sensors, the electrodes act as the source/captor of electrons transferred between the electrode and the analytes in solution. To play this role efficiently, electrodes need to possess excellent electrical conductivity. While many electroactive species produce identical electrochemical signals, electrodes may also respond differently depending on the potentials applied.

Modification to obtain a heterogeneous nanostructured electrode surfaces is aimed at enhancing signals through increasing the active surface area and working potential window of electrodes (Shirakawa et al., 1977; Shrivastava et al., 2016), and to facilitate immobilisation of biorecognition elements (ElKaoutit, 2014; Gerard et al., 2002).

The use of conductive polymers (CPs) has the potential in protecting electrode surfaces from interfering materials in a sample matrix while ensuring maximum redox activity. CPs consist of a group of organic and inorganic compounds with very specific properties. Common examples used in electrochemical research are polyaniline (PANI), polypyrrole (PPy), polythiophene, PEDOT:PSS (Krampa et al., 2017) and their derivatives (Shrivastava et al., 2016).

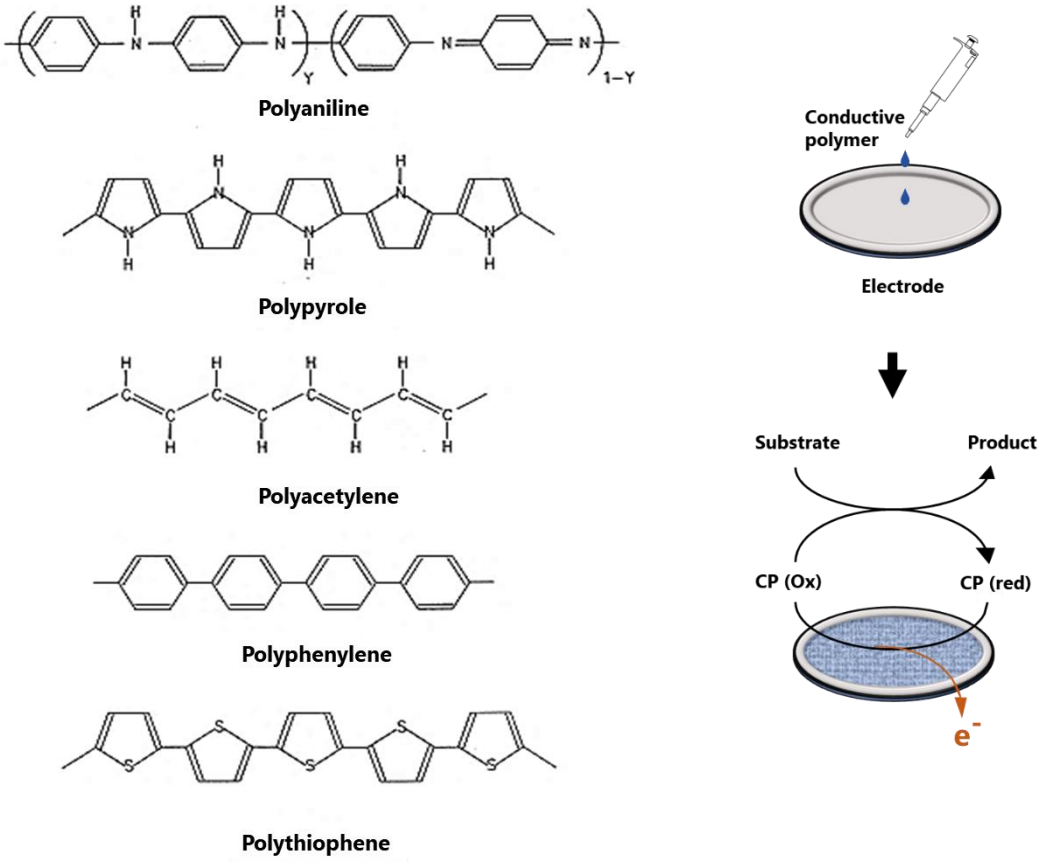

Figure 2. 9 Structures of some conducting polymers commonly used in biosensors and pathway of electron transfer.
(Deng et al., 2013; Gerard et al., 2002; Ruecha et al., 2014)

The unique properties that make CPs suitable for sensor fabrication include lightweight, flexibility, scalability, resistance to corrosion, and ease of customisation for particular needs (Shrivastava et al., 2016).

Nanocomposites composed of CPs along with other nanomaterials of electrochemical significance can act synergistically as a highly active electroactive compound better than the individual components. Nanocomposites have been demonstrated to possess improved electroanalytical properties that address some limitations of pure CPs (Prakash et al., 2013)

Nanomaterials have been used alongside CPs in nanocomposites, examples include metal nanoparticles, carbon nanotubes (CNTs), graphene, MIPs, and ionic liquids (ILs). The interest in using polymer nanocomposites in electrochemical sensor designs has increased owing to their ability to promote electron transfer, large surface area, and high electrical conductivity. These attributes directly impact on a sensor's sensitivity and detection limits. Metal and metal oxide nanoparticles possess advantageous features such as their small size; unique Physico-chemical and electronic properties and easy manipulation (Siangproh et al., 2011).

A range of chemically modified electrodes have been applied in electrochemical sensors. The incorporation of nanocomposite combinations into sensor designs has led to enhanced electrocatalytic efficiency, giving rise to several significant applications in analyte detection. Some examples of the nanocomposites include; TiO_2 nanoparticles and TiO_2 nanotubes (TNTs)-PANI (Zhu et al., 2015), ZnO–PPy (Devi et al., 2011), PANI–ZnO (Jain et al., 2014), PANI-graphene (Fan et al., 2011), PPy–graphene (Gao et al., 2014), poly(ionic liquid)-functionalized polypyrrole–graphene oxide nanosheet (PIL–PPy–GO) (Mao et al., 2015), PEDOT–rGO (W. Wang et al., 2014), PEDOT–graphene (Lu et al., 2013), PPy–MWCNT (Singh et al., 2012), PANI–MWCNT (Karolia et al., 2015), oligo(phenylene ethynylene) and chemically reduced graphene oxide (OPE-NH2–rGO) (Deng et al., 2013), PANI–polyvinylpyrrolidone (PVP)-graphene (Ruecha et al., 2014), PVP–AuNP–Grp (Wang et al., 2015), PANI–AuNP–chitosan–graphene sheet (Li Wang et al., 2014), polyaniline nanofibers (PANI-NF)–AuNP (Spain et al., 2011), and PPy–pyrrolepropylic acid–rGO (Wang et al., 2015) and graphene nanoplatelets-PEDOT:PSS (Cataldi et al., 2018).

2.4.3 Strategies for immobilizing biological receptors

Advances in new recognition elements for biosensors developments coupled with the application of nanotechnology have greatly improved the analytical performance (sensitivity, selectivity, the limit of detection (LoD)) and signal-to-noise ratio) of biosensors (Justino et al., 2013). The methods used to immobilise bioreceptors in sensor designs directly influences its efficiency and operational performance (Justino et al., 2015). While biomolecules are required to remain tightly bound to the surface of the transducer throughout its operation without desorption, it is equally important that they retain their structure and orientation for maximum biological activity after being immobilised. Biomolecule stability after immobilisation affects accuracy of measurements, operational lifetimes and is responsible for inconsistencies in sensor-to-sensor reproducibility. It is therefore imperative to incorporate successful immobilisation approaches into sensor designs in order to assure maximum performance. The classical strategies used in bioreceptor immobilisation include: adsorption, covalent linkage, entrapment, cross-linking and affinity–(Physical or chemical) (Liebana & Drago, 2016; Prieto-Simon et al., 2008). A combination of the strategies can be applied depending on the biomolecule, the transducer or mode of detection.

Sometimes, the final application of the sensor influences the choice of immobilization technique. The focus turns to the characteristics desired from the sensor rather than producing the ideal biosensor. For instance, a trade-off in stability for improved sensitivity and cost; or reproducibility while overcoming the difficulty of the immobilisation process.

Physical adsorption or passive adsorption is the method in which recognition molecules (often proteins) are directly attached to transducer surfaces via non-covalent

interactions. Although this form of attachment is simple and maintains the bioactivity after the immobilisation, non-covalent bonding like electrostatic force, ionic bond, hydrogen bond, and hydrophobic interaction are weak bonds and result in a weak attachment (Wang et al., 2008). The problem arises considering that initially adsorbed particles may be desorbed during assay procedures like washing (Ben Rejeb et al., 1998; Martín-Palma et al., 2004). Moreover, the method is still prone to random orientation (Sadir et al., 2014). In covalent attachment, irreversible interaction are formed between functional groups of biomolecules and a modified transducer (Rusmini et al., 2007; Yu et al., 2015). Chemical coupling agents such as carbodiimides and succinimidyl esters (frequently applied for carbodiimide/N-hydroxysuccinimide protocols) are used to generate carboxylic groups on electrode surfaces that bind with free amino groups of antibodies or protein, as shown in Figure 2.12 (Lai et al., 2011).

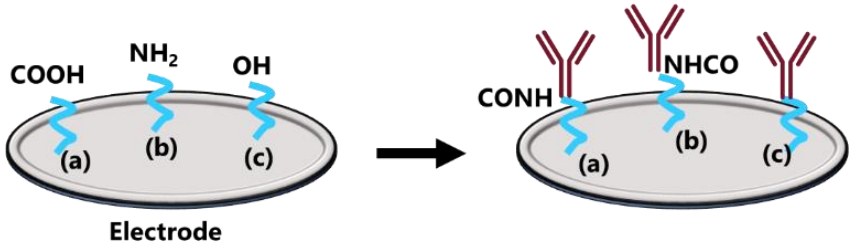

Figure 2. 10 Covalent immobilisation via free amino groups on antibodies.
(a) activation of carboxylic groups (COOH) on the WE with carbodiimides and succinimyl esters; (b) amine surface (NH_2) activation using isothiocyanates, epoxides, or aldehydes; (c) alcohol surface activation periodate oxidation, isothiocyanates, epoxides, aldehydes, and cyanogen bromide.

Different reactive linkers like thiol derivatives (Azrilawani Ahmad & Moore, 2012; Limbut et al., 2006; Nassef et al., 2008), 3-aminopropyl)triethoxysilane (APTES) (Wilson, 2005), 3-glycidoxypropyl)-trimethoxysilane (GPTMS) (Wei et al., 2009), 3-mercaptopropyltrimethoxy-silane (MPTMS) (Mansur et al., 2005), diazonium cation

(Corgier et al., 2005) can be used to generate functional groups on electrodes that bind proteins through cross-linking with aldehydes or epoxides. Amine and alcohol groups on the proteins are activated by aldehydes (mostly glutaraldehyde) and epoxides. The disadvantage associated with covalent linkages and cross-linking is that harsh coupling chemicals products may denature biomolecules and result in the loss of activity.

To ensure high stability and bioactivity, biomolecules can be entrapped within a gel or conductive polymer. Thin-film sol-gels and hydrogels, commonly, chitosan, dextran and carboxymethyl cellulose (Wu et al., 2006) are porous matrix with excellent biocompatibility and have been applied to entrap antibodies in electrochemical immunoassays (Dai et al., 2003; Du et al., 2003; Tan et al., 2006, 2007; Tripathi et al., 2006). Although entrapment methods do not predispose biomolecules to chemical reactions that may affect their activity, the formation of gel layers may inhibit signal transduction.

In remedying the partial or complete loss of biomolecule activity that results from random orientation and structural deformation, captured biorecognition molecules can be immobilised in a manner that exposes the recognition sites to a sample solution. Oriented immobilisations strategies that have improved immunosensor's performance include interactions between a functional group and an affinity tag on a protein sequence such as avidin-biotin (Yang et al., 2008), protein A/G (Arora et al., 2006; Fowler et al., 2007), lectin-carbohydrate (Zeng et al., 2012), metal cation–chelator and DNA-directed immobilisation (Boozer et al., 2005).

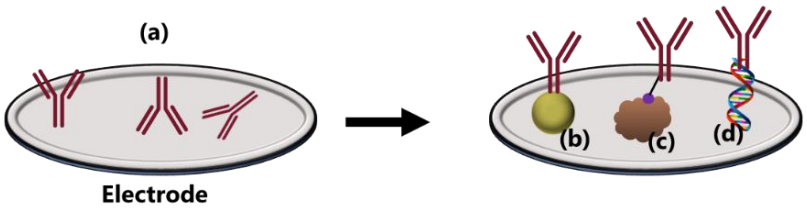

Figure 2. 11 Physiosorbed and oriented immobilization strategies of antibodies
(a) randomly immobilised antibodies; immobilisations through different bioaffinity systems involving (b) avidin-biotin, (c) protein A/G and (d) and DNA-directed.

2.4.4 Performance criteria of biosensor responses: analytical properties

Table 2. 1 Important analytical parameters of biosensors

Analytical properties	**Description**	**References**
Selectivity	Specificity of the bioreceptor towards a target analyte amidst other contaminants	(McNaught & McNaught, 1997; Umezawa et al., 2007)
Sensitivity	A function of the slope of the calibration curve gradient versus concentration	(Thevenot et al., 2001)
Linearity	The accuracy of measurements for increasing analyte concentrations.	(Stephen, 2004)
Dynamic/linear range	Defined from a series of analyte concentrations for which the measurement changes linearly between the lower and upper limits of quantification.	(Thevenot et al., 2001)
Reproducibility	Drifts in a series of responses over time symbolising the sensor's capacity to produce identical responses in repeated experiments.	(Thevenot et al., 2001)
Stability	Disturbances in or around biosensing system that may predispose responses to errors. The bioreceptor and the transducer are of particular concern which can be affected by operational procedures like temperature and lengthy incubation.	(Thevenot et al., 2001)

2.5 Electrochemical biosensors

Electrochemical biosensors are based on the concepts of electrochemistry, hence specific interactions between an electrode and the solution at its surface. It relies on the measurement of electrical charges from reactions of electroactive species occurring at an electrode-electrolyte interface using redox reactions. This provides a medium for electrons to flow between the two phases of different conductivity and produce signals which can be directly proportional to the species/analyte's concentration. A theoretical background underlying electrochemistry and electrochemical transduction is detailed in Section 2.3.1.

The popularity of electrochemical biosensors for clinical analysis has increased steadily due to key advantages in their design, assay simplicity, and superior analytical performance over conventional laboratory methods (Belluzo et al., 2008; Wang, 2008). These qualities make it suitable for POC application amidst continued efforts to improve and miniaturise electrochemical systems for portable devices. Electrochemical biosensors are categorised into their mode of signal transduction after the biorecognition event, namely; amperometric, potentiometric, impedimetric and conductometric (Gerard et al., 2002).

2.5.1 Amperometric sensors

Amperometric sensors apply a fixed potential between a sensing and a reference electrode to measure the current produced by an electroactive species as a function of time. The current which is as a result of electron transfer from oxidation/reduction reaction of an analyte is proportional to its concentration. This method has evolved through three generations. Initially, electrochemical responses from a reaction were

measured as the products diffused to the transducer. In order to enhance signals, specific mediators were employed between the reaction and transducer. The current generation probes the occurrence of the reaction itself without the need for mediators or product diffusion to the transducer (Saxena & Malhotra, 2003; Wang, 2008). The main drawback of amperometric methods is its dependence on a fixed potential which can result in interferences from other electroactive species in a sample matrix leading to false signals and low specificity (Lowe, 2008; Perumal & Hashim, 2014). The integration of mediators, selectively permeable membranes or sample dilution has been used to circumvent or minimise interferences (Belluzo et al., 2008; D'Orazio, 2003; Shinde et al., 2012).

2.5.2 Potentiometric Sensors

Potentiometric methods measure the potential difference in the form of charge build-up that accumulates between the transducer and a reference electrode upon analyte-receptor binding (Grieshaber et al., 2008). Ion-selective electrodes are mostly applied in potentiometric sensors used in clinical chemistry for physiologically relevant electrolytes. However, the method is less sensitive and slower than amperometry (Makarychev-Mikhailov et al., 2008).

2.5.3 Conductometric biosensors

Variant concentrations of electroactive species influence electrical conductivity, forming the basis of conductometric sensors where analytical information is obtained from the conductivity of electrolyte species within an electrochemical cell.

Conductometric methods have been employed in modelling inexpensive devices for food quality monitoring (Arora et al., 2011) but are faced with limited sensitivity attributable to interfering signals from the buffer (Jdanova et al., 1996).

2.5.4 Impedimetric biosensors

Impedimetric transduction is based on the measurement of conductivity when an electrical frequency sweep is applied to an electrode (McGuinness & Verdonk, 2009). It functions by analyte-bioreceptor interactions which can be monitored by changes in either capacitance and electron transfer resistance (R_{CT}) across a transducer surface caused by analyte binding. The impedance changes across the transducer surface changes with increasing analyte concentrations, making impedimetric systems highly sensitive and selective because they rely on specific receptor/ligand interactions and not affected by other analytes in a sample matrix. An important advantage over the other electrochemical methods is that, it is suitable for both label-free detection of analytes with or without the need for a redox probe (Parkinson & Pejcic, 2005; Pejcic et al., 2006). It is however, prone to variable reproducibility, and has the likelihood of nonspecific binding events occurring (Bogomolova et al., 2009; Daniels & Pourmand, 2007).

2.6 Immunosensors

Immunosensors are the most researched affinity biosensors. Due to its reliance on the theoretical basis of immunoreaction where an antibody or an antigen is used as a biorecognition agent, immunosensors are to an extent mistakenly associated with

biomedical application or disease diagnosis alone. A good accounts of their widespread applications involving antibodies immobilised as probes for the detection of pesticide residues (Jiang et al., 2008), drug compounds (Gandhi et al., 2015) toxins (Wang & Wang, 2008) and in food and drink industries (Thakur & Ragavan, 2013) have been well documented.

The specificity of the selected antibody towards the target is its most significant feature and immunoreaction complex can be monitored via a labelled or label-free assay format. Antibodies select for antigens ranging from small molecules to macromolecules in a given sample. Five classes of antibodies (IgG, IgA, IgE, IgM, and IgD) are defined based on structures and biological roles. IgG is abundant in blood and extracellular fluid and binds many kinds of pathogens, therefore, immunoassays have often employed its use. IgGs have a "*Y-shaped*" consisting of four polypeptide units (2 heavy chains and 2 light chains) (Figure 2.8); The upper segments of the *Y-shape*, denoted as Fab fragments, are the sites that bind with antigen.

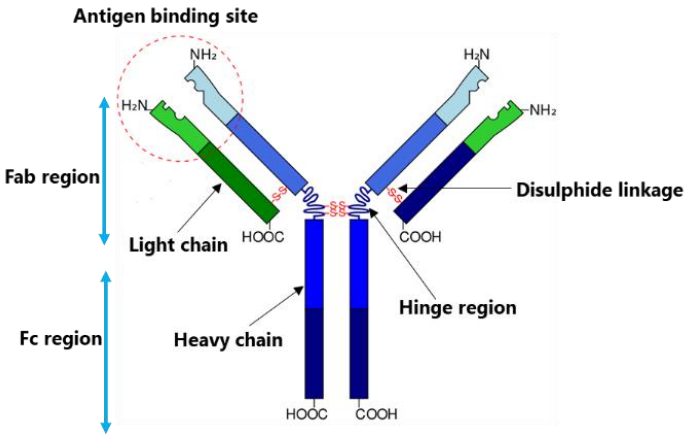

Figure 2. 12 Schematic representation of an IgG.

Among immunoglobulins, IgG, the most widely used in the developed immunosensors. Abs are bivalent and can bind with two specific antigens according to size, shape, and chemical compatibility. The Ag-binding site, the paratope binds the complementary region on the antigen called the epitope. Antibodies are classified either as monoclonal antibodies (mAbs) or polyclonal antibodies (pAbs). mAbs are produced from identical immune B cells and are used as a primary antibody in immunosensors to target a single epitope of an antigen. Owing to their monovalent affinity they are highly specific towards an antigen. On the other pAbs hand are a heterogeneous mixture of immunoglobulins produced by different B cell clones. Each pAbs them can recognize and bind to different epitopes of a specific antigen. (Lipman et al., 2005).

2.7 Immunoassay formats of electrochemical Immunosensing

The distinction between immunosensors and immunoassays is based on the site of immunocomplex between the antibody and the antigen. In immunoassay systems such as the conventional Enzyme-Linked-Immunosorbent Assay (ELISA), the immunocomplex processes takes place elsewhere whereas in immunosensors, the formation of the immunocomplex and diagnosis occur on the same platform (Wang et al., 2008). In ELISA the detectable signal is a colour change readable by an optical transducer (Mistry et al., 2014). The optical immunoassay approach is liable to drawbacks depending to the type of measurements applied (direct ELISA, indirect ELISA, competitive ELISA, and sandwich ELISA). These limitations can be associated with the potential false signals arising from coloured samples, a relatively long analysis time, a requirement of power-intensive light sources and detectors, as well as sample size and usage problem outside the classical diagnostic laboratory (Arduini et al., 2016).

In this regard, the use of immunosensors is a promising alternative to optical immunoassay approach for diagnosis of clinically important analytes due to high sensitivity and selectivity (Diaconu et al., 2013; Karunakaran et al., 2015). Furthermore, they provide the possibility of progression of immunoreactions at detector surfaces in real time. The use of electrochemical immunosensors simplifies the analysis with rapid and reliable signals.

Immunosensors are categorised as labelled and label-free formats (H Ju et al., 2011), illustrated in Figure 2.9. Labelling strategies require tagging immunoreagents with molecules such as fluorophores, magnetic beads and enzymes that produce detectable analytical signals upon immunoreaction. Label-free formats, on the other hand, do not require any labels during the immunoreaction. Labelled assays could be homogeneous or heterogeneous. A homogeneous immunoassay does not require unbound reagents to be separated from the immunocomplex reactions during operational procedures; similar to agglutination (Englebienne et al., 2000), capillary electrophoresis (Moser & Hage, 2008), fluorescence polarisation (Nielsen et al., 2000), and fluorescence resonance energy transfer-based immunoassays (Pulli et al., 2005).

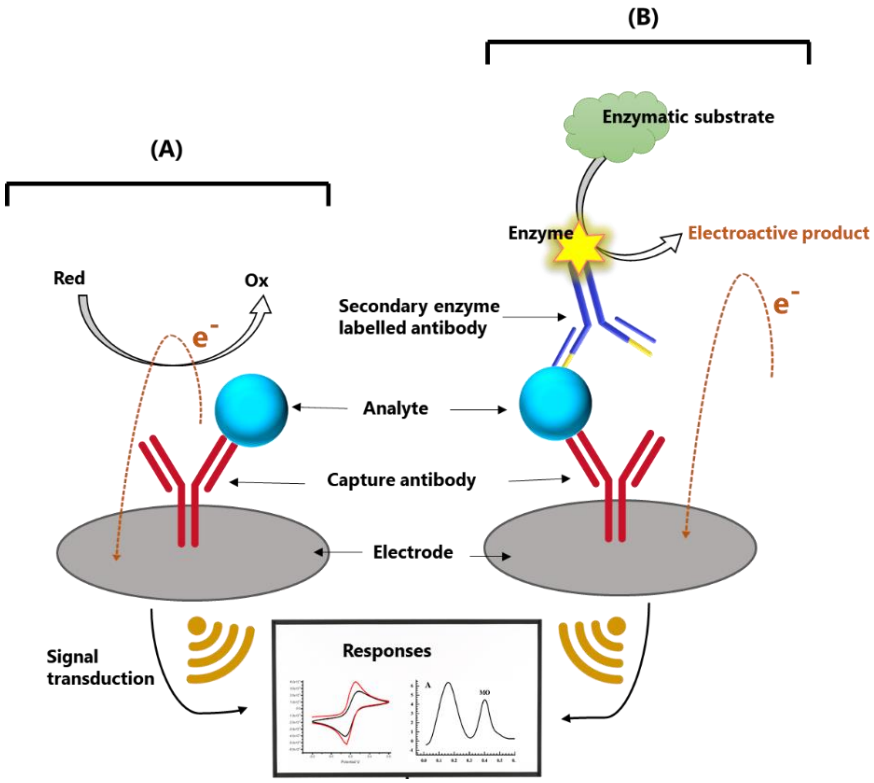

Figure 2. 13 Assay strategies applied in electrochemical biosensors.
(A) involves a one-step label-free immunosensor with signals induced by antigen-antibody binding, and (B) is a labelled sandwich-type immunoassay involving multiple steps. In the labelled assay signals are obtained from the reaction between an enzymatic label and a substrate.

Heterogeneous immunoassay formats involve separation of unbound immune reagents from immunocomplexes so that only the analytes of interest remain on the transducer surface while unbound ones are washed away. Heterogeneous immunoassay formats, commonly the sandwich-type are more popular because they augment sensitivity, specificity and throughput. However, the numerous steps involved prolong the turnaround time and makes them labour intensive and can be relatively expensive due to the use of different chemicals. Moreover, the analyte concentration measured is based on signals generated through the product of a secondary event. Labels can be fluorophores, magnetic beads, active enzymes with an easily detectable product, or anything that allows facile target conjugation and convenient detection. The labels can

change the binding properties of the biomolecules, which could, in turn, affect their binding affinity for targets (Haab, 2003). Label-free detection has been vastly applied in impedance sensors. Interaction between a biomolecule and a probe-functionalised electrode results in alterations in the electrical properties of the electrode surface. Therefore, no labelling is required, and real-time detection can be achieved in impedance sensing of proteins through immunocomplexes.

CHAPTER 3

RESULTS OF SPECIFIC OBJECTIVES 1 AND 2

3.1 Development and characterisation of electrochemical transducers for biosensing application

Overview

To achieve objectives 1 and 2, electrochemical studies were conducted on SPCEs to evaluate the suitability as a base transducer. This was followed by enhancement of the electrode surfaces with conducting nanocomposites to improve their electroanalytical properties. The modified electrodes were then applied to the detection of important analytes to demonstrate their suitability as electrochemical sensing platforms.

The chapter is based on two related publications.

Related publications

1. Krampa, F., Aniweh, Y., Awandare, G., & Kanyong, P. (2017). A Disposable amperometric sensor based on high-performance PEDOT: PSS/ionic liquid nanocomposite thin film-modified screen-printed electrode for the analysis of catechol in natural water samples. Sensors, 17(8), 1716. doi: 10.3390/s17081716

2. Krampa, F. D., Aniweh, Y., Kanyong, P., & Awandare, G. A. (2018). Graphene nanoplatelet-based sensor for the detection of dopamine and N-acetyl-p-aminophenol in urine. *Arabian Journal of Chemistry*. doi:10.1016/j.arabjc.2018.10.006

3.1.1 Abstract

The development and application of disposable sensors for the detection of catechol and simultaneous voltammetric determination of dopamine (DA) and N-acetyl-p-aminophenol (APAP) is reported. The sensors were fabricated by drop-coating conducting polymer-based composite material of poly(3,4-ethylenedioxythiophene) (PEDOT): poly(4-styrenesulfonate) (PSS) doped with a room temperature ionic liquid (IL), 1-ethyl-3-methylimidazolium tetrafluoroborate ([EMIM][BF_4]) and graphene nanoplatelets (GNPs)-Nafion (Naf) nanocomposite onto the working area of a screen-printed electrode (SPE). The sensors were characterized by scanning electron microscopy (SEM), Raman spectroscopy, electrochemical impedance spectroscopy (EIS) and cyclic voltammetry (CV). The composites exhibited a nano-porous microstructure and was found to be highly stable and conductive with enhanced electrocatalytic properties. PEDOT:PSS/IL was utilised in conjunction with amperometry towards catechol, a priority environmental pollutant, and differential pulse voltammetry applied at the GNPs/Naf for simultaneous analysis DA and APAP in their binary mixtures. The sensors showed excellent selectivity and sensitivity toward the target analytes, with limit of detection of 23.7 μM for catechol and 0.13 μM and 0.25 μM for DA and APAP, respectively. The catechol sensor produced recoveries exceeding 99.0% when applied to natural water samples and the performance of the APAP/DA sensor in human urine samples were found to be well over 97.0%.

3.1.2 Introduction

Electrochemical transduction has received the most credit among several mechanisms of transduction in biosensor designs owing to its simplicity, minimal instrumentation cost, capability of miniaturization, and automation. The use of screen-printed electrodes (SPEs), have contributed to the success of biosensors in terms of reliability, reproducibility, mass production, and low cost.

Nanomaterials are capable of providing improved electrocatalytic activity and minimise the fouling of electrode surfaces, rendering their use extremely advantageous in the development of biosensors. Biosensors based on SPEs modified with nanomaterials have been widely reported for the detection of several analytes (Arduini et al., 2014; Scognamiglio, 2013). The modification techniques involve drop casting with nanomaterial dispersions (Arduini et al., 2010; Cinti et al., 2014), addition of nanomaterial to inks during manufacturing (Arduini et al., 2012), electrodeposition (Ping et al., 2011), the Langmuir-Blodgett film approach (Michopoulos et al., 2014), and electrospray methods (Welle & Jacobs, 2005).

With the aim of improving the analytical characteristics of electrochemical transducers, their modification with a variety of nanomaterials been explored with successful results in most cases. Several conductive polymers and carbonaceous materials have been used to modify SPEs in order to improve analyte detection in clinical, food and environmental fields (Bahadir & Sezgintürk, 2015). These advancement places SPEs as leads to in the realization of POCT. However, there are still some drawbacks with regards to cost of electrode, electrode complexity and inactivation, and stability of electrode modifiers; thus, it is important to find low-cost electrode materials that allows for selective simultaneous analysis.

Among the different types of conductive polymers, the polythiophene-derived macromolecule species poly(3,4-ethylenedioxythiophene) (PEDOT) is known to be the best in terms of conductivity, stability and processability (Elschner et al., 2010; Terasawa & Asaka, 2016). Also, colloidal dispersions of PEDOT can be readily made through the addition of poly(4-styrenesulfonate) (PSS) to form the doped compound PEDOT:PSS. This doped version of the polymer has excellent conductivity and exhibits good mechanical properties (Shahinpoor & Kim, 2004); thus, it has been applied to the development of various devices and sensors (Hallett & Welton, 2011; Moczko et al., 2012; Sheng et al., 2015).

Room temperature ionic liquids (ILs) are organic/inorganic salts that are liquid at room temperature and are usually considered to be 'green solvents'. They are known to have good chemical stability, high ionic conductivity, negligible vapour pressure, low flammability and has been used in many technological fields (Kanyong, et al., 2016a). Because of the high affinity of ILs with conductive polymers and their ability of supramolecular ordering, ILs were used as a dopant in the conductive polymer PEDOT:PSS to enhance the charge transfer rate of PEDOT:PSS for catechol. Consequently, different percentages of the ionic liquid, 1-ethyl-3-methylimidazolium tetrafluoroborate ([EMIM][BF_4]) were prepared in PEDOT:PSS and used to modify working area of a screen-printed carbon electrode (SPCE) and dried at 40 ºC for about 1 hr. The specific advantages of screen-printed sensors and the synergistic effect of PEDOT:PSS and [EMIM][BF_4] are assembled to fabricate a low-cost, disposable and simple sensor for the analysis of catechol in natural water samples. Catechol is a phenolic compound listed as a priority pollutant (European Parliament and Council, 2008; "UNITED STATES ENVIRONMENTAL PROTECTION AGENCY," 2012) because it has a poor biodegradability and is extremely toxic on human health and the

ecosystem (Nambiar et al., 2013; Palanisamy et al., 2014). Currently, the analysis of catechol is limited by complex, time-consuming and laborious tools like mass spectrometry, high-performance liquid chromatography and electrochemiluminescence (Govindhan et al., 2015; Nagaraja et al., 2001; Pistonesi et al., 2006; Sun et al., 2000). Owing to the electroactive nature of catechol, application of electrochemical techniques, especially at modified electrodes offers a simple, sensitive and rapid analytical alternative (Govindhan et al., 2015; Kanyong, et al., 2016; Kanyong, Rawlinson, et al., 2016c).

Subsequently, a nanocomposite of graphene nanoplatelets (GNPs) solubilized in Nafion (Naf) was used to develop a sensor for the single and simultaneous analysis of relevant clinical markers; dopamine and *N*-acetyl-*p*-aminophenol in urine samples.

Details of the fabrication, characterization and application of the sensors are described and discussed.

3.1.3 Experimental

3.1.3.1 Apparatus and reagents

Electrochemical experiments were conducted using PGSTAT204 Autolab Potentiostat/ Galvanostat/EIS FRA32M Module (Metrohm-Autolab, The Netherlands) with Nova 2.1 Software for data acquisition and experimental control. Electrochemical impedance spectroscopy in 5.0 mM potassium hexacyanoferrate ($[Fe(CN)_6]^{3-}/[Fe(CN)_6]^{4-}$) was carried out at open circuit within the frequency range of 100 kHz - 0.1 Hz at an applied potential of 0.25 V. Under the optimized conditions, unless otherwise stated, differential pulse voltammetry (DPV) was recorded with pulse amplitude, pulse time, voltage step time, voltage step and scan rate of 50 mV, 50 ms, 500 ms, 5 mV, and 50

mV/s, respectively. The disposable screen-printed carbon electrodes (Ref DS 410) utilized in the sensor design have a carbon working electrode, carbon counter electrode and silver reference electrode and were purchased from DropSens, Spain. Scanning electron microscopy (SEM) was performed by JEOL JSM-610PLUS/~LA SEM (JEOL Ltd, Japan). Raman spectrum was obtained with a LabRAM 300 system (HORIBA Scientific, UK) using He-Ne (632.8 nm) laser.

Poly(3,4-ethylenedioxythiophene) (PEDOT): poly(4-styrenesulfonate) (PSS), 1-ethyl-3-methylimidazolium tetrafluoroborate ([EMIM][BF_4]), graphene nanoplatelets were purchased from the US Research Nanomaterials, Inc, Houston, Texas, Nafion, potassium hexacyanoferrate ($[Fe(CN)_6]^{3-}$/$[Fe(CN)_6]^{4-}$), hydrogen peroxide (H_2O_2) (30 % (w/w) in H_2O), phosphate buffered saline (PBS) tablets, dopamine hydrochloride, *N*-acetyl-*p*-aminophenol and catechol were purchased from Sigma-Aldrich, USA. All other chemicals were of analytical grade and used without further purification. Pooled normal human urine samples were purchased from Innovative Research, USA.

3.1.3.2 Fabrication of GNPs-Naf/SPE

Firstly, graphene nanoplatelets (GNPs) powder (0.5 mg) was dispersed in ethanol/water (3:1 v/v) solution. Thereafter 10.0 µL of Nafion (5 wt% solution in a mixture of water and ethanol) was added to the GNPs slurry, sonicated for 10 min and stirred on VWR® Rocking Platform shaker for 2hr at room temperature. The working area (12.57 mm^2) of bare screen-printed electrode (SPE) was then covered with 5.0 µL of GNPs/Naf nanocomposite and allowed to dry at 40 ºC for 1hr to form GNPs-Naf/SPE. Prior to use, the surface the GNPs-Naf/SPE was thoroughly rinsed with distilled H_2O to remove any loosely bound nanocomposite materials. Once prepared, the sensors were stored in

room temperature conditions. The fabrication process of the GNPs-Naf/SPCE is shown in Figure 3.1.

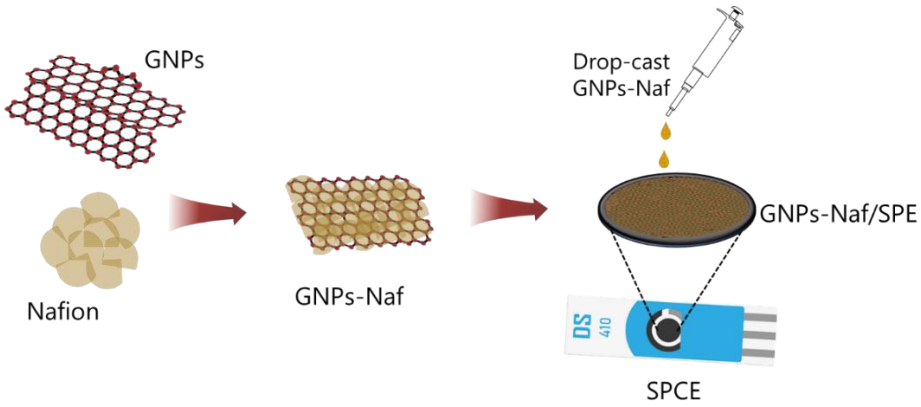

Figure 3. 1 Fabrication of the GNPs/Naf/SPCE

3.1.3.3 Fabrication of PEDOT:PSS/20%IL/SPCE

The bare Screen-Printed Carbon Electrode (SPCE) was modified by drop-coating 2.0 µL each of PEDOT:PSS and EMIM][BF_4], and dried at 40 ºC for 1hr to form PEDOT:PSS/SPCE and IL/SPCE, respectively. Difference percentages of IL (v/v) (1.0, 2.0, 5.0, 10.0, 20.0, 30.0, 50.0 %) in PEDOT:PSS were also prepared and 2.0 µL of the composite drop-coated on the SPCE and allowed to dry as previously described. The fabrication process is illustrated in Figure 3.2. The surfaces of all the modified SPCEs were thoroughly rinsed in PBS to remove any unbound species. Once prepared, the sensors were stored at room temperature conditions.

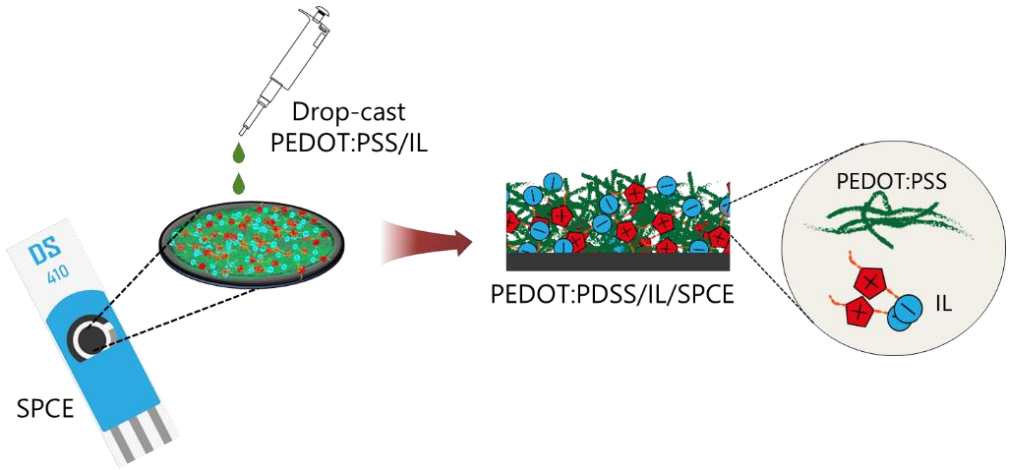

Figure 3. 2 Fabrication of the PEDOT:PSS/20%IL/SPCE sensor.

3.1.3.4 Sessile contact angle measurement

The contact angle measurements were carried out by the sessile drop technique; a water droplet was placed onto a flat surface of the bare SPCE and PEDOT:PSS/20%IL/SPCE, and the contact angle of the droplet with the surface measured. Reported values are the average contact angle (right and left) of 10 droplets. During the measurement time (~50 s), no change in contact angle was observed. A variation of 5º is generally considered to be sufficient to differentiate materials (Kanyong, et al., 2016c).

3.1.4 Results and discussion

3.1.4.1 Optimization of the percentage of IL in PEDOT:PSS/IL composite

To ascertain the amount of IL in PEDOT:PSS required for optimum electrocatalytic response of the modified SPCE, composites with different percentages of IL (1.0, 2.0, 5.0, 10.0 20.0. 40.0 and 50.0%) in PEDOT:PSS were formulated and used to fabricate PEDOT:PSS/IL/SPCE sensors. Thereafter, the voltammetric responses from the PEDOT:PSS/IL/SPCE were measured in PBS (pH 7.4) containing 5.0 mM

hexacyanoferrate ($[Fe(CN)_6]^{3-}/[Fe(CN)_6]^{4-}$) and 0.1 M KCl. It should be mentioned that, similar procedure was used to fabricate PEDOT:PSS/SPCE and IL/SPCE. Figure 3.3A shows cyclic voltammograms recorded at SPCEs modified with different percentages of IL in PEDOT:PSS in 5.0 mM ($[Fe(CN)_6]^{3-}/[Fe(CN)_6]^{4-}$) in PBS (pH 7.4) while Figure 3.3B shows a plot of the peak currents vs. the percentage of IL in the composites formulated. It can be seen in Figure 3.3A and 1B that the voltammetric peaks increased gradually from 1.0% IL up to 20.0% IL. Subsequent increases in the percentage of IL did not show any increase in the voltammetric response of the modified sensors. Consequently, 20.0% IL was chosen as the optimum amount of IL required in PEDOT:PSS/IL composite to give the highest conductivity. Figure 3.3C shows a comparison of voltammograms recorded using the bare SPCE, IL/SPCE, PEDOT:PSS/SPCE and PEDOT:PSS/20%IL/SPCE in 5.0 mM ($[Fe(CN)_6]^{3-}/[Fe(CN)_6]^{4-}$) solution. In comparison to both PEDOT:PSS/SPCE and IL/SPCE, the I_{pa} and I_{pc} of the PEDOT:PSS/20% IL/SPCE was more enhanced and prominent; this enhancement in electrocatalytic properties is attributed to the synergistic effect of the PEDOT:PSS and IL. Consequently, the PEDOT:PSS/20%IL/SPCE was used throughout the remainder for this study.

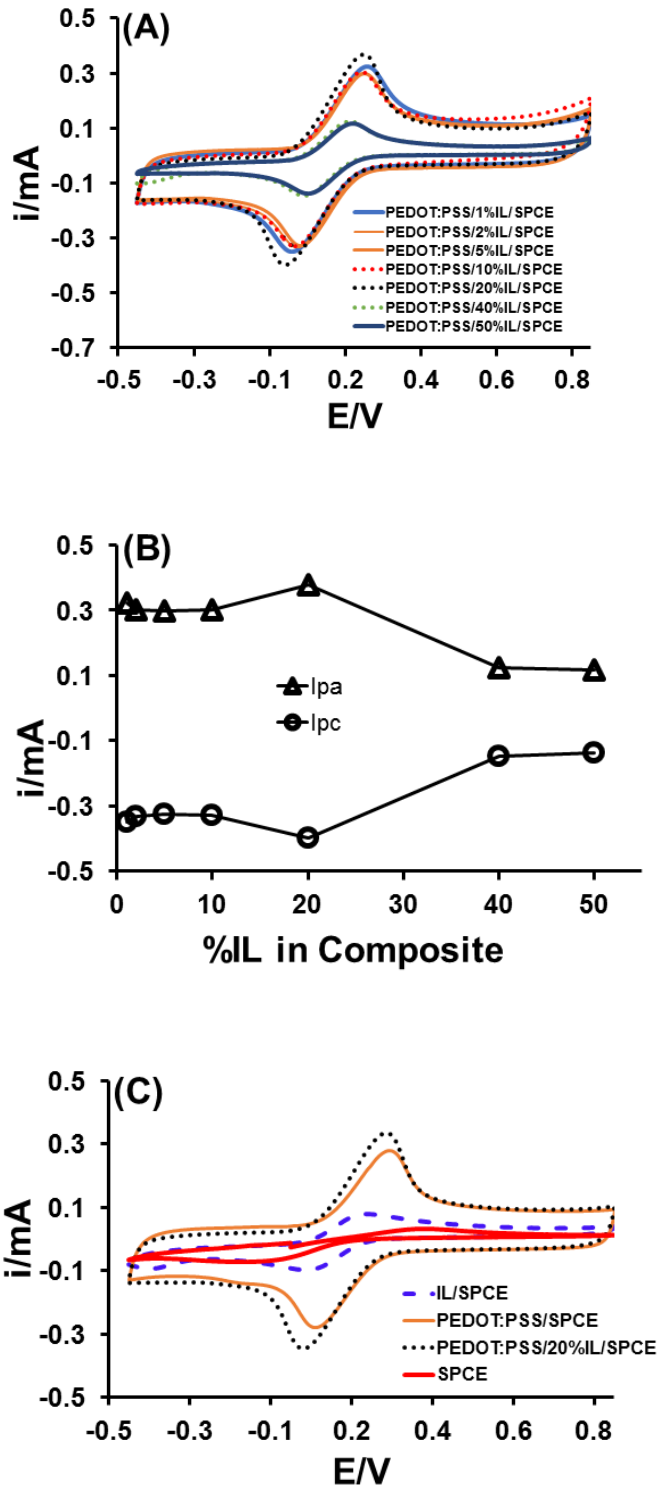

Figure 3. 3 Cyclic voltammograms of different IL% in PEDOT:PSS
(a) Cyclic voltammograms of PEDOT:PSS/IL/SPCE prepared with different amounts of IL (1.0, 2.0, 5.0, 10.0 20.0. 40.0 and 50%) in PEDOT:PSS/IL composite; (b) Plot of anodic (I_{pa}) and cathodic (I_{pc}) peak currents for $[Fe(CN)_6]^{3-}/[Fe(CN)_6]^{4-}$ vs. amount of IL (%) in PEDOT:PSS/IL composite; (c) CVs of SPCE, IL/SPCE, PEDOT:PSS/SPCE and PEDOT:PSS/20%IL/SPCE. All CVs were recorded in 5.0 mM hexacyanoferrate ($[Fe(CN)_6]^{3-}/[Fe(CN)_6]^{4-}$) in PBS (pH 7.4) containing 0.1 M KCl.

3.1.4.2 Characterisation of SPCE and PEDOT:PSS/20%IL/SPCE

3.1.4.2.1 ***Cyclic voltammetry***

Figure 3.4A shows a comparison of cyclic voltammograms recorded at the bare SPCE and PEDOT:PSS/20%IL/SPCE in PBS (pH 7.4) containing 5.0 mM $[Fe(CN)_6]^{3-}/[Fe(CN)_6]^{4-}$ and 0.1 M KCl at a scan rate of 100 $mV.s^{-1}$. As expected, when compared with what occurred on the bare SPCE (curve a), the PEDOT:PSS/20%IL/SPCE (curve b) exhibited a characteristic increase of both the anodic and cathodic peak currents for $[Fe(CN)_6]^{3-}/[Fe(CN)_6]^{4-}$ redox couple, thus, confirming the successful modification of the SPCE with the composite. Higher peak currents and a smaller peak-to-peak potential separation (ΔE_p) were observed at the PEDOT:PSS/20%IL/SPCE (I_{pa} = 336.8 µA, I_{pc} = 345.9 µA; ΔE_p = 202.6 mV) when compared with the bare SPCE (I_{pa} = 32.4 µA, I_{pc} = 69.9 µA; ΔE_p = 346.6 mV). This is attributed to the higher electrocatalytic properties of the PEDOT:PSS/IL composite which allowed the increase of the total active area of the modified electrode. The presence of the PEDOT:PSS/IL composite produced a negative shift in the anodic potential and a positive shift in the cathodic potential, giving rise to a smaller peak-to-peak separation (ΔE_p = 202.6 mV). This more than ten-fold increase in the anodic peak current and five-fold increase in the cathodic peak current for $[Fe(CN)_6]^{3-}/[Fe(CN)_6]^{4-}$ can be attributed to the electrocatalytic effect of the PEDOT:PSS/IL composite.

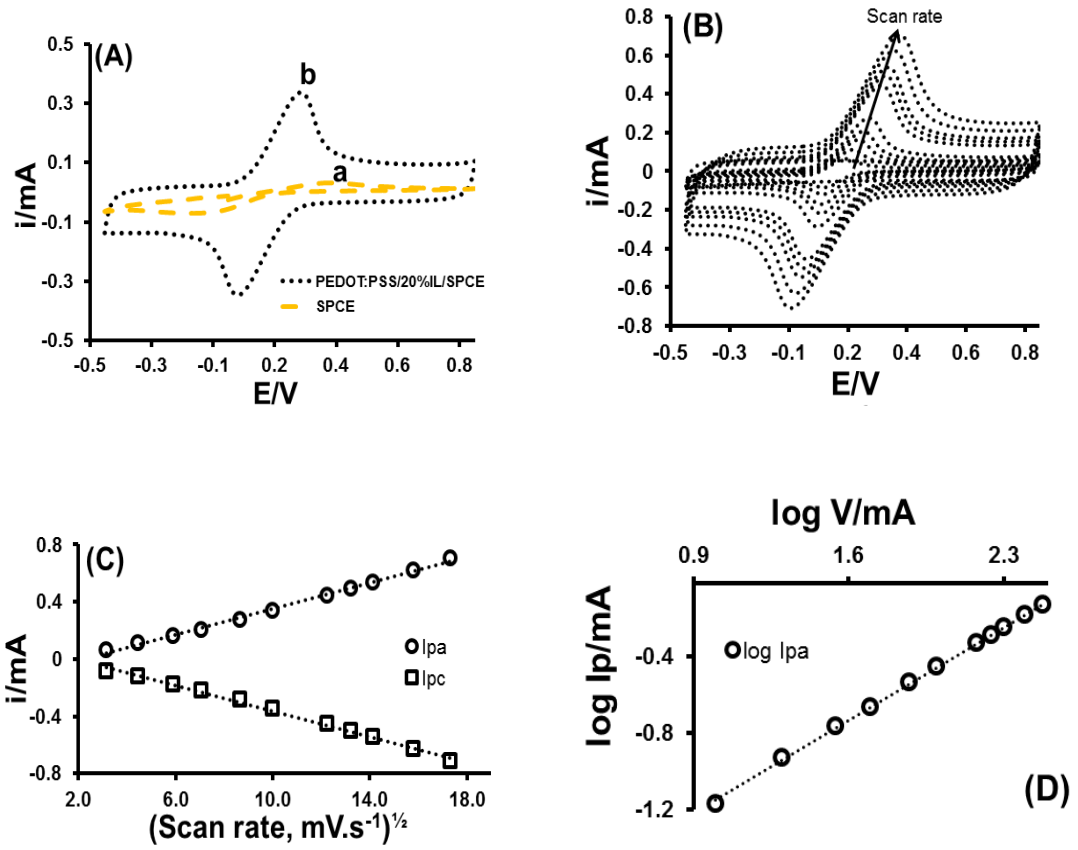

Figure 3. 4 Voltammetric responses of 20% IL in PEDOT:PSS
(A) Cyclic voltammograms recorded using SPCE (curve a) and PEDOT:PSS/20%IL/SPCE (curve b) at 100 $mV.s^{-1}$ scan rate; (B) CVs recorded using PEDOT:PSS/20%IL/SPCE at 10, 20, 35, 50, 75, 100, 150, 175, 200, 250 and 300 $mV.s^{-1}$ scan rates; (C) Peak current vs. square root of scan rate; (D) log I_{pa} vs. log *V*. All CVs were recorded in 5.0 mM hexacyanoferrate ($[Fe(CN)_6]^{3-}/[Fe(CN)^6]^{4-}$) in PBS (pH 7.4) containing 0.1 M KCl.

The effect of scan rate (v) on the voltammetric behaviour of the PEDOT:PSS/20%IL/SPCE was also examined by CV (Figure 3.4B). At the scan rates investigated (10.0 to 300.0 mV/s), a plot of the square root of the scan rate (*v*) vs. the anodic (I_{pa}) and cathodic (I_{pc}) peak currents exhibited a linear relationship (Figure 3.4C), which is typical of a diffusion-controlled process (Gosser, 1993; Morrin et al., 2003). A linear relationship was also observed when both log I_{pa} and log I_{pc} were plotted against log *v* (Figure 3.4D) with slope values of 0.697 and 0.637, respectively. These

slope values are comparable with the theoretically expected value of 0.5 for purely diffusion controlled currents (Gosser, 1993); thus, confirming that the electrochemical process is diffusion-controlled and that the surface of the modified SPCE was not fouled.

3.1.4.2.2 ***Electrochemical Impedance Spectroscopy***

The interface properties of the bare SPCE and PEDOT:PSS/20%IL/SPCE were further characterised by Faradaic electrochemical impedance spectroscopy (EIS) in the presence of 5.0 mM hexacyanoferrate $[Fe(CN)_6]^{3-}/[Fe(CN)^6]^{4-}$ (Figure 3.5). The impedance spectrum associated with the bare SPCE (curve a) consists of a semicircle part in the high frequency region and a linear part in the low frequency region, corresponding to electron transfer and diffusion processes, respectively. The diameter of the semicircle represents the charge-transfer resistance (R_{CT}) at the surface of the electrode (Kanyong, et al., 2016d). At the bare SPCE (curve a), a semicircle with a larger diameter was obtained. However, on the PEDOT:PSS/20%IL/SPCE (curve b), the diameter of the semicircle was negligible. This significant change in R_{CT} value is attributed to the enhanced charge transfer rate across the modified interface and the large surface area provided by the PEDOT:PSS/IL composite. This impedance results are in agreement with the results obtained from the cyclic voltammetric measurements; thus, confirming the successful modification of the SPCE.

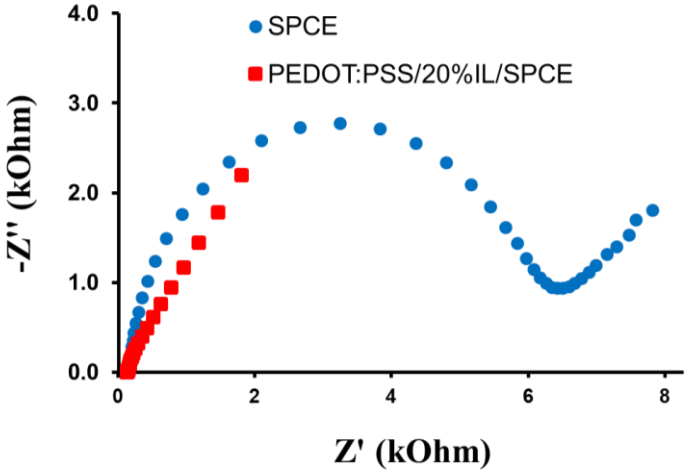

Figure 3. 5 Nyquist plots observed for EIS at bare and modified SPCE
Nyquist plots for the bare SPCE (curve a) and PEDOT:PSS/20%IL/SPCE (red curve) in PBS (pH 7.4) containing 5.0 mM $[Fe(CN)_6]^{3-}/[Fe(CN)_6]^{4-}$ and 0.1 M KCl.

3.1.4.3 Scanning Electron Microscopy and profilometry

Additionally, the morphological features of both the bare SPCE and PEDOT:PSS/20%IL/SPCE were characterised by scanning electron microscopy (SEM) as well as profilometry. Figure 3.6A and 3.6B show the view of the SPCE and PEDOT:PSS/20%IL/SPCE, respectively. The morphology of the bare SPCE is typical for graphite materials with grains that are stacked in flakes. As shown in Figure 3.6B, a uniform film was formed on the electrode surface, indicating successful deposition of the PEDOT:PSS/IL composite. When compared with the bare SPCE (Figure 3.6A), the PEDOT:PSS/20%IL/SPCE (Figure 3.6B) showed a highly porous morphology, consisting of several interconnected ginger-like dots; this greatly increased the surface area of the modified electrode. Profilometry measurements revealed that the average surface roughness of the SPCE (Figure 3.6C) and PEDOT:PSS/20%IL/SPCE (Figure 3.6D) were 1.44 µm and 6.29 µm, respectively; which is in agreement with the SEM images.

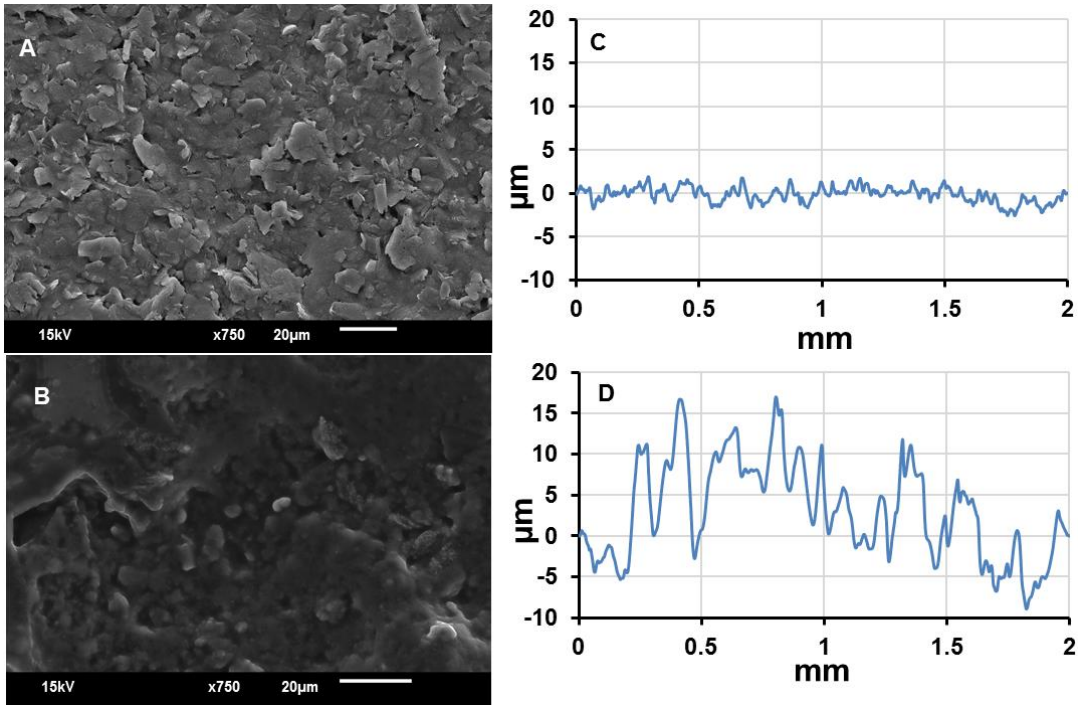

Figure 3. 6 Scanning electron micrographs and surface roughness for PEDOT:PSS/20%IL modified electrodes.
SEM images of SPCE (A) and PEDOT:PSS/20%IL/SPCE (B). C and D correspond to the surface roughness of SPCE and PEDOT:PSS/20%IL D respectively) obtained from profilometry.

3.1.4.4 Sessile contact angle measurements

In addition to these, the measurement of water contact angle for the PEDOT:PSS/IL thin film on the surface of the SPCE was performed. The contact angle of water at the surface of the bare SPCE was found to be ~74.3º. However, it decreased after coating the SPCE with PEDOT:PSS/IL composite to ~50.8º. This increase in the hydrophilicity of the coated electrode means that the properties of the PEDOT:PSS/IL composite can be manipulated in buffer solution; thus, making it a suitable surface for the immobilisation of biomolecules. This is of considerable relevance for a variety of applications including sensors for biomedical applications as well as studying biointerfaces (Kanyong, et al., 2016c).

3.1.4.5 Electrochemical characterization of SPE and GNPs-Naf/SPE

The surface morphological features of the SPE and GNPs-Naf/SPE were examined by SEM and Raman spectroscopy. Figure 3.7A,B,C show the view of the SPE and GNPs-Naf/SPE, respectively. The morphology of the SPE is typical for graphite materials with grains that are stacked in flakes (Figure 3.7A). The heterogenous distribution of graphene nanoplatelets sheets of submicron dimension is clearly visible throughout the GNPs/Naf/SPE with wrinkles on the surface (Figure 3.7B) and well-formed architecture of large open area porous surface structure (Figure 3.7C). Further characterization of the GNPs/Naf/SPE (Figure 3.7D) show D, G and 2D peaks, which are typical features of thick graphene stacks (Cançado et al., 2008; Ferrari, 2007).

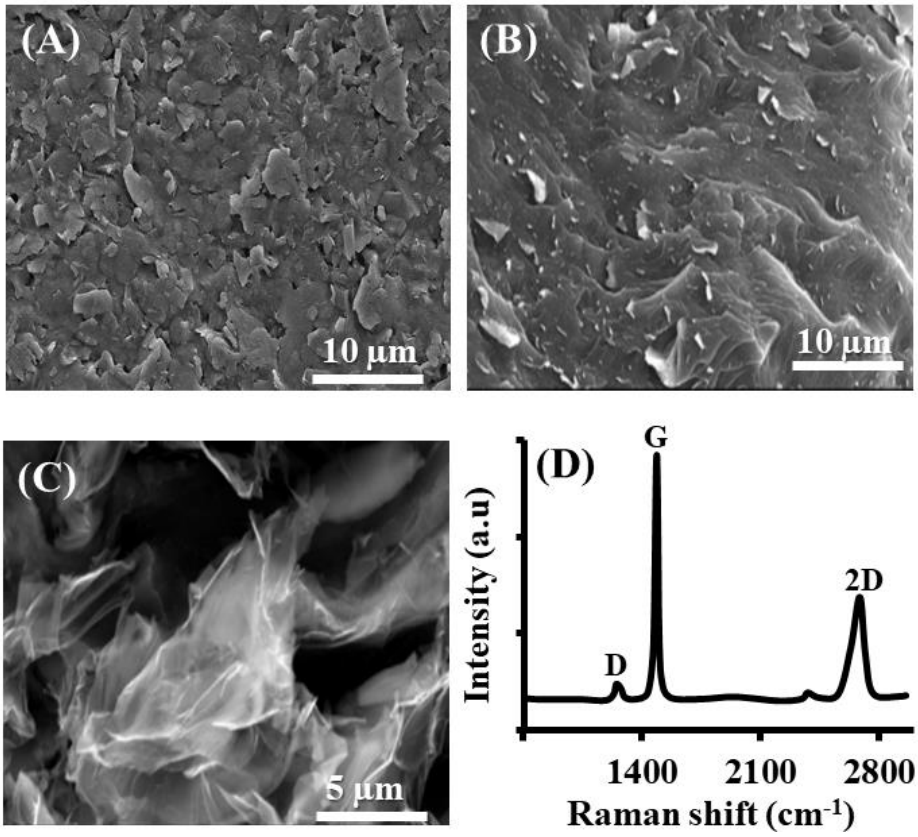

Figure 3. 7Scanning electron micrographs and Raman spectrum of bare and GNPs-Naf modified electrodes
(A) bare SPE; (B) top and (C) cross-section of GNPs-Naf/SPE, and (D) Raman spectrum of GNPs-Naf/SPE measured using 632.8 nm laser.

The interface of the SPE and GNPs-Naf/SPE were further characterized by Faradaic electrochemical impedance spectroscopy (EIS) in the presence of 5.0 mM $[Fe(CN)_6]^{3-}/[Fe(CN)_6]^{4-}$. Figure 3.8 illustrates experimental Nyquist spectra for both the bare SPE and GNPs-Naf/SPE. The impedance spectrum associated with the bare SPE (curve a, Figure 3.8) consists of a semicircle in the high-frequency region and a linear part in the low-frequency region, corresponding transfer and diffusion processes, respectively. The diameter of the semicircle represents the charge-transfer resistance (R_{ct}) at the electrode (Kanyong, et al., 2016c; Suni, 2008). In comparison to what was observed at the GNPs-Naf/SPE (curve b, Figure 3.8), the diameter of the semicircle of the bare SPE was larger. This shows that the charge-transfer rate increased upon employing the GNPs, which facilitated the $Fe(CN)_6]^{3-}/[Fe(CN)_6]^{4-}$ redox process.

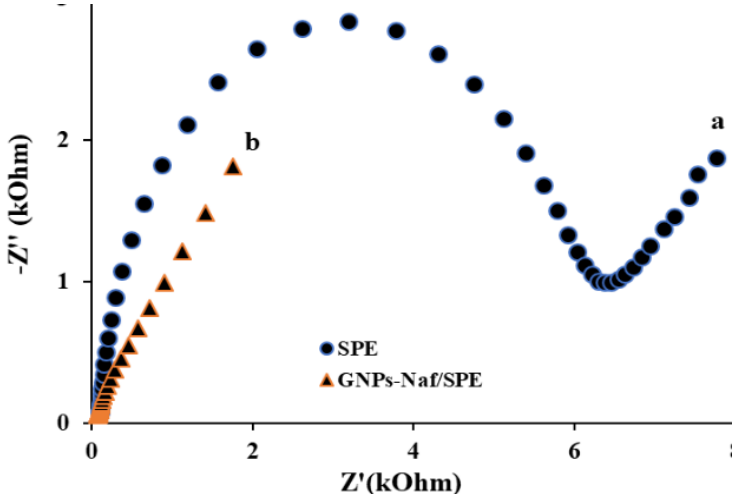

Figure 3. 8 Nyquist plots for EIS at bare and GNPs-Naf modified electrodes.
Electrochemical impedance spectroscopy at bare SPE (curve a) and GNPs-Naf/SPE (curve b) in PBS (pH 7.4) containing 5.0 mM $[Fe(CN)_6]^{3-}/[Fe(CN)_6]^{4-}$ and 0.1 M KCl.

The electrocatalytic behaviour of the sensors was characterized by cyclic voltammetry. Figure 3.9A is a comparison of cyclic voltammograms recorded at the bare SPE and GNPs-Naf/SPE in PBS (pH 7.4) containing 5.0 mM $Fe(CN)_6]^{3-}$/$[Fe(CN)_6]^{4-}$ and 0.1 M KCl at 100 $mV.s^{-1}$ scan rate. When compared to what occurred on the bare SPE (curve a, insert of Figure 3.9A), the GNPs-Naf/SPE (curve b, Figure 3.9A) exhibited a characteristic increase of both the anodic and cathodic peak currents for the $Fe(CN)_6]^{3-}$/$[Fe(CN)_6]^{4-}$ redox couple, thus, confirming the successful modification of the SPE with the GNPs composite. Higher peak currents and smaller peak-to-peak potential separation (ΔE_p) were observed at the GNPs-Naf/SPE (I_{pa} = 1.35 mA, I_{pc} = 1.38 mA; ΔE_p = 200 mV) when compared with the bare SPE (I_{pa} = 0.03 mA, I_{pc} = 0.07 mA; ΔE_p = 276 mV). The more than 40-fold increase in the anodic peak current and 20-fold increase in the cathodic peak for $Fe(CN)_6]^{3-}$/$[Fe(CN)_6]^{4-}$ redox couple can be attributed to the higher electrocatalytic properties of the GNPs composite which led to an enhancement of the total electroactive area of the GNPs-Naf/SPE (Krampa et al., 2017a). The presence of the GNPs also produced a negative and a positive shift in the anodic and cathodic potentials, respectively; thus, giving rise to a smaller peak-to-peak separation (ΔE_p = 200 mV). This cyclic voltammetry data agrees with the results obtained from faradaic impedance analysis; thereby confirming the successful modification of the SPE with graphene nanoplatelets.

The effect of scan rate (ν) on the voltammetric behaviour of GNPs-Naf/SPE towards $Fe(CN)_6]^{3-}$/$[Fe(CN)_6]^{4-}$ redox couple was examined. At the scan rates investigated (Figure 3.9B), a plot of the square root of the scan rate (v) vs. the anodic (I_{pa}) and cathodic (I_{pc}) peak currents exhibited a linear relationship (insert of Figure 3.9B), which suggests a behaviour consistent with surface confined voltammetry and corresponding 'thin-layer' type voltammetry (Kanyong, et al., 2016c). The slight deviations from

linearity may reflect on the transport processes to and from the electrode resulting from the porosity of the GNPs composite films (Kanyong, et al., 2016c; Streeter et al., 2008). A linear relationship was also observed when the absolute values of log I_{pa} and log I_{pc} were plotted against log *v* (not shown) with slope values of 0.50 and 0.69, respectively. These slope values are comparable with the theoretically expected value of 0.5 for purely diffusion-controlled currents (Gosser, 1993), which suggests that the electrochemical process is diffusion-controlled and that the surface of the modified SPE is not fouled.

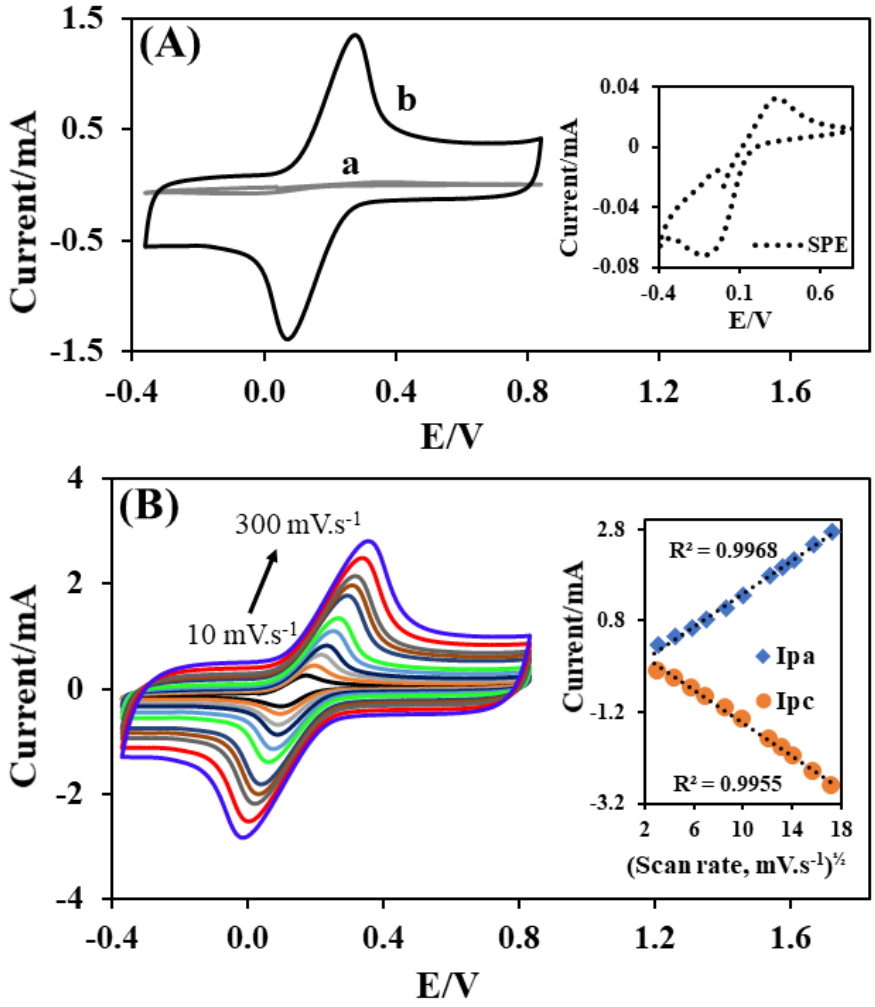

Figure 3. 9 Electrochemical characterization of the GNPs-Naf/SPE sensor
(A) Cyclic voltammograms recorded using bare SPE (curve a) and GNPs-Naf/SPE sensor (curve b) at 100 $mV \cdot s^{-1}$ scan rate; insert is CV of bare SPE; (B) CVs recorded using GNPs-Naf/SPE at 10, 20, 35, 50, 75, 100, 150, 175, 200, 250, and 300 $mV \cdot s^{-1}$ scan rates; insert is peak current vs. square root of scan rate. All CVs were recorded in 5.0 mM $[Fe(CN)_6]^{3-}$/$[Fe(CN)^6]^{4-}$ in PBS (pH 7.4) containing 0.1 M KCl.

3.1.4.6 Application of PEDOT:PSS/20%IL/SPCE to catechol analysis

3.1.4.6.1 ***Cyclic voltammetry***

Figure 3.10A shows cyclic voltammograms for catechol at the bare SPCE (curve a) and PEDOT:PSS/20%IL/SPCE (curve b). During the forward scan, two prominent oxidation peaks at 0.27 V (a1) and 0.50 V (a2) were observed on the PEDOT:PSS/20%IL/SPCE. The anodic peak (a1) can be attributed to the formation of *o*-semiquinone intermediates while the second peak (a2) pertains to the oxidation of the catechol to *o*-quinone (Yang et al., 2014) . Previous studies identified the formation of the *o*-semiquinone and found the redox potential of catechol/*o*-semiquinone pair to be 0.53 V (Yang et al., 2014), which is in agreement with this finding. On the reverse scans, a cathodic peak (c1 = 0.01 V) on PEDOT:PSS/20%IL/SPCE was observed. This cathodic peak (c1) corresponds to the reduction of the *o*-quinone (Nematollahi & Dehdashtian, 2008). A peak current ratio (I_{pc1}/I_{pa2}) for the repetitive recycling of potential was found to be near unity, which is a criterion for the stability of *o*-quinone produced at the surface of electrode (Khalafi et al., 2013; Nematollahi et al., 2004). These findings agree with the oxidation of catechol at similar surfaces (Khalafi et al., 2013; Nematollahi & Dehdashtian, 2008; Nematollahi et al., 2009). The two oxidation peaks (a1 and a2) and cathodic peak (c1) broadened and shifted to more positive potentials (a1 = 0.44 V, a2 = 0.63 V, c1 = 0.04 V) with a significant decrease in the peak currents at the bare SPCE. In comparison to what occurred at the bare SPCE, the PEDOT:PSS/20%IL/SPCE exhibited a characteristic increase of both the anodic and cathodic peak currents for catechol. The enhanced prominence and the shifts in peak potentials to less positive values, and the more than 4-fold increase in peak currents are attributed to the electrocatalytic properties of the PEDOT:PSS/IL composite.

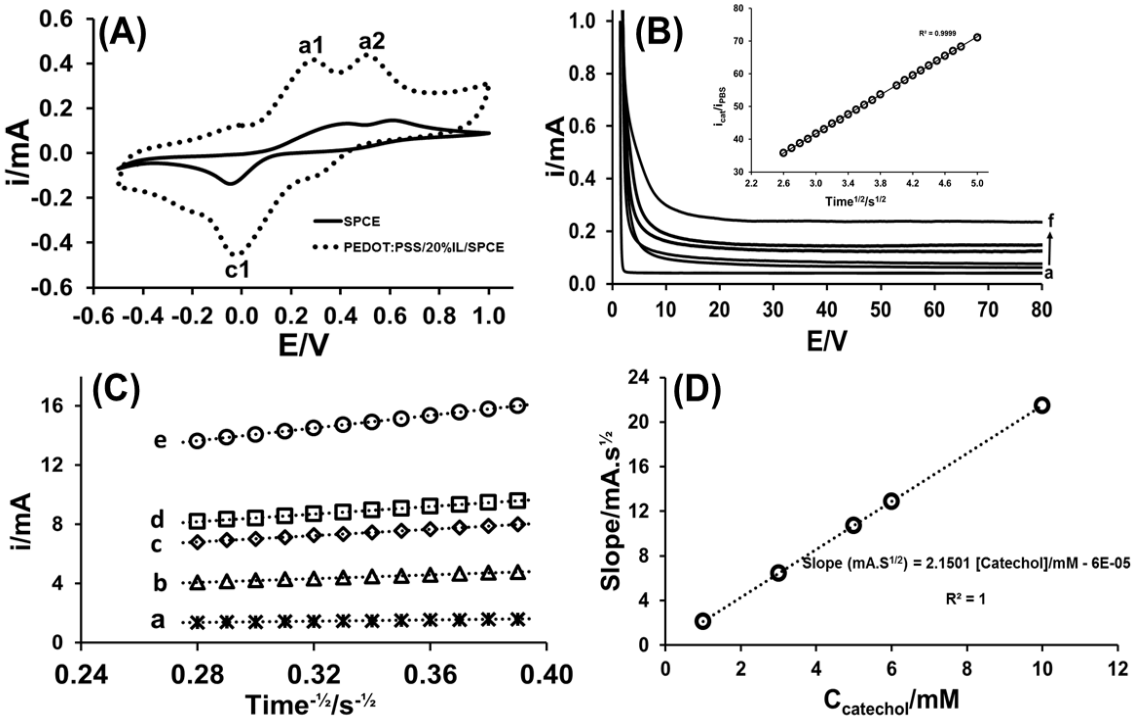

Figure 3. 10 Electrochemical detection of catechol at PEDOT:PSS/20%IL/SPCE (A) Cyclic voltammograms recorded using the bare SPCE and PEDOT:PSS/20%IL/SPCE in 5.0 mM catechol solution in PBS (pH 7.4) at a scan rate of 100 $mV.s^{-1}$;(B) Chronoamperograms obtained at PEDOT:PSS/20%IL/SPCE in the presence of (a) 0; (b) 1.0; (c) 3.0; (d) 5.0; (e) 6.0 and (f) 10.0 mM catechol in PBS (pH 7.4). Insert; i_{cat}/i_{PBS} vs. $t^{½}$ plot derived from chronoamperomeric data for PBS (a) and 1.0 mM catechol (b); (C) Linear segments of plot i vs. $t^{-½}$ for (a) 1.0; (b) 2.0; (c) 5.0; (d) 6.0 and (e) 10.0 mM catechol and; (D) plot of the slopes from graph C vs. concentration of catechol.

The effect of scan rate on the voltammetric behaviour of catechol at the PEDOT:PSS/20%IL/SPCE was examined by CV. The oxidation and reduction peak currents increased linearly with increasing scan rate; thus, suggesting a behaviour consistent with surface-confined voltammetry and corresponding 'thin-layer' type voltammetry (Kanyong, et al., 2016c).

To further evaluate the electrochemical behaviour of the PEDOT:PSS/20%IL/SPCE, the influence of scan rate on both the anodic peak potentials and cathodic peak potential of catechol were analysed. With increase in scan rate, the anodic peak potential shifted

towards a positive value and a linear relationship was observed in the range of 10 to 300 mV.s^{-1}. The equation of this behaviour for E_{pa2} can be expressed as:

$$Epa2\ (V) = 0.183 \log v\ (V.s^{-1}) + 0.709;\ R^2 = 0.9995 \qquad (15)$$

According to Laviron's expression for an electrochemical process [34, 35], E_p is governed by:

$$Ep = E^{0\prime} + \frac{(2.303RT)}{(\propto n' F)} log \frac{(RTk^0)}{(\alpha\, n' F)} + \frac{(2.303RT)}{(\propto n' F)} \log v \qquad (16)$$

where *v* is the scan rate, *n′ is* the number of electrons transferred before the rate-determining step, α is the transfer coefficient, $E^{0\prime}$ is the formal standard redox potential and k^0 is the standard heterogeneous rate constant of the reaction, and the other symbols have their usual meaning. The value of $\alpha n'$ can be calculated using the slope of E_{pa2} vs log *v* plot (here slope = 0.183). Taking *R* = 8.314J.K^{-1}.mol^{-1}, *T* = 298 K, and F = 96480 C.mol^{-1}, the value of $\alpha n'$ was calculated to be 0.323.

According to Bard and Faulkner (Bard et al., 1980),

$$\alpha = \frac{(47.7)}{(Ep - Ep/_2)}\ mV \qquad (17)$$

where (Ep-Ep)/2 is the potential at which the current is at half its peak value. From this, the value of α was calculated to be 0.152. Consequently, the number of electrons (*n*) involved in the electrochemical process was calculated to be ~2.0; which indicates that the reaction is a two-electron transfer process.

3.1.4.6.2 ***Chronoamperometry***

The catalytic rate constant (K_{cat}) and diffusion coefficient (D) of catechol for PEDOT:PSS/20%IL/SPCE were estimated by chronoamperometry. Chronoamperometric measurements were carried out in PBS (pH 7.4) containing various concentrations of catechol (1.0, 2.0, 5.0, 6.0 and 10.0 mM) at an applied potential of +0.5 V (Figure 3.10B). The catalytic rate constant K_{cat}, was calculated using the equation (Rotariu et al., 2010):

$$\left(\frac{i_{cat}}{i_{PBS}}\right) = \pi^{½}(K_{cat}.C.t)^{½} \qquad (18)$$

where i_{cat} and i_{BRB} are the currents obtained at the PEDOT:PSS/20%IL/SPCE for catechol and PBS solution, respectively, *C* is the concentration of catechol and *t* is time in seconds. The catalytic rate constant was calculated from the slope of the plot of i_{cat}/i_{PBS} vs. $t^{1/2}$ (insert of Figure 3.10B) for 1.0 mM catechol concentration. A value of ~6.99 × 10^4 $M^{-1}s^{-1}$ was calculated for the PEDOT:PSS/20%IL/SPCE, which is satisfactory for the analysis of catechol (Nematollahi et al., 2004).

The slope of the linear parts of *i* vs. $t^{-1/2}$ plots (Figure 3.10C) for the different concentrations of catechol (1.0, 2.0, 3.0, 5.0, 6.0 and 10 mM) were selected and used to construct the $i.t^{1/2}$ vs. $C_{catechol}$ plot (Figure 3.10D). The slope of $i.t^{-1/2}$ vs $C_{catechol}$ plot was used in conjunction with the Cottrel expression (Rotariu et al., 2010):

$$i = \left(\frac{nFAD^{½}C}{\pi^{½}t^{½}}\right) \qquad (19)$$

where *i* is current (in A), *n* is the number of electrons (here n = 2), *F* is Faraday's constant, *A* is the electrode are (*A* = 0.12566 cm^2), *C* is the concentration (1.0 x 10^{-6} $mol.cm^{-3}$) and *D* is the diffusion coefficient (in cm^2s^{-1}) and *t* is time (s)] to estimate the diffusion coefficient (D) for catechol and was calculated to be ~1.17 × 10^{-6} $cm^2.s^{-1}$.

3.1.4.6.3 ***Amperometry in stirred solution***

The amperometric response of catechol was measured in PBS (pH 7.4) on the PEDOT:PSS/20%IL/SPCE at constant potential of 0.5 V, which was the oxidation potential of catechol (a2) (Figure 3.11A). As shown in Figure 3.11, the amperometric current vs time (i-t) curve of catechol showed that the PEDOT:PSS/20%IL/SPCE had a rapid response to varying concentrations of catechol in stirred buffer solution. The establishment of well-defined steady-state current responses to catechol additions indicates that the sensor is sensitive. A linear range was recorded from 0.1 µM to 330.0 µM with a sensitivity of 18.2 mA.mM.cm^{-2} and a calculated limit of detection (based on 3× the baseline noise) of 23.7 µM; which are considered to be satisfactory for routine analysis of catechol in natural water samples (Khalafi et al., 2013; Nematollahi et al., 2004).

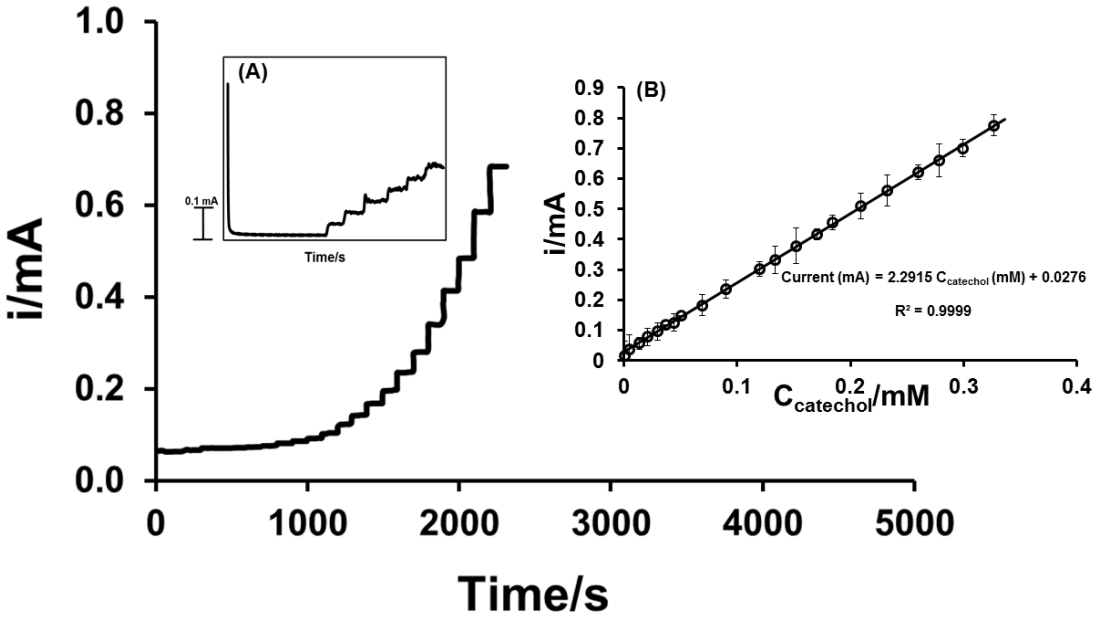

Figure 3. 11 Detection of catechol by amperometry in stirred solution
Amperometric responses of the PEDOT:PSS/20%IL/SPCE in stirred PBS (pH 7.4) at an applied potential of 0.5 V to varying concentrations of catechol from 0.1 µM to 330.0 µM; insert (A) zoom at the first 7 standard additions of catechol and (B) plot of steady state current vs catechol concentration.

3.1.4.7 Stability of PEDOT:PSS/20%IL/SPCE

The stability of the conducting polymer composite is crucial for any practical applications. In order to investigate the stability and durability of the electrocatalytic activity of the PEDOT:PSS/20%IL composite, several voltammograms were recorded using the PEDOT:PSS/20%IL/SPCE in 5.0 mM catechol solution. In general, unstable electrodes have unstable voltammograms. Figure 3.12, shows 40 repetitive voltammograms recorded for 5.0 mM catechol and their corresponding anodic ($I_{pa1,}$ I_{pa2}) and cathodic (I_{pc}) peak currents for selected cycles are shown in the insert of Figure 3.12. The standard deviation values for I_{pa1}, I_{pa2}, and I_{pc1} were found to be 1.84 %, 0.59 %, and 1.27 %, respectively. These standard deviation values indicate a highly reproducible electrode modification procedure.

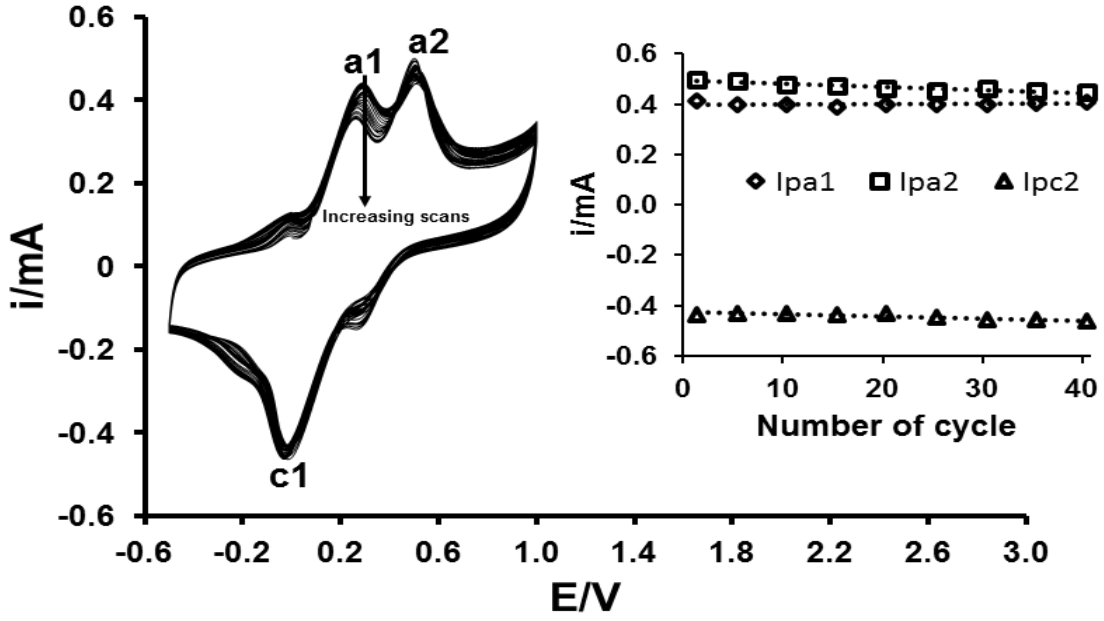

Figure 3. 12 Stability of PEDOT:PSS/20%IL/SPCE towards catechol
Repetitive cyclic voltammograms (40 scans) recorded at PEDOT:PSS/20%IL/SPCE; insert is peak current vs. cycle number. Voltammograms were recorded in 5.0 mM catechol in PBS (pH 7.4) containing 0.1 M KCl and at a scan rate of 100 $mV.s^{-1}$.

3.1.4.8 Analysis of natural water samples

To demonstrate the feasibility of the PEDOT:PSS/20%IL/SCPE sensor for routine analysis, the sensor was used to analyse natural water samples. Prior to this analysis, the water samples were analysed for the presence (or otherwise) of endogenous catechol; this analysis indicated that there is no detectable catechol in the water sampled. After verifying the absence of endogenous catechol in the water samples, amperometry, in conjunction with the method of standard additions, was employed to determine the recovery of catechol spiked into the water samples. The analytical performance data for three repeated measurements are summarised in Table 1. The recoveries were found to be well over 99.0% with coefficient of variations of 0.035 and 0.315. Clearly, the presence of interfering species in the water samples did not interfere with the analysis of the compound; thus, the sensor can be used for routine quantification of catechol in the natural water samples.

Table 3. 1 Recovery of spiked catechol from natural water samples

Spiked urine sample	**Amount Added (µM)**	**Amount Found (µM)**	**Recovery (%)**
River water (n=3)	20	19.94±0.04	99.7
Tap water (n=3)	20	19.81±0.6	99.1

3.1.4.9 Electrochemical behaviour of DA and APAP at SPE and GNPs-Naf/SPE

Cyclic voltammograms (CVs) were recorded for 0.5 mM each of DA and APAP at the bare SPE and GNPs-Naf/SPE in PBS (pH 7.4) at a scan rate of 100 $mV.s^{-1}$. A comparison of the CVs for DA and APAP at the SPE and GNPs-Naf/SPE is illustrated in Figure 3.13. A pair of well-defined, quasi-reversible anodic and cathodic peaks for DA was observed at 160.4 mV and 102.1 mV, respectively, on the GNPs-Naf/SPE. The anodic peak can be attributed to the oxidation of DA to dopamine-quinone while the cathodic peak can be attributed to the reduction of the dopamine-quinone back to DA (Kanyong, et al., 2016c; Loget et al., 2013). At the bare SPE, DA has an anodic peak and a broadened cathodic peak; which is an indication of a sluggish electron transfer process. This behaviour of DA at the bare SPE can be attributed to the conductivity of the SPE material and/or electrode fouling caused by the deposition of DA and its associated redox products on the electrode (Kanyong, et al., 2016c). The redox peaks shifted to more positive potentials with a marked decrease in the peak currents (I_{pa} = 2.5 mA; I_{pc} = 0.4 mA) at the bare SPE. A significantly enhanced peak currents (I_{pa} = 5.7 mA; I_{pc} = 1.5 mA) with peak-to-peak potential separation (ΔE_p) of 58.3 mV for DA was observed at the GNPs-Naf/SPE; which is considerably close to the 59.0 mV value expected for Nernstian one-electron reactions (Kanyong, et al., 2016c). Similar electrochemical behaviour of dopamine has been reported elsewhere (Kanyong, et al., 2016e, 2016a; Morrin et al., 2003). The smaller ΔE_p value suggests that the reversibility of DA at GNPs-Naf/SPE is remarkably improved and the enhanced peak currents also suggests an enhancement of the electron-transfer rate by the GNPs at the surface of the electrode.

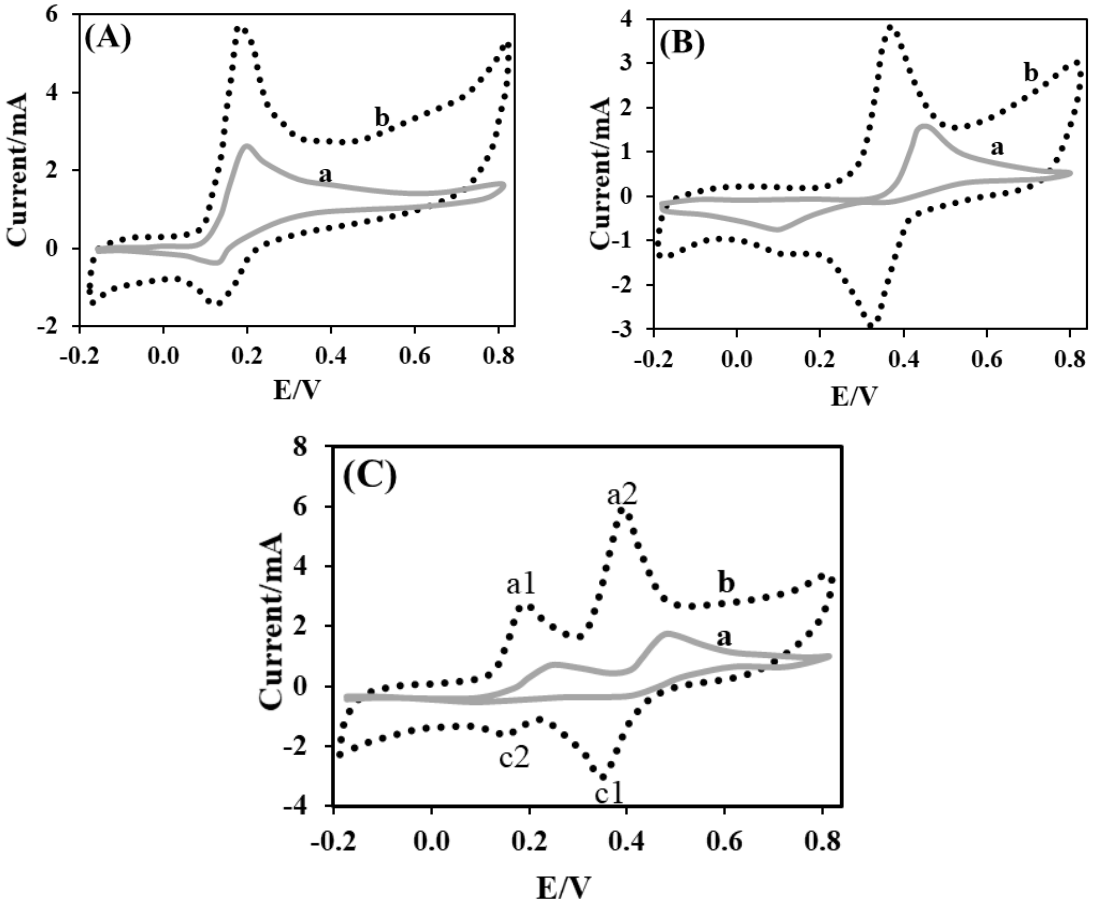

Figure 3. 13 Voltammetric detection of APAP and DA.
CV of (A) 0.5 mM dopamine (DA); (B) 0.5 mM *N*-acetyl-*p*-aminophenol (APAP); and; (C) simultaneous determination of binary mixtures of DA and APAP (0.5 mM each) in PBS (pH 7.4) at bare SPE (curves a) and GNPs-Naf/SPE (curves b).

Figure 3.13B shows CV recorded in 0.5 mM APAP in PBS (pH 7.4) at 100 $mV.s^{-1}$. The voltammogram shows an anodic peak (at 328.0 mV) in the positive-going scan and a cathodic counterpart peak (at 298.5 mV) in the negative-going scan which corresponds to the transformation of *N*-acetyl-*p*-aminophenol (APAP) to *N*-acetyl-*p*-benzoquinoneimine and vice versa in a quasi-reversible two-electron (ΔE_p = 29.5 mV) process (Eqn. 1) (Nematollahi et al., 2009).

However, at the SPE, there was a positive shift in the anodic peak (E_{pa} = 442.2 mV) position and a negative shift in the cathodic peak (E_{pc} = 70.0 mV) position; which

increased the peak-to-peak potential separation from 29.5 mV to 372.2 mV. This is an indication of a sluggish electron transfer process. The electrochemical behaviour of both DA and APAP on both sensors had non-unity peak current ratios (I_{pc}/I_{pa}); this can be a criterion for the instability of reaction products (Nematollahi et al., 2009) at the sensor surfaces under the experimental conditions.

The CVs for a binary mixture of 0.5 mM DA and APAP in PBS (pH 7.4) at the SPE and GNPs-Naf/SPE were also recorded (Figure 3.13C). The voltammogram for the binary mixture shows two broadened anodic peaks (a1 =232.4 mV; a2 = 456.2 mV) with no corresponding distinguishable reduction peaks at the bare SPE. However, at the GNPs-Naf/SPE, the voltammetric profiles have well-defined peaks at 166.7 mV and 374.2 mV corresponding to the oxidation of DA and APAP, respectively. The oxidation peaks of DA (a1 = 166.7 mV) and APAP (a2 = 374.2 mV) observed on GNPs-Naf/SPE formed a quasi-reversible couple with peak potentials (c2 = 135.7 mV; C1 = 135.7 mV), as observed during the oxidation of DA (Figure 3.13A) and APAP (Figure 3.13B) alone. The peak currents are also significantly higher at GNPs-Naf/SPE than at SPE. Clearly, the modification of the SPE with GNPs leads to significant increase in peak current. The presence of Nafion served as a binding agent to prevent the detachment of the GNPs from the SPE surface (Wen et al., 2012; Yao, Wen, Xu, et al., 2013; Yao, Wen, Zhang, et al., 2013). Without the presence of the Nafion, the GNPs are easily washed off the surface of the SPE when immersed in the electrochemical cell with measuring solution. Consequently, the addition of Nafion enhanced the GNPs film formation on the SPE surface.

3.1.4.10 DPV analysis of DA and APAP at GNPs-Naf/SPE

Further analysis of DA and APAP was carried out at the GNPs-Naf/SPE using differential pulse voltammetry (DPV) in PBS (pH 7.4) over concentration ranges of 0.25 – 40.0 µM and 0.25 – 30.0 µM for DA and APAP, respectively. A fresh electrode was used for each measurement, and this was done in triplicate for each concentration. The resulting plots (Figure 3.14A, C) show that the oxidation peak currents (I_{pa}) for DA and APAP increased linearly with increasing concentrations, suggesting a stable and efficient electrocatalytic activity at the GNPs-Naf/SPE. For DA detection, the corresponding linear regression equation is defined by the expression $Ipa\ (\mu A) = 0.321\ [DA](\mu M) + 0.014,\ R^2 = 0.9994$ in the range of 0.25 to 40.0 µM (Figure 3.14B) while for APAP detection, the corresponding linear regression equation is defined by the expression $Ipa\ (\mu A) = 0.398\ [APAP](\mu M) + 0.033, R^2 = 0.9994$ in the range of and 0.02 – 30.0 µM (Figure 3.14D). Using the regression equations, the calculated limits of detection for DA and APAP (based on 3x the baseline noise) were found to be 0.13 µM and 0.25 µM, respectively; these were deemed to be satisfactory for the analysis of elevated levels of both compounds in human bodily fluids.

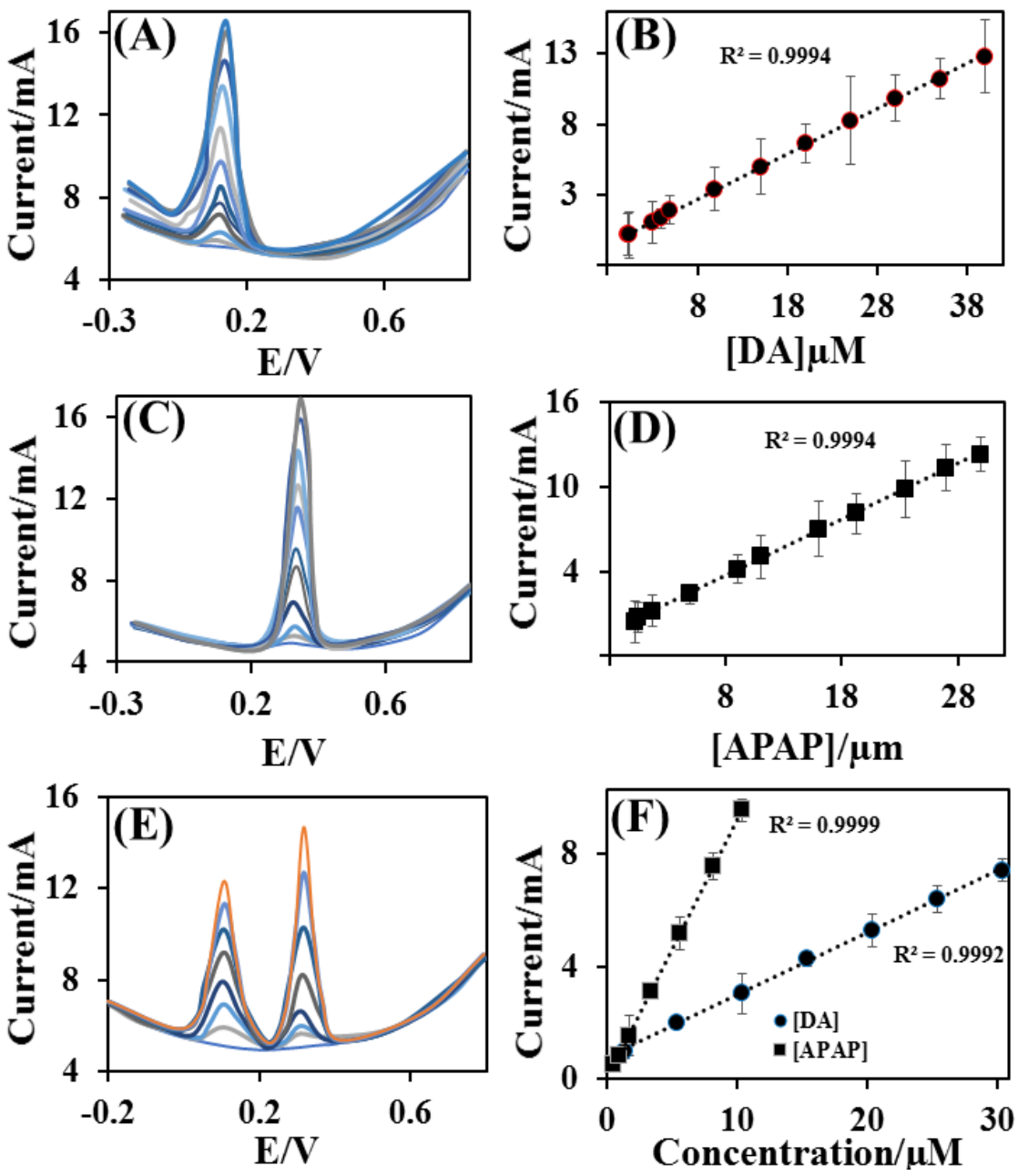

Figure 3. 14 Analysis of DA and APAP at GNPs-Naf/SPE by differential pulse voltammograms (DPV)

Differential Pulse Voltammograms with corresponding linear calibration plots for DA (A and B), APAP, (C and D) and DA + APAP (E and F) in PBS (pH 7.4) at the GNPs-Naf/SPE.

3.1.4.11 Analysis of DA and APAP in binary mixtures at GNPs-Naf/SPE

DPV analysis of binary mixtures of DA and APAP was also performed with different concentrations (DA in the range of 1-30 µM; APAP in the range of 0.1-10.0 µM) and the voltammogram for this analysis is shown in Figure 3.14E. With increasing concentrations of each compound, there was a linear increase in the anodic peak currents (Figure 3.14F) for each measurement. The corresponding linear regression behaviour for DA and APAP is defined by the equations $Ipa\ (\mu A) = 0.221\ [DA](\mu M) + 0.011, R^2 = 0.9992$ and $Ipa\ (\mu A) = 0.950\ [APAP](\mu M) + 0.101, R^2 = 0.9999,$ respectively. The limits of detection for DA and APAP were estimated to be 0.15 µM and 0.32 µM, respectively. These analytical performance characteristics are superior to published results obtained from other graphene-based sensors (Table 1), which tended to have reduced linear ranges (Adhikari et al., 2016; Kang et al., 2010; Xiong & Jin, 2011; Zhang et al., 2014) and/or poor limits of detection (Kim et al., 2017; Y. Kim et al., 2010; Mallesha et al., 2011; Wang et al., 2009; Xiong & Jin, 2011; Yang et al., 2014) when compared to this sensor.

Table 3. 2 Comparison of graphene-based electrodes for determination of DA and APAP

Dopamine			
Type of graphene	LoD/µM	Linear range/ µM	Reference
GR	-	5.0-200.0	(Ying Wang et al., 2009)
RGO	2.60	4.0-100.0	(Y. Kim et al., 2010)
RGO	0.25	3.0-60.0	(Mallesha et al., 2011)
ERGO	0.50	0.2-15.0	(Xiong & Jin, 2011)
ERGO	0.02	4.0-500.0	(Z. Zhang et al., 2014)
AG	0.33	0.5-35.0	(D. Kim et al., 2017)
ERGO	0.50	0.5-60.0	(L. Yang et al., 2014)
CRGO	0.10	0.2-80.0	(Kanyong, Rawlinson, et al., 2016b)
GNP	0.13	0.25-40.0	Current work
N-acetyl-p-aminophenol			
Type of graphene	LoD/µM	Linear range/ µM	Reference
EGNS	$2.5x10^{-3}$	$5x10^{-3}$ – 1.0	(C. Wu et al., 2015)
GNS	$4.7x10^{-3}$	0.05-45.0	(Adhikari et al., 2016)
GR	$8.6x10^{-4}$	$6.6x10^{-3}$-1.5	(Yiğit et al., 2016)
GR	$3.2x10^{-2}$	0.1-20.0	(Kang et al., 2010)
AG	$3.1x10^{-2}$	0.05-20.0	(D. Kim et al., 2017)
GNP	0.25	0.02-30.0	Current work

GR Graphene, *RGO* Reduced Graphene Oxide, *ERGO* Electrochemically RGO, *AG* Activated Graphene, CRGO Chemically RGO, *GNP* Graphene nanoplatelets, *EGNS* exfoliated graphene nanosheets.

The reproducibility of the GNPs-Naf/SPE is highlighted in Figures 3.14 B, D, F where the responses to individual increasing concentrations of DAP (Figure 3.14B) and APAP (Figure 3.14D) and in their binary mixtures (Figure 3.14F) are detailed for triplicates measurements. Standard deviations for peak current intensities for the two compounds were found to be in the range of 1.2 to 1.9%. The stability of the GNPs-Naf/SPE was

also determined in a similar fashion after storage at room temperature for 30 days; the peak current intensities for DA and APAP decayed by less than 3.1%, suggesting that the electrodes were highly stable over the 30-day period.

3.1.4.12 Analytical application of GNPs-Naf/SPE

To demonstrate the feasibility of the GNPs-Naf/SPE for routine analysis, the sensor was used to determine DA and APAP concentrations in human urine samples. All the urine samples were diluted (1:10) with PBS (pH 7.4), and then appropriate amounts were transferred to the electrochemical cell and each species determined using the GNPs-Naf/SPE and DPV. The simultaneous determination of DA and APAP was also evaluated; firstly, their binary mixture in PBS (pH 7.4) was spiked into the urine samples and DPV was used to simultaneously recover them. A fresh GNPs-Naf/SPE was used for each measurement. The recovery data (Table 2) shows that the methods is highly accurate and reproducible, indicating potential application of the GNPs-Naf/SPE for the determination of DA and APAP in real clinical samples.

Table 3. 3 Recovery of DA and APAP from fortified urine samples (n=3)

Spiked urine sample	Amount Added (µM)	Amount Found (µM)	Recovery (%)
DA	50	49.47 ±0.49	98.9
APAP	50	49.17 ±0.55	98.3
DA + APAP mixture (DA 25µM; 25 µM)	25	49.17	97.0
DA+APAP mixture (DA	25	48.83	97.7

3.2 Conclusion

Two high performing and stable composites combining the synergistic effects of the conducting polymer PEDOT:PSS and the room temperature ionic liquid [EMIM][BF_4]); and GNPs-Naf were developed and applied in two independent sensors. In the first sensor, a disposable screen-printed electrode was modified with the PEDOT:PSS/IL composite and the resulting sensor was utilised as an analytical tool for the analysis of catechol, a priority pollutant, by amperometry in stirred solution. The prepared PEDOT:PSS/IL composite exhibited a highly nano-porous microstructure, excellent stability and enhanced electrocatalytic properties towards catechol. The sensor was used to analyse catechol with satisfying selectivity and sensitivity. Potential applicability in the analysis of catechol in natural water samples was demonstrated with stable, accurate results obtained.

The GNPs-Naf/SPCE was reliable and could be used for routine analysis of these compounds in human urine samples. The sensor was selective toward DA and APAP detection in the presence of common biological interfering factors within urine, and it also showed a stable performance over time in storage. The developed method is reliable with recovery of spiked urine samples of 97.0 %. This suggests that the sensor is good and suitable for use in the analysis of the compounds in clinical samples.

This demonstrates that the sensors have prospects for routine application in the analysis of this priority pollutant. In future, sensors based on the transduction capabilities of the PEDOT:PSS/IL and GNPs-Naf composites could be developed for biomedical diagnostic applications.

CHAPTER 4

RESULTS OF SPECIFIC OBJECTIVES 3 &4

Overview

In achieving these objectives, two label-free impedimetric immunosensors were developed to detect detection *Plasmodium falciparum* histidine-rich protein-2 (PfHRP-II) and hepatitis B surface antigens (HBsAg). The sensors were developed on screen-printed gold microelectrodes and applied covalent crosslinking to immobilize capture antibodies to the target antigens.

4.1 Manuscript 3: Development of a simple sensitive impedimetric immunosensor for detection of *Plasmodium falciparum* histidine rich protein-II

Authors: Francis D. Krampa[1,2], Yaw Aniweh[1], Jonathan Adjimani[1,2], Osbourne Quaye[1,2], Gordon A. Awandare[1,2], Prosper Kanyong[1,3].

[1]West African Centre for Cell Biology of Infectious Pathogens (WACCBIP), University of Ghana;

[2]Department of Biochemistry, Cell & Molecular Biology, University of Ghana; [3]Department of Chemistry, Physical & Theoretical Chemistry Laboratory, University of Oxford, Oxford OX1 3QZ, UK

*corresponding author; prosper.kanyong@chem.ox.ac.uk; p.kanyong@waccbip.org

4.1.1 Abstract

In this work, the development of a label-free electrochemical impedance immunosensor for the quantitative detection of *Plasmodium falciparum* histidine-rich protein-2 (PfHRP-II) is reported. First, physisorption, covalent binding and polydopamine assisted binding were evaluated for immobilizing capture anti-PfHRP-II antibodies unto a screen printed gold microelectrode surface. A robust covalent coupling between anti-PfHRP-II antibodies and an amine layer glutaraldehyde crosslinking produced a sensitive immunosensor. With the help of the amino groups located on the surface of antibodies, anti-PfHRP-II covalently attached to a glutaraldehyde crosslinker. Cyclic voltammetry and Electrochemical impedance spectroscopy are employed in the presence of $[Fe(CN)_6]^{-3/-4}$ redox species to characterize the electrode and the step-by-step development of the label-free detection of *Pf*HRP-II. The impedimetric immunosensor demonstrated high reproducibility and sensitivity, with an impressively low detection limit of 38 pg/mL in buffer.-

4.1.2 Introduction

Malaria prevails in tropical and subtropical regions of the world (Jain et al., 2014; WHO, 2016). The etiologic agent is an Apicomplexan protozoan of the genus *Plasmodium* and five species, namely, *P. falciparum, P. malariae, P. knowlesi, P. ovale, P. knowlesi* and *P. vivax* are known to cause infection in humans. The World Health Organization (WHO) reported that, in 2014, only 78% of suspected malaria cases, excluding undocumented cases, had access to diagnostic tests in public health facilities (WHO, 2015). In 2016, over 216 million cases in 91 countries and 400,000 mortalities were reported (WHO, 2018).

4.1.2.1 Parasite development in humans, biomarkers, and diagnosis

The developmental cycle of *Plasmodium* species that infect humans and the tools applied in their is briefly illustrated in Figure 4.1 (Scherf et al., 2008). The cycle begins with the injection of sporozoites into the host's circulation by an infected female *Anopheles* mosquito. The sporozoites then target and enter hepatocytes where they multiply and differentiate into merozoites. This stage of the parasite life cycle is known as pre-erythrocytic. In infections involving *P. vivax* and *P. ovale,* dormant forms of the liver stage, called hypnozoites may persist in the liver (Mueller et al., 2009) and cause relapse of the infection, thereby making it difficult to eradicate. The pre-erythrocytic stage is essential in the establishment of malaria infection. This stage is asymptomatic, however, it is difficult for diagnostic tools to detect sporozoites because hepatocytes invasion occurs within 30–45 min after sporozoites are inoculated by the infected mosquito (Cerami et al., 1992; Sinnis et al., 1996). This short time and low numbers of sporozoites injected leaves little time for their detection. Some efforts in finding biomarkers for detection of early liver stage or the dormant form have identified the

Plasmodium liver-specific protein 2 (LISP2) (Gupta et al., 2019; Orito et al., 2013). The sporozoite surface circumsporozoite proteins (CSP), which functions to interact with receptors on the hepatocyte, has also been targeted for diagnostic potential (Nam et al., 2014).

The erythrocytic stage of infection begins when merozoites released from the invade red blood cells (RBCs) and grow from the rings to trophozoites and schizonts stages of development. Schizonts egress to release merozoites that continue the cyclical asexual cycle. In the process, some of the parasites differentiate into gametocytes to begin the sexual phase of the life cycle. The gametocytes are taken up by female Anopheles mosquitoes during blood meal. This subsequently develops in the midgut through to ookinete and their transition into the salivary glands as sporozoites ready to be injected during blood meal to initiate infection in humans.

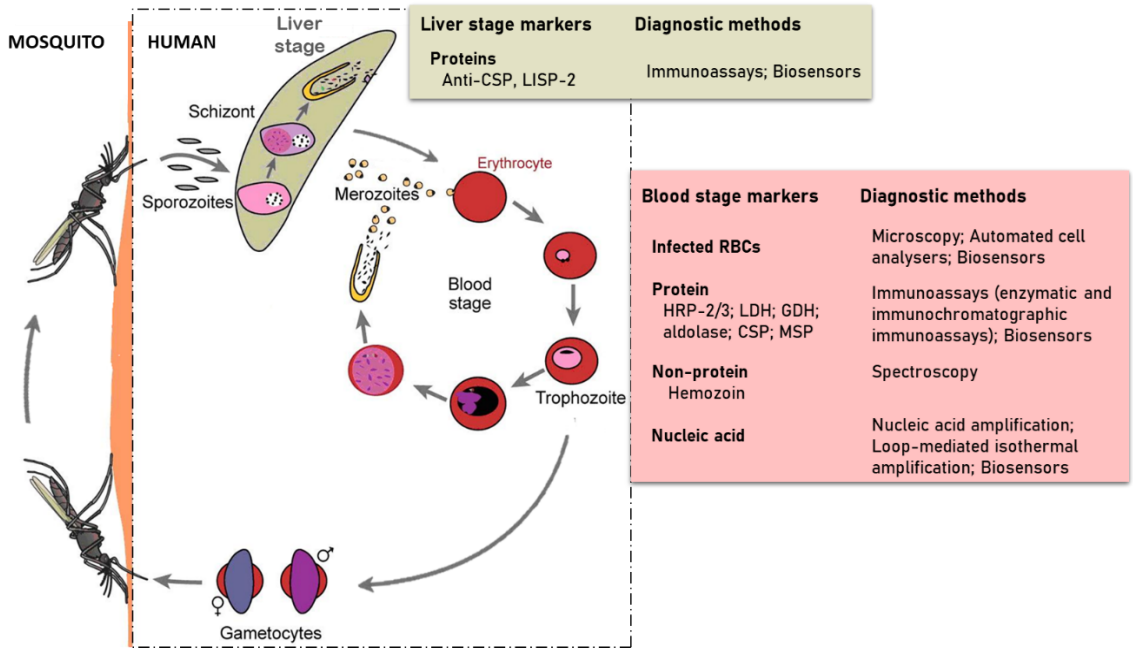

Figure 4.1 Developmental cycle of human *Plasmodium* species in a mammalian host and the strategies used in detecting parasite specific markers. Redesigned from Scherf et al. 2008.

Various parasite detection methods have been employed over the years in diagnosing malaria cases. It is ideal to detect infection at the erythrocytic stage because of exponentially elevated parasite numbers, abundance of nucleic acid markers or the production of soluble antigenic proteins that can illicit immune responses. Using a microscope and efficient staining of peripheral blood, popularly Giemsa-stained thick and thin blood films, parasitized RBCs can be visualized and the different parasite species distinguished morphologically in: ring, trophozoite, schizont, and gametocyte. Although microscopy offers advantages such as good sensitivity and the capacity to determine parasitemia and the type of species, it is time-consuming and requires a highly skilled microscopist. Cases are sometimes misdiagnosed or undetected due to poor sensitivity at low parasitemia, which lead to inappropriate and/or delayed treatment (Amexo et al., 2004; Reyburn, 2010). These limitations associated with the routine use of microscopy have led to the development of alternative diagnostic methods such as polymerase-chain reaction (PCR)-based nucleic acid amplification tests that target specific genes or transcriptomes of the parasite at the erythrocytic stage. The commonly targeted genes or RNA transcripts and some recent advances in nucleic acid-based techniques have been extensively reviewed (Britton et al., 2016; Krampa et al., 2017b; Roth et al., 2016; Yanow, 2016). However, these alternative methods tend to be expensive, require trained personnel, lengthy turnaround time, and a level of sophistication that is not suitable for uptake in rural and poor healthcare settings (The malERA Consultative Group on Diagnoses, 2011).

The detection of a variety of other parasite-specific biomarkers including but not limited to histidine rich proteins 2 and 3 (HRP-II/III), lactate dehydrogenase (LDH), glutamate dehydrogenase (GDH), aldolase, merozoite surface protein 3 (MSP-3), and

the biocrystal hemozoin have been explored order for a faster and easier diagnosis in the field.

Immunochromatographic tests are popular for point-of-care (POC) diagnosis of malaria (B. Li et al., 2017; Reyburn, 2010). Commonly called a 'rapid diagnostic test' (RDT), it is based on a lateral flow immunoassay technique integrated into a cassette for single-step, cost-effective, simple and fast detection of parasite specific biomarkers. These attributes have made the RDTs immensely popular in the field for POC application since its introduction, with the distribution reaching a global estimate 1.92 billion RDT units between 2010 and 2017 (Amreen Ahmad et al., 2019). Africa is the biggest consumer with more than 80% of the total RDT sales in 2017 alone (223 million out of the 276 million units) (World Health Organization, 2018a). Although RDTs have dominated point-of-care-tests (POCT) for malaria, there have been major concerns about the stability and performance relating to sensitivity and specificity which constrains their impact (Derda et al., 2015; Gubala et al., 2012; Luppa et al., 2011). Currently, the commercially available RDTs are about 1000-fold lower in sensitivity than alternative laboratory-based techniques (Hu et al., 2014; Posthuma-Trumpie et al., 2009; Zhan et al., 2017), thus they do not provide the sensitivity and quantitation comparable to the gold-standard microscopy or PCR (Posthuma-Trumpie et al., 2009). This limitation necessitates the need to develop other diagnostic technologies with improved sensitivities (David Bell et al., 2006; Perkins & Bell, 2008), while ensuring simplicity, robustness, and cost-effectiveness. Some of these recent advances have included chip-based microfluidics, surface plasmon resonance and biosensors, many of which have achieved comparable sensitivities with traditional diagnostic methods.

4.1.2.2 Detection of PfHRP-II in Clinical Samples

Plasmodium falciparum histidine rich protein 2 (PfHRP-II) is specific to *P. falciparum* and the main target for RDTs that detect *P. falciparum* infection. The antigen is secreted into peripheral blood during parasite growth and development where it plays a role in heme detoxification. Although primarily abundant in blood, trace amounts can be found in cerebrospinal fluid, urine, and saliva of infected patients (Parra et al., 1991; Rodriguez-del Valle et al., 1991), which offer an opportunity for non-invasive testing. Nonetheless, blood is preferred because of small sample volumes required to target the antigen. Painless testing has attractive public health benefits of voluntary testing and participation in screening programs geared towards malaria control (Sin et al., 2014). However, only a few publications have attempted urine or saliva analysis as non-invasive malaria diagnostics (Castro-Sesquen et al., 2016).

Electrochemical techniques have been shown to outperform optical methods in many modelled POC tests. Nanoparticles, primarily gold (AuNP) have been adopted in signal amplification for amperometric immunosensors (Cao et al., 2011; Ju et al., 2011; Lei & Ju, 2012). Their small size and ease of immobilizing bioconjugate probes allow for increased surface concentration of enzyme-tagged detection antibodies, hence higher signals from the catalytic reaction of enzyme and substrate. Sharma et al. were first to report an electrochemical immunosensor to detect PfHRP-II in blood by amperometry (Sharma et al., 2008). The disposable immunosensor utilized multi-walled carbon nanotubes (MWCNTs) and gold nanoparticles (Nano-Au) to modify screen printed electrodes (SPE); resulting in Nano-Au/MWCNT/SPEs onto which rabbit-derived anti-PfHRP-II were immobilized as capture antibodies. A sandwich enzyme-linked immunosorbent assay format was employed for the biosensor with alkaline phosphatase (ALP)-conjugated antibodies. Amperometric measurements were applied using ALP

hydrolysis of 1-naphthyl phosphate. The Nano-Au/MWCNT/SPE had a limit of detection (LoD) of 8.0 ng/mL (compared to 80.0 ng/mL for bare SPE and 20.0 ng/mL for MWCNT/SPE). This enhanced performance was attributable to the synergistic effect of MWCNTs and AuNP. More importantly, the immunosensor had a superior analytical performance compared with a commercial immunochromatographic lateral flow test in the analysis of microscopy positive patient sample (sensitivity: 96% vs. 79%, specificity; 94% vs. 81% respectively).

In assessing exposure to malaria parasites, recombinant PfHRP-II was used as a recognition element for anti-PfHRP-II antibodies in an amperometric immunosensor for early stages of malaria and at low parasitemia (Sharma et al., 2010). SPEs were modified with alumina sol-gel (Al_2O_3) and AuNP to obtain AuNP/Al_2O_3 sol-gel/SPE after which PfHRP-II was bound. Rabbit anti-PfHRP-II and anti-rabbit IgG-ALP conjugate were directed against capture antigens and the analytical responses determined by amperometry. In comparison to 'gold standard' microscopy, the immunosensor exhibited a sensitivity of 92% and a specificity of 90%. In another study that detected monoclonal antibodies to recombinant PfHRP-II (MoaPfHRP-II), a gold chip was pre-treated with 4-mercaptobenzoic to immobilize recombinant PfHRP-II, then monitored for interactions between the antigen and antibody (Sikarwar et al., 2014). Label free surface plasmon resonance (SPR) screening of the interaction between the recombinant protein and target antibody produced a LoD of 5.6 pg.

Magnetic nanoparticles (MNPs) have also been applied in the development of a highly sensitive malaria immunosensor. Anti-HRP-2 was covalently attached to MNPs as capture elements and a second monoclonal antibody that binds a different epitope of the target antigen was labelled with horse radish peroxidase (HRP) to provide an electrochemical signal (Castilho et al., 2011). The anti-HRP-2-MNPs were captured

onto a magnetic graphite-epoxy composite electrode incubated with HRP-2-spiked serum and anti-HRP-2-HRP in a sandwich assay format. Amperometric measurements produced an LoD of 0.36 ng/mL, much lower than Sharma et al. (Sharma et al., 2008) reported. Translating this strategy to the field would require magnetic supports for electrodes (Castilho et al., 2011).

More recently, Hemben et al. used anti-PfHRP-II monoclonal antibodies to capture PfHRP-II at the surface of a screen printed gold electrode (Hemben et al., 2017). The captured antigen was targeted with HRP-labelled antibodies and the quantification of PfHRP-II derived from the substrate (TMB-H_2O_2)-enzyme reaction by amperometry (Figure 2A). The LoDs in buffer and spiked human samples were determined as 2.14 ng/mL and 2.95 ng/mL, respectively. Labelled antibodies were subsequently conjugated to gold nanoparticles (AuNP) to amplify the sensor signal which improved the sensitivity and LoD in buffer (36.0 pg/mL) and spiked serum samples (40.0 pg/mL). Besides using molecular labels and nanoparticles for improved diagnostics, some assays can probe the intimate recognition between the receptor and target alone. The benefits of using such label-free formats include a reduction in the assay complexity, preparation time, and analysis cost as it eliminates potentially confounding chemical labels. These strategies are better suited to field applications and under resourced settings where laboratories and skilled personnel are unavailable. A label-free a piezoelectric immunosensor for PfHRP-II was designed by applying mixed self-assembled monolayers (SAMs) of thioctic acid and 1-dodecanethiol on gold quartz crystal microbalance (QCM) Anti-PfHRP-II antibodies were covalently immobilized unto the SAM-modified electrodes via EDC-NHS activation and the frequency change resulting from binding of different concentrations of PfHRP-II measured (Sharma et al., 2011). The immunosensor exhibited a LoD of of 12.0 ng/mL with a linear range of

15.0–60.0 ng/mL for analysis of PfHRP-II in buffer. This was higher than their previously reported amperometric immunosensor (8 ng/mL (Sharma et al., 2008) vs. 12ng/mL (Sharma et al., 2011)), and weaker responses were observed for PfHRP-II concentrations lower than 25.0 ng/mL. However, application of the sensor to clinical samples produced comparable sensitivities with a commercial immunochromatographic test (ICT) kit (NOW® Malaria, Binax, Inc., Scarborough, Maine, USA).

Electrochemical impedance spectroscopy (EIS)-based methods present with numerous advantages that make them suitable candidates for POC application (Prodromidis, 2010). Their high sensitivity is evident from lower LoDs they tend to produce compared with other electrochemical methods. The lowest LoD yet reported for malaria was achieved by impedimetric detection of PfHRP-II (Paul et al., 2016). In the sensor design, copper doped zinc oxide nanofibers (CZnONF) was drop-casted on glassy carbon electrode (GCE/CZnONF) followed by SAM modification and chemisorption of anti-PfHRP-II (Figure 2B). The highly sensitive nanosensor (28.5 kΩ/(g/mL)/cm^3) attained a detection limit of 6.8 ag/mL. The authors subsequently reported a flexible chemiresistive immunosensor in which the transducer comprised a 1-dimensional MWCNT-zinc oxide (MWCNTs-ZnO) nanofiber drop-casted on micro gold electrodes (Paul et al., 2017). Capture antibodies, anti-PfHRP-II were immobilized on MWCNTs-ZnO by EDC-NHS crosslinking and resistance changes (ΔR) measured to monitor the formation of PfHRP-II-anti-PfHRP-II complexes. The device demonstrated good analytical performance as well as potential towards the development of POCTs with a linear response ranging from 10 fg/mL to10 ng/mL, LoD of 0.97 fg/mL and high specificity for PfHRP-II over non-specific antigens.

With the current trends aiming at microfluidic and multiplexed detection of analytes, microelectrodes offer well-established advantages for integration owing to their relatively small surface area which enables the use of use micro volumes of test sample (Li et al., 2009), integration of multiple processes (Budai, 2010; Selimovic & Martin, 2013), rapid/high-throughput analysis (Zhang et al., 2012) in detecting biologically significant compounds.

This chapter reports on the design and characterisation of an impedimetric immunosensor for *Pf*HRP-II antigens based on an amine modified screen-printed gold microarray electrodes.

4.1.3 Materials and methods

4.1.3.1 Reagents

Phosphate buffered saline (PBS), potassium ferrocyanide and potassium ferricyanide ($K_3[Fe(CN)_6]$, $K_4[Fe(CN)_6]$), Hellmanex III, potassium chloride (KCl), sodium bicarbonate, sodium carbonate anhydrous, bovine serum albumin (BSA), cysteamine (Cys) and glutaraldehyde (GA, 50%) were purchased from Sigma–Aldrich (Sigma–Aldrich, UK). Ethanol (99.5%) was obtained from Merck (UK) and recombinant *Plasmodium falciparum* histidine-rich protein-2 (*Pf*HRP-II) and human anti-*Pf*HRP-II antibody was supplied by BioRad (Hemel Hempstead, UK).

4.1.3.2 Solutions

The redox probe consisted of 5.0 mM $[Fe(CN)_6]^{3-/4-}$ prepared in PBS (pH 7.4) containing 0.1M KCl as the electrolyte. Sodium bicarbonate buffer (pH 9.6) was prepared by mixing sodium bicarbonate (0.58g) and anhydrous sodium carbonate

(0.33g) in 100mL of ddH_2O. Ferrocyanide, cysteamine and glutaraldehyde were freshly prepared before use. All other solutions and buffers were stored appropriately at 4°C or room temperature.

4.1.3.3 Apparatus and instrumentation

Electrochemical measurement was performed in an electrochemical cell using an in-house gold-sputtered screen-printed gold microelectrode (SPGµE). The SPGµE consist of a gold micro-disc working electrode (0.4 mm diameter) and were used alongside with a disposable reliable silver RE and gold CE. All electrochemical measurements were performed in a faradaic cade with an AUTOLAB Potentiostat model PGSTAT204 equipped with a Frequency Response Analyser module (FRA32M) (Metrohm, Utrecht, The Netherlands) coupled to a computer with NOVA 2.1 software for experimental control and data acquisition.

4.1.3.4 Fabrication of the PfHRP2 immunosensor

4.1.3.4.1 ***Electrodes preparation***

The SPGµ were initially washed in 50% Hellmanex III solution (1:1 v/v Hellmanex III:ddH_2O). Briefly, the electrodes were immersed in a 50.0 mL falcon tube partly filled with the wash solution and rocked slowly for 1 hr, rinsed twice with ddH_2O and air-dried.

4.1.3.4.2 ***Preparation of the sensing layer***

After the cleaning step, three strategies for biofunctionalization were prepared; physisorption, dopamine-assisted immobilisation consisting electrodeposition of a

quinone-rich polydopamine layer (ePDA) and an amine coupling process using cysteamine-glutaraldehyde (GA-cys) complex. Antibody immobilisation strategies were preceded by specific modifications of the WE, illustrated in figure 4.1.

4.1.3.4.3 ***Preparation of ePDA/SPGµE***

A controlled electrodeposition of functional polydopamine (PDA) thin films was performed by repeated CV scans (10 cycles) between −0.5 V and −1.5 V at 100mV/s scan rate in PBS (pH 7.4) containing 5mM dopamine hydrochloride. The modified ePDA/SPGµE were thoroughly rinsed with ddH_2O and air-dried at room temperature.

4.1.3.4.4 ***Assembly of the GA-cys/SPGµE sensing layer***

The general schematic representation of the proposed GA-cys assembly sensing layer for conjugating capture antibodies is demonstrated in Figure 4.1. SPGµEs were incubated in 20mM cysteamine (prepared in absolute ethanol) for 1hr 30mins to generate a self-assembled monolayer (SAM) of amine functional groups. Sulphur atoms on cysteamine bind to gold leaving free amine groups. The cysteamine treated electrodes were rinsed in ddH_2O to remove excess unbound cysteamine, air-dried and placed in of 2.5% glutaraldehyde (prepared in ddH_2O) for 1 hour at room temperature to form the GA-cys/SPGµE. GA was used as a cross-linker to facilitate covalent conjugation of capture antibodies to cysteamine SAM.

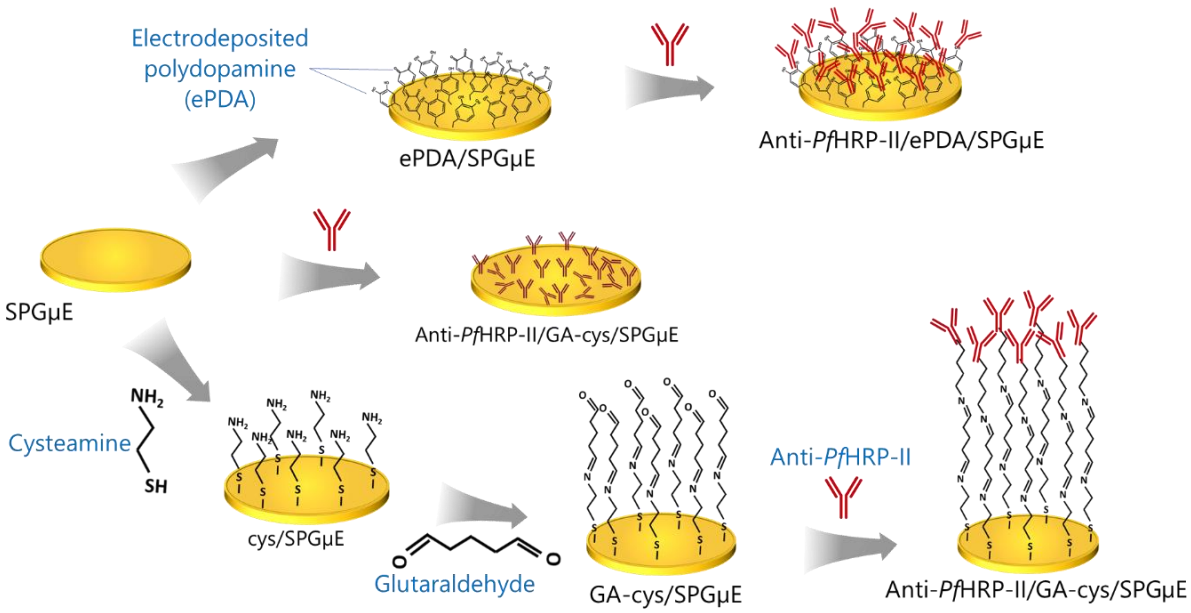

Figure 4. 2 Immobilization strategies applied for the PfHRP-II sensor.
An outline of physisorption and surface modification of SPGµE for *Pf*HRP-2 detection using glutaraldehyde as a crosslinking agent to immobilise anti-*Pf*HRP-2 to a cysteamine modified microelectrode.

4.1.3.4.5 ***Capture antibody immobilization***

The SPGµE, ePDA/SPGµE and Glu-cys/SPGµE were incubated with the antibody. Briefly, 8.0 µL of 100 µg/mL anti-*Pf*HRP-II antibodies (in PBS, pH 7.4) was casted over the WE and incubated overnight at 4°C under controlled-humidity conditions. The resultant anti-*Pf*HRP-II/SPGµE, anti-*Pf*HRP-II/ePDA/SPGµE and anti-*Pf*HRP-II/GA-CA/SPGµE were rinsed with ddH_2O to remove excess unbound antibodies. BSA (2% in PBS) was used to saturate the sensor surface and prevent nonspecific binding for 30 mins at 37°C after which it was rinsed with ddH_2O and air-dried. The functionalised sensors were stored at 4°C when not in use.

4.1.3.5 Detection of malaria antigen PfHRP-II and evaluation of the analytical performance

A step-by-step performance of each sensing layer was evaluated which consisted of incubating the functionalised sensors with increasing standard concentrations of recombinant *Pf*HRP-II; 0.5-20 ng/mL prepared in bicarbonate buffer (pH 9.6). The incubation steps consisted of covering the immunosensor surfaces with 8.0 µL of recombinant antigen (0.5 ng/mL, 5.0 ng/mL, 10.0 ng/mL, 15.0 ng/mL, 20.0 ng/mL and 30.0 ng/mL) for 20 minutes at 37°C under controlled humidity. After incubating with each concentration, the sensing layers were washed and EIS measured to evaluated electrical properties in the presence of 5.0 mM $[Fe(CN)_6]^{3-/4-}$ redox probe and 0.1M KCl. The assays were repeated in triplicates. Using the slope of the calibration plot, standard deviation from blank solutions (n = 5) and the electrode area, the LoD was calculated using the expression (Eqn 21 and 221):

$$\boldsymbol{LoD} = \ (3 \times SD(blank))/slope \tag{20}$$

$$\boldsymbol{Sensitivity} = \ slope/(Electrode\ area) \tag{21}$$

4.1.3.6 Electrochemical studies

All electrochemical studies were conducted using 1X PBS (pH 7.4) containing 5.0 mM $[Fe(CN)_6]^{3-/4-}$ redox probe and 0.1M KCl as the electrolyte. CV and DPV were used in characterising the SPGµE. EIS was acquired using an applied AC amplitude of 10.0 mV rms, DC potential of 0.24 V and a frequency range of 100 kHz - 0.05 Hz. Nyquist plots were used to indicate the frequency response of the electrochemical system (Z”

vs Z") and R_{ct} assumed by the diameter of the semi-circle. The resistance to charge transfer (R_{ct}) was evaluated using relevant Randle's equivalent circuits to fit acquired Nyquist plots using NOVA 2.1 software.

4.1.4 Results and discussion

4.1.4.1 Electrochemical characterisation of the SPGµE

Electrochemical analyses were initially carried out on the SPGµE. The electrochemical responses of SPGµE was characterised by CV and EIS in $[Fe(CN)_6]^{3-/4-}$, as described in Figure 4.2. Cyclic voltammograms showed peaks characteristic of a reversible electrochemical reaction. Prior to washing, the SPGµE wase slightly resistive, limited the charge transfer (Figure 4.2A & B) and accounted for the poor reversibility of the redox couple with comparatively lower I_{pa} and I_{pc} values (Figure 4.2C). The response was improved after washing, as shown by the more prominent peak in the voltammograms (red plot) in Figure 4.2A. In a similar manner, the washed SPGµE showed lower resistance to charge transfer (R_{ct}) than the unwashed electrode, exhibited by the smaller semicircle domain from the Nyquist plot (Fig 5.2 B). This observation could be attributed to removal of residual inks and insulating materials from the printing process and that may have formed on the gold surfaces. The peak-to-peak separation potential (ΔE_p) of approximately 100.0 mV (greater than the theoretical 59.0 mV/s) is indicative of the quasi-reversible behaviour of $[Fe(CN)_6]^{3-/4-}$ at the SPGµE (Ito et al., 1983; Morrin et al., 2003). Scan rate studies demonstrated a strong linear relationship between peak currents and the square root of the scan rates, with no significant alterations in peak potentials (Figure 4.2D). This implies a typical diffusion-controlled process and assumes the absence of any secondary reactions that may affect the kinetics

of electron transfer (Laviron et al., 1980; Srivastava et al., 2013). Repetitive CV scans recorded at 100.0 mV/s revealed reproducible peaks for all 25 scans (Figure 4.2E) with no specific adsorption.

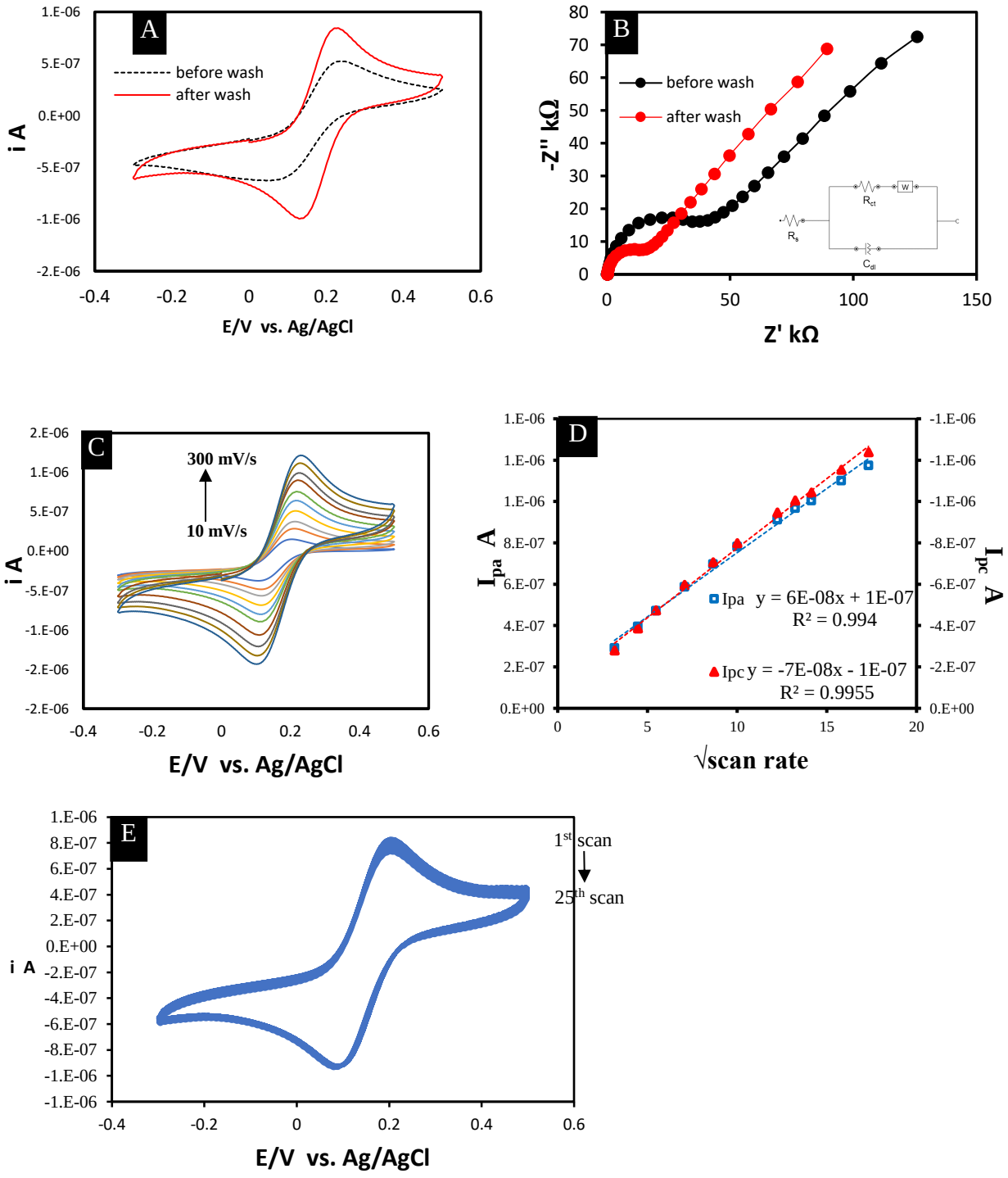

Figure 4. 3 Electrochemical characterisation of the printed gold microelectrode. (A) Cyclic voltammograms obtained at 100mV/s before (black dashed) and after (red) cleaning SPGµE (B) Nyquist plots of SPGµE; (C) Cyclic voltammograms of SPGµE at different scan rates: 10, 20, 35, 50, 75, 100, 150, 175, 200, 250 and 300 mV/s. (D) Calibration plots of peak currents (I_{pa} and I_{pc}) vs the square scan rate with regression equations (E) Cyclic voltammograms of 25 cycles at the SPGµE at of 100 mV/s. All measurements shown were conducted in 5.0 mM $[Fe(CN)_6]^{3-/4-}$ and 0.1M KCl (pH 7.4).

4.1.4.2 Assembly of the sensing layer

To confirm the changes occurring at the electrode surface during the immunosensor development, chemical modifications and antibody immobilization was monitored through EIS (Figure 4.3). It was observed that, chemical changes made at the electrode surfaces and the additional amounts of proteins bound accounted for different changes in the diameter of the semicircles in the Nyquist plots. The amine SAMs resulted in an initial decrease in R_{ct}, probably as a result of positive charges carried by amine functional groups after cysteamine treatment (Sharma et al., 2018) which attract electrons and facilitate the charge transfer process. After cross-linking and immobilization of capture antibodies, the Rct increased significantly. There were significant increases in R_{ct} after physisorption and GA-cys crosslinking of capture antibodies observed in Nyquist graphs. For physisorption (Figure 4.3A), the R_{ct} of SPGµE increased from 9046 ± 253 Ω (n = 3) to 19846 ± 553 Ω (n = 3) when incubated with anti-*Pf*HRP-II. Immobilization of capture antibodies on the GA-cys layer also showed an increase in R_{ct} to 24133 ± 1221 Ω (n = 3). These changes confirmed immobilisation of antibodies on the sensing layers and could be explained by two factors. First is the thickening of sensing layer (Cordeiro et al., 2019) causing electrostatic barrier, hence a slower reaction to 5.0 mM $[Fe(CN)_6]^{3-/4-}$ and secondly, the relatively weak negative charges of immunoglobulins at physiological conditions (Filoti et al., 2015; Yang et al., 2019) which may create an addition impediment for electron transfer between the sensing layer and $[Fe(CN)_6]^{3-/4-}$. For ePDA/SPGµE (Figure 4.3C), the increased R_{ct} is due to poor electrical conductivity of PDA films (Meredith & Sarna, 2006). Further increases in R_{ct} values after antibody incubation suggests the linkage of antibodies to the ePDA layer. The remarkable advantages of

PDA coated surfaces is their ability to bind biomolecules through amino groups and thiol groups without using any coupling agent (Lynge et al., 2011).

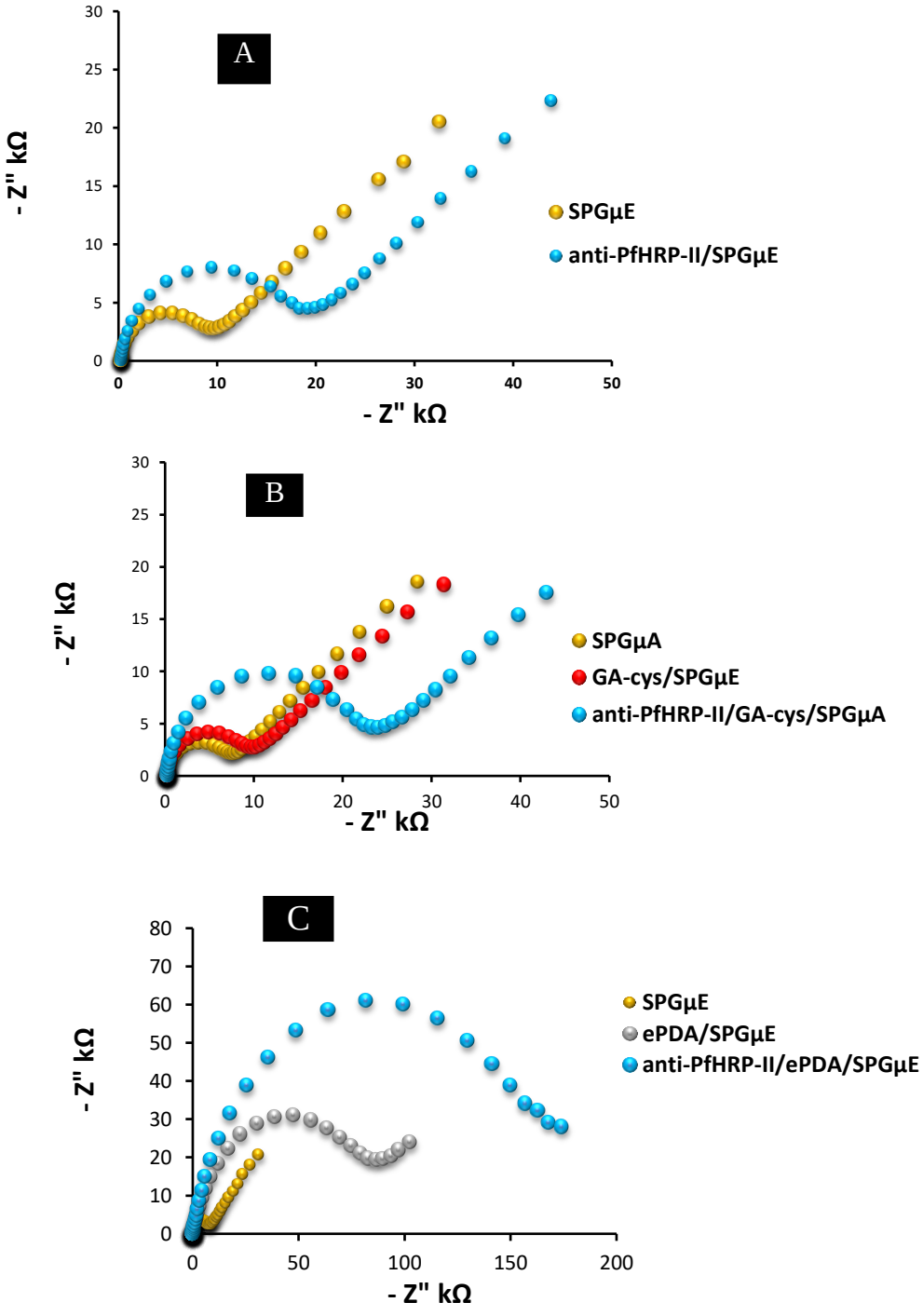

Figure 4. 4 Nyquist of EIS at different stages of PfHRP-II sensor development. (A) bare SPGµE and anti-*Pf*HRP-II; (B) SPGµE, GA-cys/SPGµE and anti-*Pf*HRP-II /GA-cys/SPGµE in 5mM $[Fe(CN)_6]^{3-/4-}$ and 0.1M KCl aqueous solution (pH 7.4). The Randles equivalent circuit is shown in insert.

In determining the suitability of the three strategies to detecting target proteins, BSA-blocked anti-*Pf*HRP-II/SPGµE, *Pf*HRP-II/ePDA/SPGµE and anti-*Pf*HRP-II/GA-cys/SPGµE were incubated with different concentrations of *Pf*HRP-II. Blocking with BSA showed further increases in charge transfer which could be due to additional insulation created on the immunosensor (Figure 4.4, 4.5A & 4.6A). In all the setups, R_{ct} of the sensing layer increased progressively despite saturation of all the active binding saturated with BSA. It can be deduced that; the capture antibodies retained their bioactivity in both methods and bound to the antigens which caused an additional hinderance for the redox probe to access the WE. However, responses from physically adsorbed antibodies seemed fairly uneven compared to antibody attachment by GA-cys covalent crosslinking (Figure 4.5B and 4.6B). It could be that, weak electrostatic, ionic and hydrophobic interactions from physically-linked anti-*Pf*HRP-II on WE were not sufficiently stable for multistage processes of the sensor development. On the other hand, the amine activated GA layer might have bound antibodies with higher stability and the led to the formation of SAMs. This resulted in a better linear trend with minimal error bars.

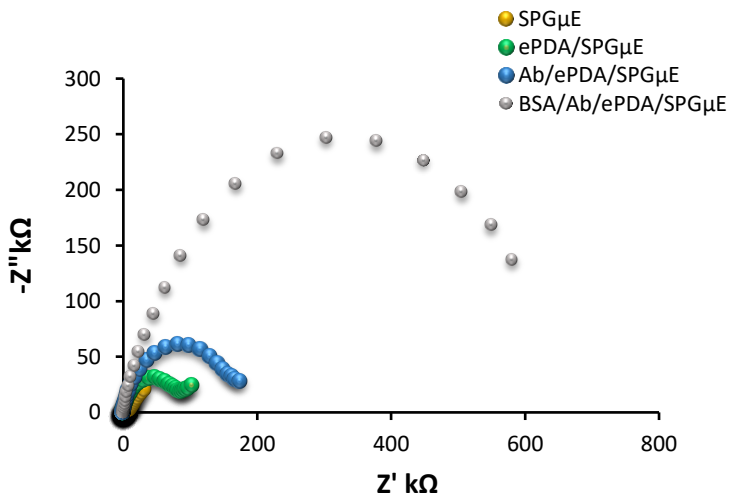

Figure 4. 5 Nyquist plot of BSA-blocked Impedimetric responses of anti-PfHRP-II/ePDA/SPGµE

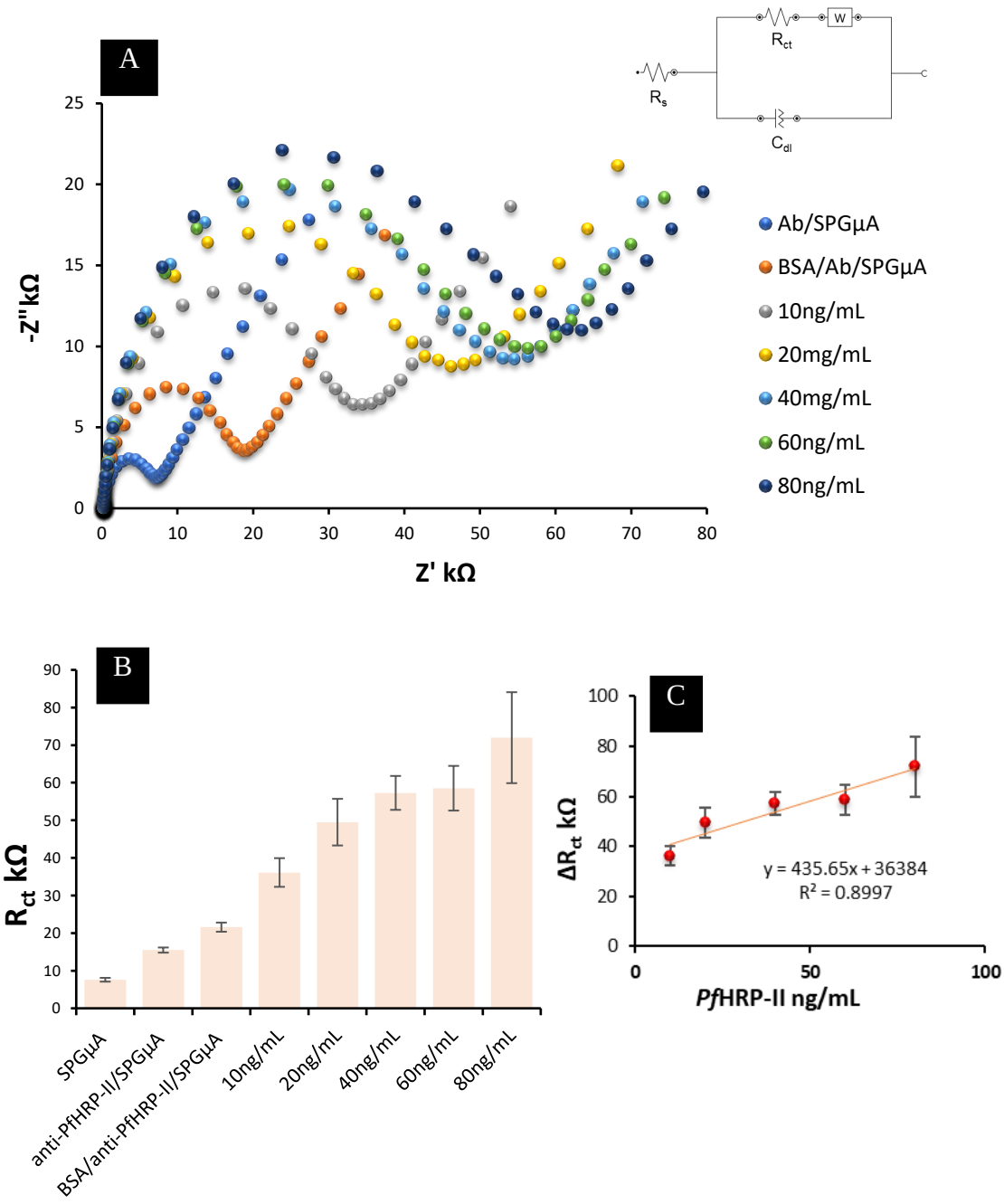

Figure 4. 6 Impedimetric responses of physiosorbed antibodies to PfHRP-II
Nyquist plot (A) and the responses of the sensor fabrication steps. Inset (C): the linear relationship between R_{ct} values and antigen concentrations obtained after stepwise fabrication. Measurements were performed in 5mM $[Fe(CN)_6]^{3-/4-}$ and 0.1M KCl aqueous solution (pH 7.4). The Randles equivalent circuit is shown in insert.

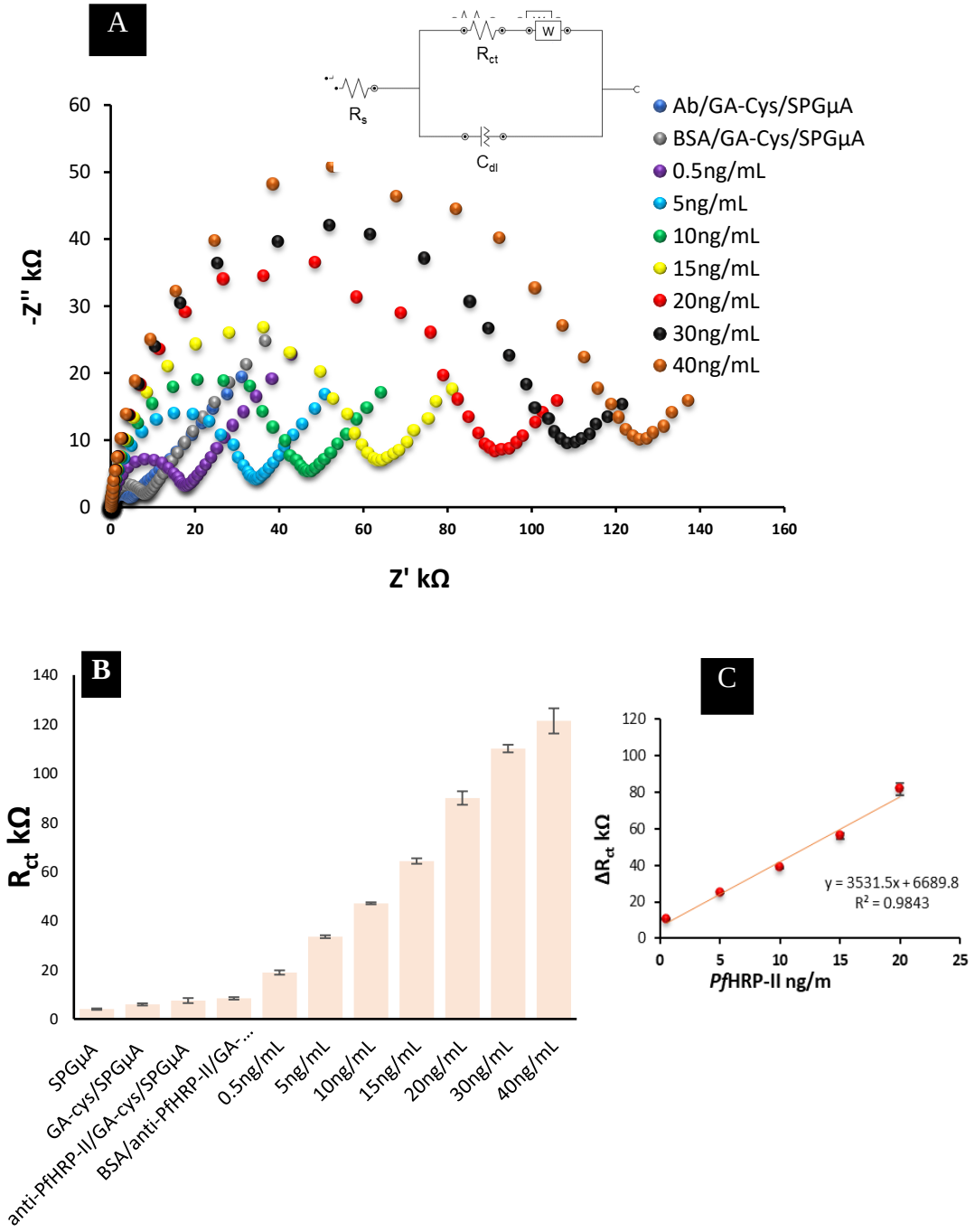

Figure 4. 7 Impedimetric responses of covalently crosslinked antibodies to PfHRP-II

Nyquist plot (A) and the responses of the sensor fabrication steps. Inset (C): the linear relationship between R_{ct} values and antigen concentrations obtained after stepwise fabrication. Measurements were performed in 5mM $[Fe(CN)_6]^{3-/4-}$ and 0.1M KCl aqueous solution (pH 7.4). The Randles equivalent circuit is shown in insert.

The limits of detection and sensitivity for both methods were calculated according to equations 21 and 22 (n=3). Physisorption produced a LoD of 0.3 ng/mL and sensitivity of 0.00035 kΩ/(g/mL)cm^2 whereas the GA-cys crosslinking method detected antigens as low as 40 pg/mL with a sensitivity of 4.4 kΩ/(g/mL)cm^2.

Despite the high biocompatibility of PDA and the apparent facile method of physisorption, reliable data could not be obtained with the anti-*Pf*HRP-II/ePDA/SPGµE. Subsequently, only anti-*Pf*HRP-II/GA-cys/SPGµE platforms were used in the final sensor design.

4.1.4.3 Analytical performance of the PfHRP-II immunosensor

Owing to the superior analytical performance of the sensing layer, further analysis applied the anti-*Pf*HRP-II/GA-cys/SPGµE to increasing concentrations of *Pf*HRP-II. The Nyquist plot and corresponding calibration curve are shown in Figure 4.7 and 4.8 for two independent experiments with a different batch of SPGµE over a range concentration 0.5-20.0 ng/mL. For all repeats, EIS measurements showed that increasing concentrations of *Pf*HRP-II, increased R_{ct} of $[Fe(CN)_6]^{3-/4-}$ at the sensing layer and gave a strong linear relationship between ΔR_{ct} and *Pf*HRP-II. The limits of detection were comparable (LoD of 38.0 pg/mL vs and t) to those obtained during the stepwise monitoring. With significant differences observed between the blank and first standard of the calibration plot.

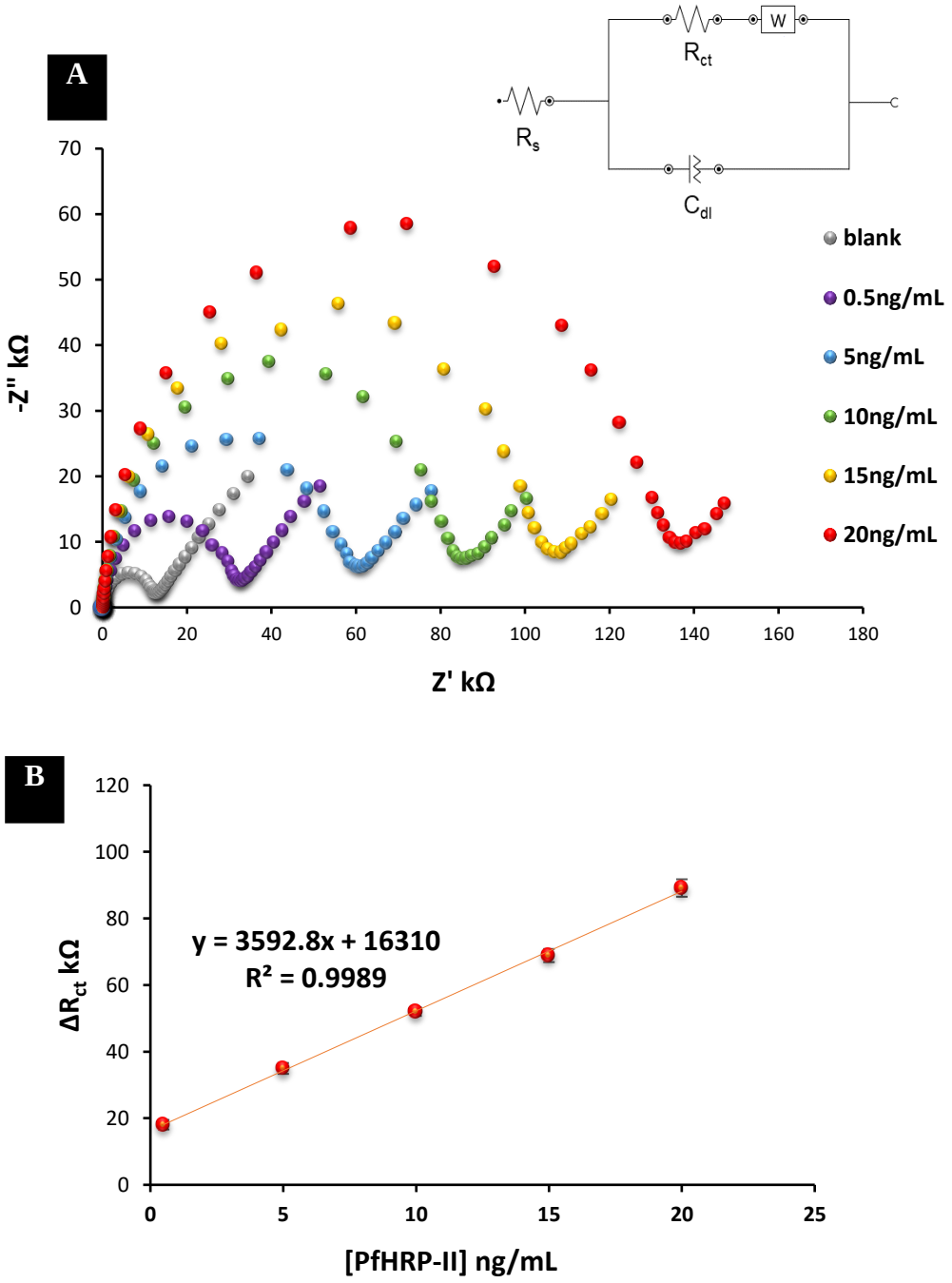

Figure 4. 8 Impedimetric responses of the anti-PfHRP-II/GA-cys/SPGµE sensor Nyquist plot and a corresponding calibration curve of *Pf*HRP-II detection in Each data point is an average of three independent measurements from the same batch of electrodes. Measurements were performed in 5mM $[Fe(CN)_6]^{3-/4-}$ and 0.1M KCl aqueous solution (pH 7.4). The Randles equivalent circuit is shown in insert.

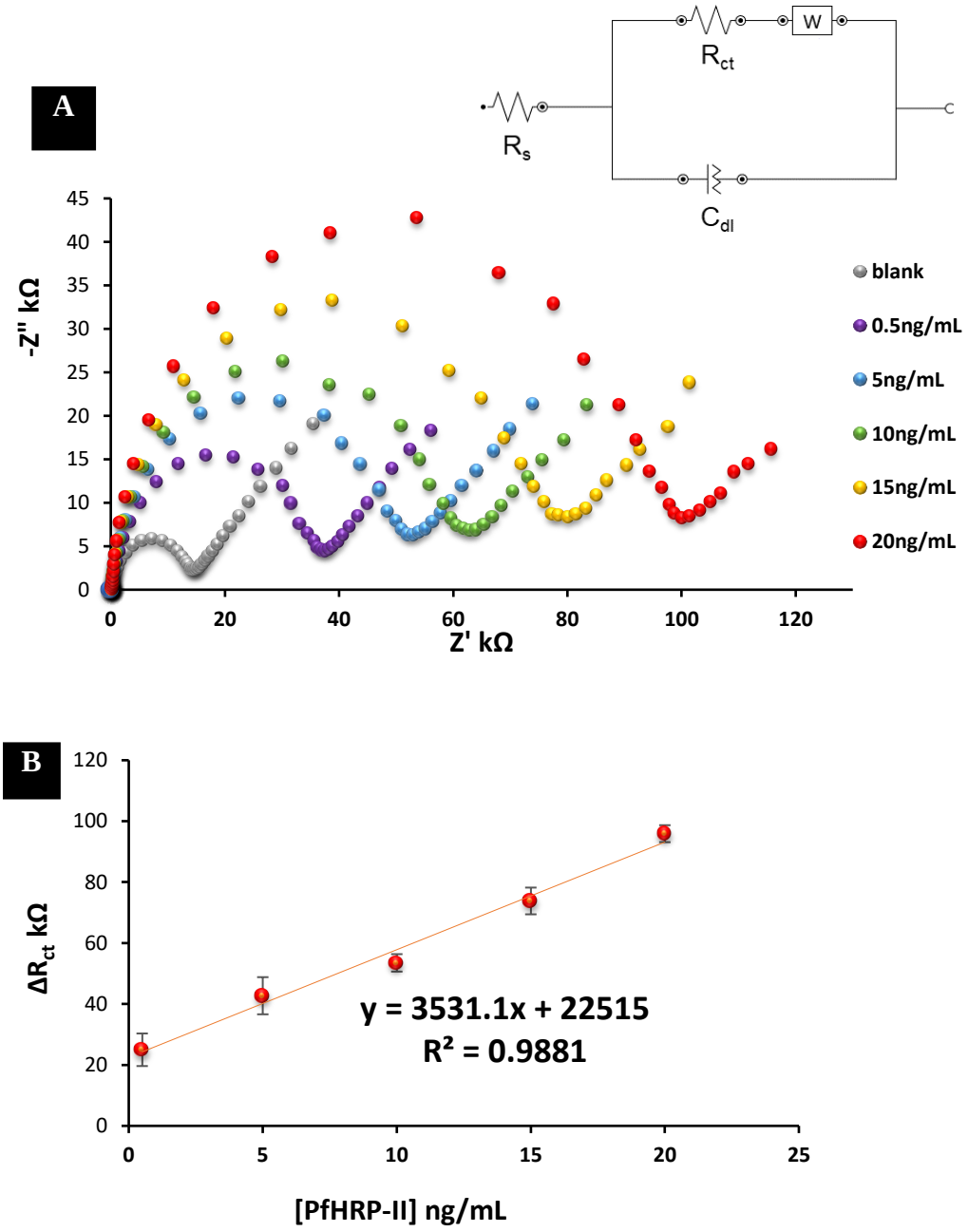

Figure 4. 9 Impedimetric responses of the anti-PfHRP-II/GA-cys/SPGµE sensor Nyquist plot and corresponding calibration curve of *Pf*HRP-II detection in a different batch of electrodes. Each data point is an average of three independent measurements performed in 5mM $[Fe(CN)_6]^{3-/4-}$ and 0.1M KCl aqueous solution (pH 7.4). The Randles equivalent circuit is shown in insert.

A comparison of the performances of selected biosensing technologies for detecting *Pf*HRP-II are summarised in Table 4.1. Compared with the previously published sensing systems, this study demonstrates the proof-of-concept of a relatively lower LoD. This improved performance shows that, impedimetric detection coupled with the efficiency of the GA-cys immobilization methods can enable detection of low concentrations of an analyte. It also implies that *Pf*HRP-II can be low detection limits in biological samples can be sensitively probed of that sensor has prospects of detecting low titres of the *Pf*HRP-II in blood for which many tests cannot detect a positive result.

Table 4. 1 A summary of the selected *Pf*HRP-II biosensors

Sensing platform	Receptor	LoD	Reference
Mercaptopropylphosphonic acid functionalized copper doped zinc oxide nanofibers	anti-*Pf*HRP-II	6.8 ag/mL	(Paul et al., 2016)
Printed gold electrodes functionalized with GNPs	anti-*Pf*HRP-II tagged with HRP	40 pg/mL	(Hemben et al., 2017)
Carbon nanofiber forest grown on glass microballons	anti-HRP-II	25 pg/mL	(Gikunoo et al., 2014)
Nanofiber based flexible chemiresistive biosensor	anti-HRP-II	0.97 fg/mL	(Paul et al., 2017)
Magnetic nanoparticle with graphite-epoxy composite	anti-*Pf*HRP-II	0.36 ng/mL	(De Souza Castilho et al., 2011)
SPE modified with MWCN and Au/MWCN	anti-*Pf*HRP-II	16 ng/mL	(Lillehoj et al., 2013)
magnetic particle-based immunoassay.	anti-*Pf*HRP-II	12 ng/mL	(M. K. Sharma et al., 2011)
Graphite–epoxy composite magneto electrodes	anti-*Pf*HRP-II	0.36ng/mL	(Mukesh K. Sharma et al., 2010)
Mobile based electrochemical immunosensor detector	anti-*Pf*HRP-II	20 ng/mL	(Nemiroski et al., 2014)

4.1.4.4 Reproducibility and stability of the malaria immunosensor

The reproducibility of the immunosensor on different batches of electrodes were investigated for 18 different electrodes across 4 batches (Figure 4.9) and the percent relative standard deviation (%RSD) determined for *Pf*HRP-II (0.5, 5.0, 10.0, 15.0 and 20.0 ng/mL). The RSD for inter-electrode reproducibility ranged between 15.0%-30.0%, and batch-to-batch RSD averaged approximately 30.0%. This indicates that the immunosensor has an acceptable reproducibility.

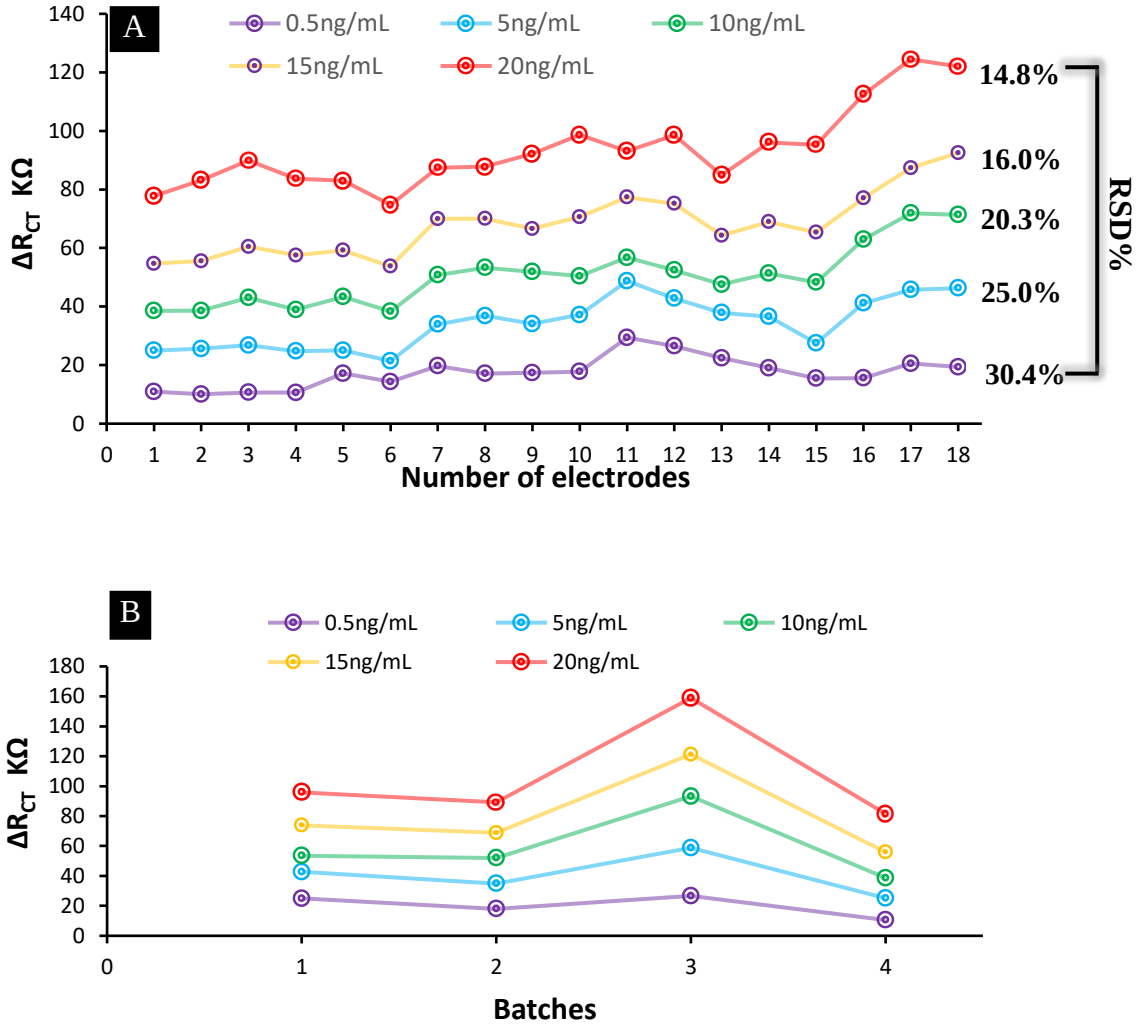

Figure 4. 10 Variations in electrodes batches used for the PfHRP-II sensor.
The (A) electrode-to-electrode and (B) batch-to-batch reproducibility of the sensing system showing ΔR_{ct} of different concentrations of *Pf*HRP-II (0.5-20 ng/mL) measured for 18 selected immunosensors in 0.1 M KCl containing 5 mM $[Fe(CN)_6]^{3-/4-}$. Data point from the batch-to-batch plots consist the means of triplicates from each batch.

4.1.4.5 Conclusions

In summary, a facile, sensitive and efficient immunosensor was developed for the detection of *Pf*HRP-II. Aided by a robust covalent coupling between antibodies and an amine layer GA crosslinking, the sensor produced a turnaround time <30mins. The reliable SAM guided immobilisation provided a highly stable capture of antibodies and a good impedimetric performance compared to physiosorbed antibodies. In comparison to physisorption, covalent linkage of capture molecules showed superior sensitivity and quantified target antigens up to 8-times lower. The combination of SAMs and EIS is an attractive concept for label-free biosensor designs and integration into PoCTs. The simplicity of the method and the good linear relationship between the electron-transfer resistance and increasing *Pf*HRP-II concentrations makes it a prospective tool in detecting malaria and other immunocomplexes involved in other infectious diseases. The low LoD obtained using printed microelectrode was impressive and can be applied for sensitive detection of relevant biomarkers, particularly in the case of malaria where the lack of a sensitive tool for asymptomatic diagnosis is a major drawback in malaria diagnosis. More importantly, the high reproducibility of inter/intra-electrode comparisons makes the SPGµE a potential candidate for multiplexed assay designs. This would allow for the acquisition of multiple analytical parameters from microvolumes of biological fluids simultaneously. In view of the fact that covalent binding provides a much stronger attachment than physical adsorption, further work could use the sensing strategy to analyse the biomarker in patient samples. Although the stability of the immunosensor was not investigated, the RSD which was within 30% demonstrates an acceptable reproducibility of using the SPGµE as a reliable sensor in malaria diagnostics.

4.2 Manuscript 4: Ultrasensitive impedimetric immunosensor for the detection of hepatitis B using gold microelectrodes

Authors: Francis D. Krampa[1,2], Yaw Aniweh[1], Jonathan Adjimani[1,2], Osbourne Quaye[1,2], Gordon A. Awandare[1,2], Prosper Kanyong[1,3].

[1]West African Centre for Cell Biology of Infectious Pathogens (WACCBIP), University of Ghana;

[2]Department of Biochemistry, Cell & Molecular Biology, University of Ghana; [3]Department of Chemistry, Physical & Theoretical Chemistry Laboratory, University of Oxford, Oxford OX1 3QZ, UK

*corresponding author; prosper.kanyong@chem.ox.ac.uk; p.kanyong@waccbip.org

4.2.1 Abstract

Hepatitis B is a viral infection of the liver and a major public health issue. In this proof-of-concept study, a miniaturized immunosensor was developed for highly sensitive detection of hepatitis B surface antigen (HBsAg) using electrochemical impedance spectroscopy (EIS) in conjunction with an in-house disposable screen-printed gold microarray (SPµE). Firstly, a thin-film of cysteamine was self-assembled on the gold microarrays to form cysteamine-activated SPµE, onto which mouse monoclonal anti-HB antibodies was cross-linked with glutaraldehyde. Finally, different concentrations of HBsAg were coupled to the surface-immobilised anti-HB antibodies to form the immunosensor. After coupling HBsAg, the resulting sensing interface changed the charge-transfer resistance (R_{CT}) characteristics of hexacyanoferrate redox couple significantly and responded to increasing concentration of HBsAg (from 0.5 ng/mL – 30.0 ng/mL) in a highly selective and sensitive manner in buffer and human serum samples. The sensor exhibited a limit of detection of 0.7 ng/mL. This strategy of utilizing glutaraldehyde/cysteamine based receptive interface on gold microarrays underpin highly selective target recruitment that can be readily applied to the clinical diagnosis of hepatitis B and extended to a broad of relevant diagnostic biomarkers.

4.2.2 Introduction

Hepatitis B virus (HBV) infection is widespread and amongst the most aggressive viral disease threats to public health globally, similar in scale to tuberculosis, malaria and HIV (Naghavi et al., 2017). It is the leading chronic viral infection affecting about 260 million persons (Schweitzer et al., 2015; WHO, 2017a). The infection is transmitted through contact with body fluids of infected persons and is about 100 times more infective than HIV (Kew, 2012). Complications include cirrhosis and liver cancer. Despite the availability of effective vaccination, the high cost of vaccines hinders widespread uptake in low-income countries. As a result, an annual incidence of 10-30 million new cases with a million deaths (WHO, 2017b) are recorded, about twice the statistics of malaria (Fitzmaurice et al., 2017; WHO, 2016). This persistent risk of HBV therefore necessitates the development of rapid, simple and sensitive detection methods in order to prevent an outbreak of infection.

It is estimated that, only about 10% of people living with hepatitis B infection in high-prevalence and low-to middle-income countries have been diagnosed. The main challenge beside limited awareness and lack of perceived risk are due to insufficient screening and referral to care (Subic & Zoulim, 2018). All the same, identification of new infections and treatment of HBV infection to prevent complicated liver disease and transmission is based solely on screening (Easterbrook, 2016; Scheiblauer et al., 2010).

Screening for HBV infection is based on the detection of surface antigens to the virus (HBsAg: Hepatitis B surface antigen) in serological tests by enzyme immunoassays, commonly ELISA and chemi-luminescence assays (Easterbrook et al., 2017). Using these methods is expensive in low-income settings and cannot be applied to screen individuals at increased risk. Inexpensive point-of-care (POC) for HBsAg in blood and plasma in the form of immunochromatographic rapid diagnostic tests (RDTs) resolved

these limitations (Easterbrook, 2016), nonetheless, enzyme immunoassays still remain more sensitive than RDTs (Scheiblauer et al., 2010).

Viral DNA testing methods among PCR is not available for routine confirmatory or quantitation in low-income countries (WHO, 2016) even though dried blood spots (DBSs) for HBV viral load testing are a good alternative to plasma because of the stability at room temperature, easy handling, storage and transport even in rural areas (Subic & Zoulim, 2018). A number of innovative nucleic acid quantification and genotyping technologies developed for POCs in resources-limited regions include a portable microchip PCR-based HBV-DNA amplification devices (Cho et al., 2006), isothermal amplification (LAMP) technology (Cai et al., 2011; S. Y. Lee et al., 2007) and a nanoplasmonic electrical field-enhanced resonating device (NE2RD) (Inci et al., 2015). However, their inherent limitations (detailed in Chapter 1) and the lack or real time detection prevents the uptake in under-resourced settings.

The diagnostic markers of HBV infection depend on the clinical course. In addition to HBsAg are the HBV envelope antigen (HBeAg), HBV surface antibodies (anti-HBs), HBV core antibodies (anti-HBc) and HBV envelope antibodies (anti-HBe antibodies). In effect, the lack of available tools to probe these markers when necessary may be attributed to underdiagnosis of HBV in these regions. A likely solution would be to develop new PoCTs that target various biomarkers in combination.

This chapter describes steps towards the design of a simple, impedimetric immunoassay based on the robust covalent coupling between antibodies cysteamine/glutaraldehyde linker on disposable gold microelectrodes.

4.2.3 Materials and methods

4.2.3.1 Reagents and apparatus

The hepatitis B surface Bs antigen (HBsAg) and antibody (HBsAb) were purchased from Genetex (Irvine, USA). PBS, ($K_3[Fe(CN)_6]$, $K_4[Fe(CN)_6]$, BSA, Cys, GA (50%) Hellmanex-III, KCl, NaCl and di-Sodium hydrogen phosphate dihydrate were purchased from Sigma–Aldrich (Sigma–Aldrich, UK). Ethanol (99.5%) was obtained from Merck (UK).

4.2.3.2 Fabrication of the immunosensor

Based on the efficacy of the GA-cys covalent crosslinking method for bioreceptor immobilisation, the immunosensor fabrication is similar to the previous chapter (Chapter IV). Figure 5.1 describes the preparation procedure of HBsAb/GA-cys/SPGμE and the general scheme of the HBsAg immunosensor. Briefly, the gold microelectrodes were first cleaned in 50% Hellmanex III solution (1:1 v/v Hellmanex III:ddH2O). Following that, the SPGμE was incubated in 20.0 mM cysteamine (prepared in absolute ethanol) for 1.5 hr to generate amine self-assembled monolayers (SAMs), accompanied with further incubation in 2.5% glutaraldehyde (prepared in ddH_2O) to form the GA-cys/SPGμE. Finally, 8.0 μL of 200 μg/mL of HBsAb (in PBS, pH 7.4) was casted over the working area of the modified SPGμE and incubated overnight at 4°C under controlled-humidity conditions. The resultant HBsAb/GA-cys/SPGμE, was rinsed with ddH_2O to remove excess unbound antibodies. BSA (2% in PBS) was used to block the sensor surface and prevent nonspecific binding for 20 mins at 37°C after which it was rinsed with ddH_2O and air-dried. The functionalised sensors were stored at 4°C when not in use. The schematic diagram of the immunosensor preparation and its working principle is illustrated in Figure 5.1.

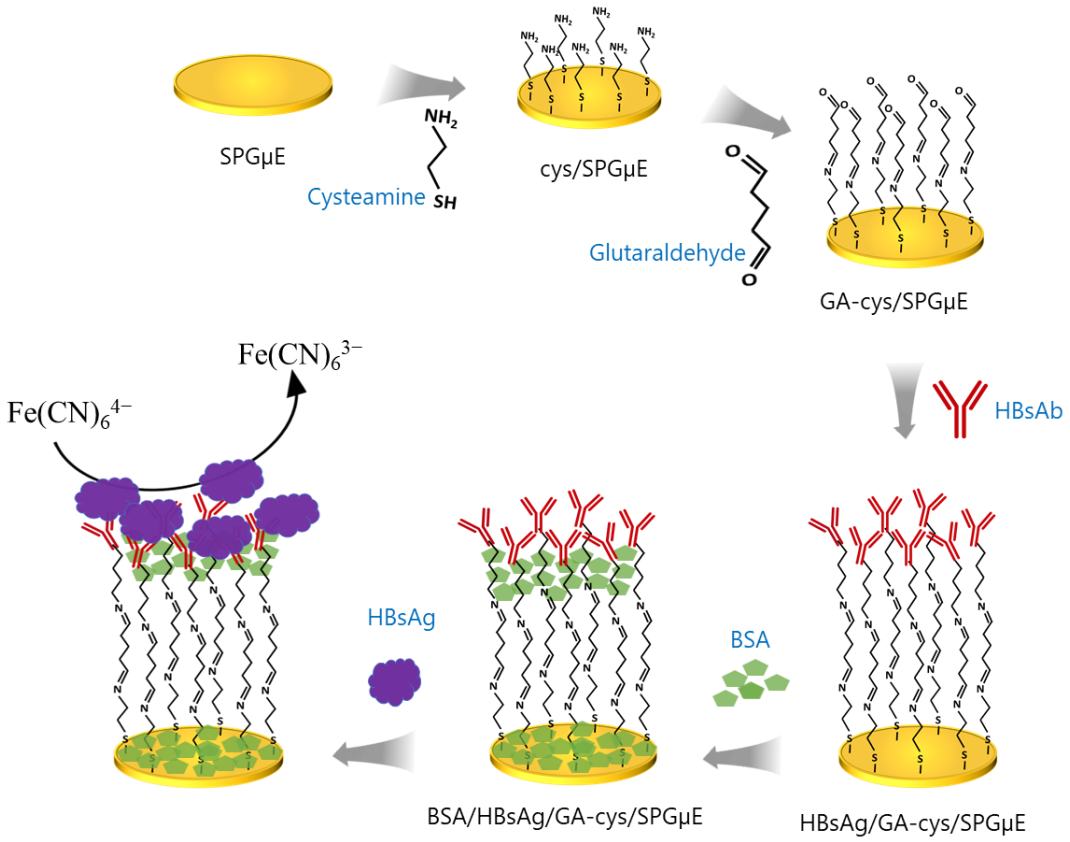

Figure 5. 1 Schematic representation of the stepwise development of the HBsAg immunosensor

Schematic representation of the stepwise des for the development of the label-free HBsAg immunosensor using a gold microelectrode crosslinked with antibodies through cysteamine -glutaraldehyde. BSA: bovine serum albumin

4.2.3.3 Detection of HBsAg

Recombinant HBsAg was prepared in sodium phosphate buffer (200 mM Na_2HPO_4 and 30 mM sodium chloride, pH 9.4) after which 8.0 µL of varying concentrations of HBsAg; 0.5-30.0 ng/mL was incubated with the sensor for 20 mins at 37 ^oC. Electrochemical detection of HBs-Ab-HBsAg interactions was accomplished using 1X PBS (pH 7.4) containing 5.0 mM $[Fe(CN)_6]^{3-/4-}$ redox probe and 0.1M KCl as electrolyte. Electrochemical impedance spectroscopy (EIS) data was acquired using an

applied AC amplitude of 10.0 mV rms, DC potential of 0.24 V and a frequency range of 100 kHz - 0.05 Hz. Frequency responses of the electrochemical system was represented through Nyquist plots (Z' vs Z'') and the electron-transfer resistance (R_{ct}) values were extracted from the Nyquist plots using relevant Randle's equivalent circuits to fit acquired Nyquist plots using NOVA 2.1 software.

4.2.4 Results

4.2.4.1 Characterisation of the immunosensor

EIS responses for the stepwise immunosensor assembly is shown in Figure 5.2. Cysteamine modification showed a decrease in the R_{ct} than the bare electrode which can be explained by the positive charges of amine groups in cysteamine that tends to facilitate charge transfer (Sharma et al., 2018). The addition of antibodies and BSA significantly increased the R_{ct}, indicating the successful immobilisation of HBsAb and the blocking step, respectively. The data was fitted to a Randles equivalent circuit, comprising solution resistance, (Rs), the double layer capacitance (C_{dl}), and the Warburg impedance (W). As shown in Fig. 3, the values of the R_{ct} varied depending on the different modification to the electrode surface.

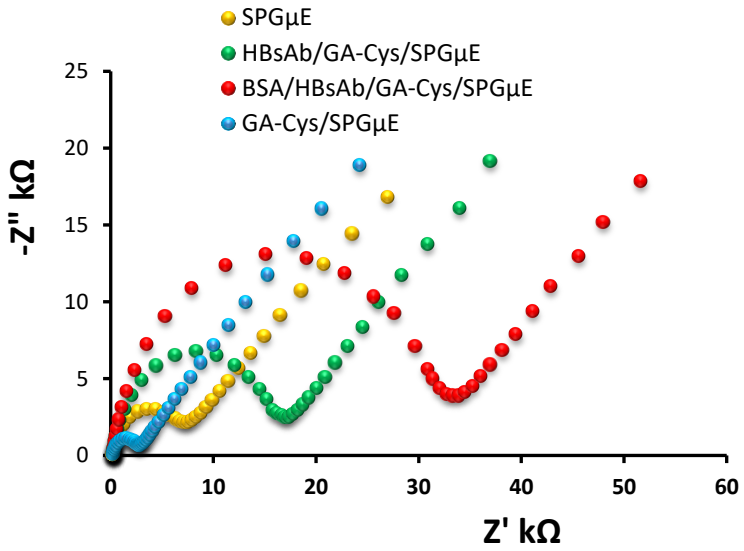

Figure 5. 2 Nyquist plots observed for EIS at at different stages of HBsAg sensor development.
EIS obtained in 5.0 mM $[Fe(CN)_6]^{3-/4-}$ and 0.1 M KCl for bare SPGµE, GA-cys, SPGµE, HBsAg/GA-cys/SPGµE and BSA/HBsAg/GA-cys/SPGµE.

4.2.4.2 Detection of HBsAg

To evaluate the suitability of the immunosensor in HBsAg detection, a calibration of the HBsAg was performed in buffer. Nyquist plots show that the sensor responded rapidly to different antigen concentrations (figure 5.3A). The corresponding calibration curve for HBsAg detection is shown in Figure 5.3B. A strong linear relationship (R^2 =0.986) (Figure 5.3B) for HBsAg concentrations was recorded from 0.5 ng/mL to 30.0 ng/mL with sensitivity of $2.8x10^9$ Ω/(g/mL)cm^2 and calculated limit of detection of 0.7 ng/mL. This low detection limit and wide linear range are superior to published sensors for HBsAg, which tended to have reduced linear range and/or poor detection limits (Table 5.1).

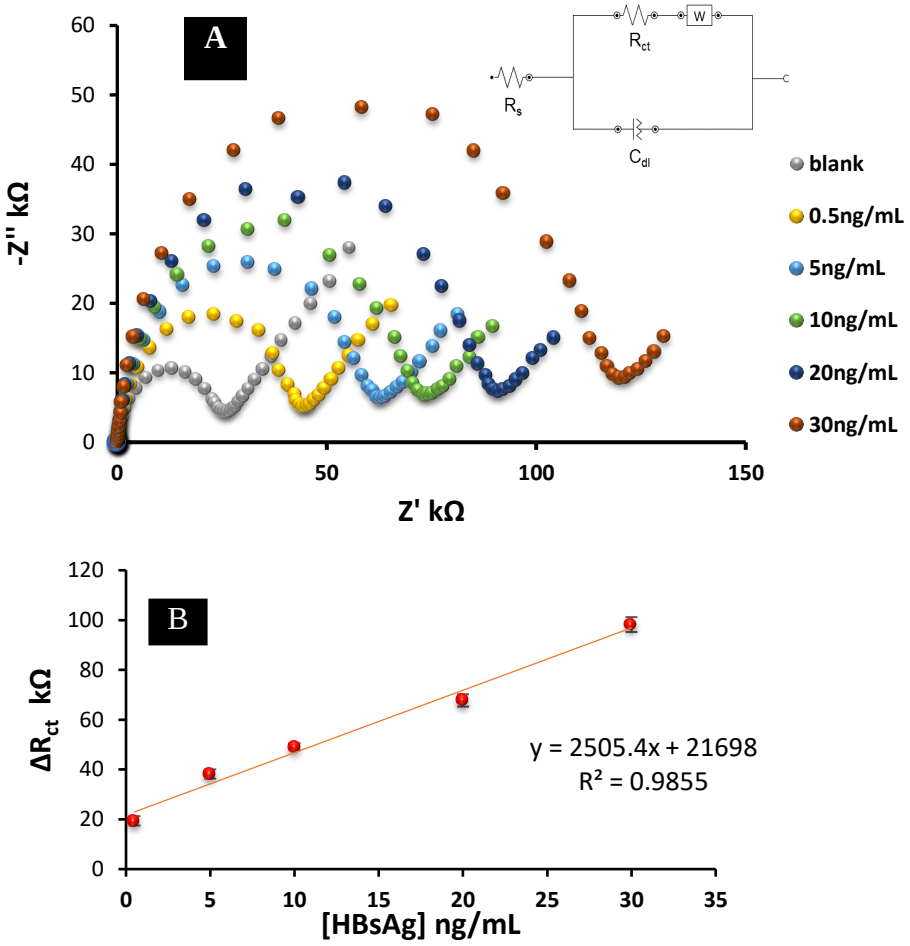

Figure 5. 3 Impedimetric response of the anti-HBsAb/GA-cys/SPGµE sensor
(A) Nyquist plots of the BSA/HBsAb/GA-cys/SPGµE with different concentrations of HBsAg from 0.5 to 30.0 ng/mL (B) Corresponding calibration curve for HBsAg. Error bars represent one standard deviation across three independent measurements.

Table 5. 1 Selected sensors developed for HBsAg detection

Platform	LoD	Author
Optical biosensor	7 ng/mL	(Tam et al., 2017)
AuNP-based biomolecular immobilization	1.3 ng/mL	(Tang et al., 2004)
CuO nanocomposite	1.8 ng/mL	(Ehsani et al., 2017)
CuO/MWCNT nanocomposite	0.85 ng/nL	
Multi-functionalized gold nanoparticles	0.358 pg/mL	(Shourian et al., 2015)
GA-cys crosslinked gold microelectrode	0.7 ng/mL	Current study

4.2.4.3 Selectivity

An advantage of using protein molecules as recognition elements in immunosensors is that, they bind targets with high selectivity. However, immunocomplexes may be liable to non-specific interactions which result in undesirable signals. This a problem is often encountered with biological samples as they contain copious amounts of proteins. Having determined that the immunosensor detected target antigens with high sensitivity and at low limits of detection, the possibility of cross-reactivity or non-specific interactions between HBsAb and other proteins was investigated. In this context, an interference assessment of the immunosensors specificity and selectivity for HBsAg was therefore investigated in a controlled experiment by incubating the prepared BSA/HBsAb/GA-cys/SPGμE with; BSA (10.0 ng/mL), HBsAb (10.0 ng/mL), HBsAg (10.0 ng/mL), and *Plasmodium falciparum* histidine rich-protein-II (PfHRP-II, 10.0 ng/mL), antibodies to *Plasmodium falciparum* histidine rich-protein-II (anti-PfHRP-II, 10.0 ng/mL) and a mixed solution 5.0 ng/mL of HBsAg prepared in 10.0 ng/mL BSA and the observation is illustrated in Figure 5.4.

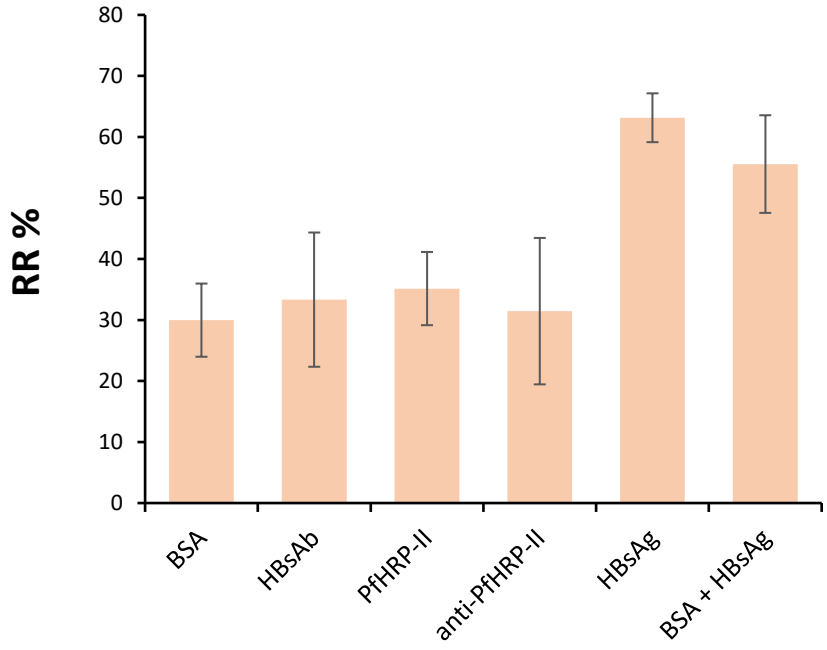

Figure 5. 4 Selectivity of the Hepatitis B immunosensor.
Selectivity of the developed sensor demonstrated by the % relative responses (%RR) of the target and some interfering proteins (BSA, PfHRP-II and anti-PfHRP-II) to examine cross-reactivity of the HBsAg immunosensor. %RR = ($\Delta R_{ct}/R_{ct}$) ×100; Error bars represent one standard deviation across three independent measurements.

The ΔR_{ct} measurements did not demonstrate any significant variations for BSA, HBsAb, PfHRP-II, and anti-*Pf*HRP-II. The specificity of the HBsAg sensor from the relative response graph (Figure 5.4) shows that the maximum responses of the BSA/HBsAb/GA-cys/SPGµE were against HBsAg and a mixture BSA + HBsAg (63% and 56% respectively). The responses for interfering proteins were around 30%. This suggests the specificity of the immunosensor towards the desired target, HBsAg and a satisfactory selectivity in the presence of other contaminating proteins.

4.2.5 Conclusions

A simple, impedimetric immunoassay of high sensitivity was developed for the detection of HBsAg based on the covalent coupling between monoclonal antibodies and gold-cysteamine interface through a glutaraldehyde linker. The sensor was label-free and highly selective in the presence of other proteins. This strategy of utilising glutaraldehyde/cysteamine based receptive interface on gold microelectrodes underpin highly selective target recruitment that can be readily applied to the clinical diagnosis of hepatitis B and other relevant biomarkers in clinical samples.

CHAPTER 5

DISCUSSIONS, CONCLUSIONS AND FUTURE PERSPECTIVE

5.1 General discussions

In an era where diagnostics has been revolutionised by nanotechnology, biosensors are forecasted as the next generation POCTs. The manifestations of its progress is exemplified in personalised blood glucose testing and many wearable devices (Bandodkar & Wang, 2014; Gawali & Wadhai, 2018; Lee et al., 2017). Biosensors have the capability to replace the traditional analytical methods by simplifying or eliminating sample preparation and making field-testing easier and faster at a significantly lower cost (Gan et al., 2010; Oujji et al., 2012).

In search for an alternative diagnostic strategy, this thesis proposed the development of a label-free electrochemical biosensor for infectious disease diagnostic application. The first objective sought to determine the suitability of printed electrodes as a base transducer, which is a fundamental to all sensing interfaces. For this purpose, SPEs were preferred to traditional electrodes in terms of its miniaturized dimensions suitable for potable electroanalytical systems. Other advantages of working with SPEs is that they allow for *in situ* analysis at low-cost through the advancements in screen-printing technologies.

However, printed electrodes are subject to differences in their printing layer which could possibly affect the electron transfer reactivity and overall analytical performance of the sensing platform. Also, since the ink characteristics are the proprietary information of the manufacturer alone, the electrochemical characteristics of the electrodes were evaluated. Voltammetric analysis of the SPCEs demonstrated clear

redox peaks in ferrocyanide solution, suggesting that the electrode did not require pre-conditioning stood response that did not require electrode pre-conditioning (Cui et al., 2001; Wang & Ploehn, 1996). SEM images showed a continuous layer of printed particles of heterogeneous sizes.

It is well-known that the carbon based sensors or electrodes are widely applied in electrochemical analysis because of its suitable properties for various sensing applications (Kirgoz et al., 2007; Ramírez-García et al., 2002). Almost all carbon-based materials are applicable in chemical or biological sensor development whether used bare or modified (Davis et al., 2003; Gilmartin & Hart, 1995; Liu et al., 2012). The next stage after investigating the electrochemical transduction properties was to enhance its signal transduction, which was achieved by modifying the working electrode surfaces with nanostructured materials and conductive polymers.

The novel nanocomposites from this study showed great improvements in signal transduction up to 10-fold increases in peak currents for the 20%IL/PEDOT:PSS nanocomposite (Krampa et al., 2017a) and 40-fold in GNP/Nafs (Krampa et al., 2018). There were also obvious negative and positive shifts in the peak potentials after modification, resulting in smaller peak-to-peak separation. Similar reports elsewhere, found improved signal transduction properties for electrodes modifies with; PANI-graphene (Fan et al., 2011), PPy–graphene (Gao et al., 2014), PEDOT/graphene oxide nanosheet (Mao et al., 2015), PEDOT/rGO (Wang et al., 2014), PEDOT/graphene (Lu et al., 2013) and GNPs/PEDOT:PSS (Cataldi et al., 2018). These nanocomposites consist conductive materials that work in synergy to enhancing the surface chemistry of the transduction platform for rapid electron transfer.

The novel smart-conducting surfaces demonstrated applicability in sensitive chemical sensing. The IL/PEDOT:PSS composite was used to probe catechol from environmental with high precision and accuracy.

Similarly, the suitability of the GNP/Nafs for analysis of inorganic and organic compounds was also demonstrated similar to other studies have been demonstrated (Kirgoz et al., 2007; Lamas-Ardisana et al., 2008; Li et al., 2007; Arribas et al., 2013).

Simultaneous and selective detection systems have become a growing trend in electroanalysis and as such, the GNP/Nafs composite showed an excellent performance in simultaneous detection of paracetamol and dopamine. Trace concentrations of these physiologically important analytes were detectable simultaneously in urine. As shown in Table 3.2, the analytical performance of the nanostructured surfaces was superior to other graphene-based sensing platforms.

For the third and fourth objectives, two proof-of concept immunosensors were developed for malaria and hepatitis B. In the malaria sensor, different immobilization strategies; physisorption, polydopamine anchorage and covalent cross-linkage were tested to anchor antibodies on gold microelectrodes. Covalent crosslinking of antibodies onto gold electrode provided the most stable and sensitive immunosensor for PfHRP-II antigens. More specifically, the sensing platform comprised of the formation of an amine SAM on the gold microelectrode followed by crosslinking of anti-PfHRP-II antibodies using glutaraldehyde. Electrochemical impedance spectroscopy (EIS) was used in the presence of ferrocyanide redox probe to monitor the immunocomplex between capture antibodies and target PfHRP-II antigens. The malaria sensor was highly reproducible and exhibited an impressive LoD, superior to

POC immune chromatographic tests which is usually ~16 nM and other sewnsing strategies reported in literature (Table 4.1).

Furthermore, based on the architectural design of the malaria sensor, the platform was repurposed for the detection of hepatitis B surface antigens. The hepatitis B sensor was also found to be highly sensitive and specific.

The stability of this immobilisation strategy, in addition to the devised label-free assay format, offer a simple and low-cost biosensing approach which can be extended to detection of any clinical biomarker of interest for diagnostics applications.

It is worth mentioning that another valuable lessons that could be learnt from this thesis is the convenience of targeting protein biomarkers. Most emerging techniques focus on genosensors based on DNA hybridisation. While genosensors provide a better specificity and avoid cross-reactivity from a diagnostic view point, systems that detect DNA would require highly specific conditions of sample pre-treatment to extract and purify nucleic acids before an assay. These requirements may complicate the assay procedure. Proteins, on the other hand, freely circulate as antigens or antibodies in samples and can form immunocomplexes directly with an immobilised receptor which can be detected directly as proven in the label-free biosensors developed in this study. In combination with impedimetric methods, protein biomarkers could be better suited for the development of self-contained, simple, one-step sensing strategy appropriate for the next generation POCTs.

5.2 Conclusions

In summary, this thesis contributed towards two main areas of the ongoing endeavours in biosensing research. The first takes advantage of the electrocatalytic properties of conductive polymers and nanomaterials to develop high performing platforms for environmental, pharmaceutical and biomedical applications. Smart conducting IL/PEDOT:PSS and GNP-Naf were successfully used as novel electrochemical transducers. The highly stable IL/PEDOT:PSS nanocomposites exhibited a good catalytic effect towards the oxidation-reduction of catechol. GNP-Naf provides a new approach for the simultaneous electrochemical detection of dopamine and acetaminophen; and broadens the application of graphene-based nanomaterials materials in the analysis of biological samples.

The second contribution entails the development of a simple, label-free and ultrasensitive immunosensor for infectious disease diagnostic applications. Preliminary data from the proof-of-concept studies demonstrate robustness and suggests the development of high performing sensing platforms for sensitive and selective analyte detection impedimetric immunosensors for the detection of malaria and hepatitis B antigens.

5.3 Perspective and further work

Nanotechnology has widened the scope for the development of (bio)sensors, with the integration of nanocomposites and printed disposable electrodes contributing to high performing but affordable POC devices. In addition to the generally low cost of printed electrodes, conductive polymers and nanocomposites can be incorporated into carbon or graphite-based inks for screen-printing to enable mass production at relatively low-cost. Label-free immunosensing in electrochemical systems without the use of additional reagents, suggest the possibility of rapid self-contained sensing systems. Considering that, screen-printed electrodes enable miniaturisation of such platforms, a combination of printed electrodes in conjunction with nanocomposites and label-free assay strategies represent a perfect biosensing system.

Although nanocomposite-modified screen-printed electrodes were developed for sensitive analysis of catechol, DA and APAP, their use as a platform for biosensing cannot be adequately discerned from the study. In contrast to the bare gold electrode that freely interact with sulphur atoms in cysteamine, the thin layer nanocomposite-modified carbon electrodes as a base transducer for SAMs modification and glutaraldehyde crosslinking of capture proteins needs further investigation. Accordingly, work from Chapter 3 should be continued in the framework of immobilizing capture/biorecognition molecules on nanocomposite-modified electrodes for biosensor development. Since many conductive polymers may not be biocompatible, it should be done in context to find a good compromise between acceptable biocompatibility as improved electrical conductivity as well as finding a good immobilization strategy. This should be done in the context of finding an appropriate immobilisation strategy. Nevertheless, the suggested approach builds a promising platform for methodologies requiring immunocomplex formation. The

impressive LoDs demonstrated by the malaria and hepatitis B immunosensors could also suggest their usefulness in probing lower titres of the biomarkers in asymptomatic cased and outside blood in an attempt for non-invasive and painless testing.

For the malaria and hepatitis B immunosensors presented in Chapters 4, two focal areas need improvement and further investigation. Firstly, the covalent immobilisation strategy applied, are based on randomly scattered amine groups on the antibody surface and therefore, does not guarantee the desired orientation. Considering the effects of antibody orientation on a sensor's sensitivity, further experiments would be required to improve the orientation of the capture antibodies. These could include the preparation of Fab fragments of antibodies or the application of bio-affinity interactions. Secondly, the sensors must be tested in physiological fluids (blood/serum, saliva, urine and other bodily fluids) in order to determine interferents that can hinder interactions between biorecognition molecules and target biomarkers

With the current advances in miniaturized electrodes and potentiostats, the achievements from this work and its recommendations for further research can be adopted to develop array-based multiplexed systems or lab-on-chip techniques. These when combined, could drive the development of rapid, cost efficient, high throughput, miniaturised and automated immunosensing devices to fulfil the needs in the health care delivery and disease diagnostics in resource-limited areas.

In anticipation of the first immunosensor in the near future, a prospective point-of-care system that fully integrates screen-printed microarray electrodes with robust immobilisation of biomolecules for multiplexed detection of infectious diseases biomarkers is illustrated in figure 5.1.

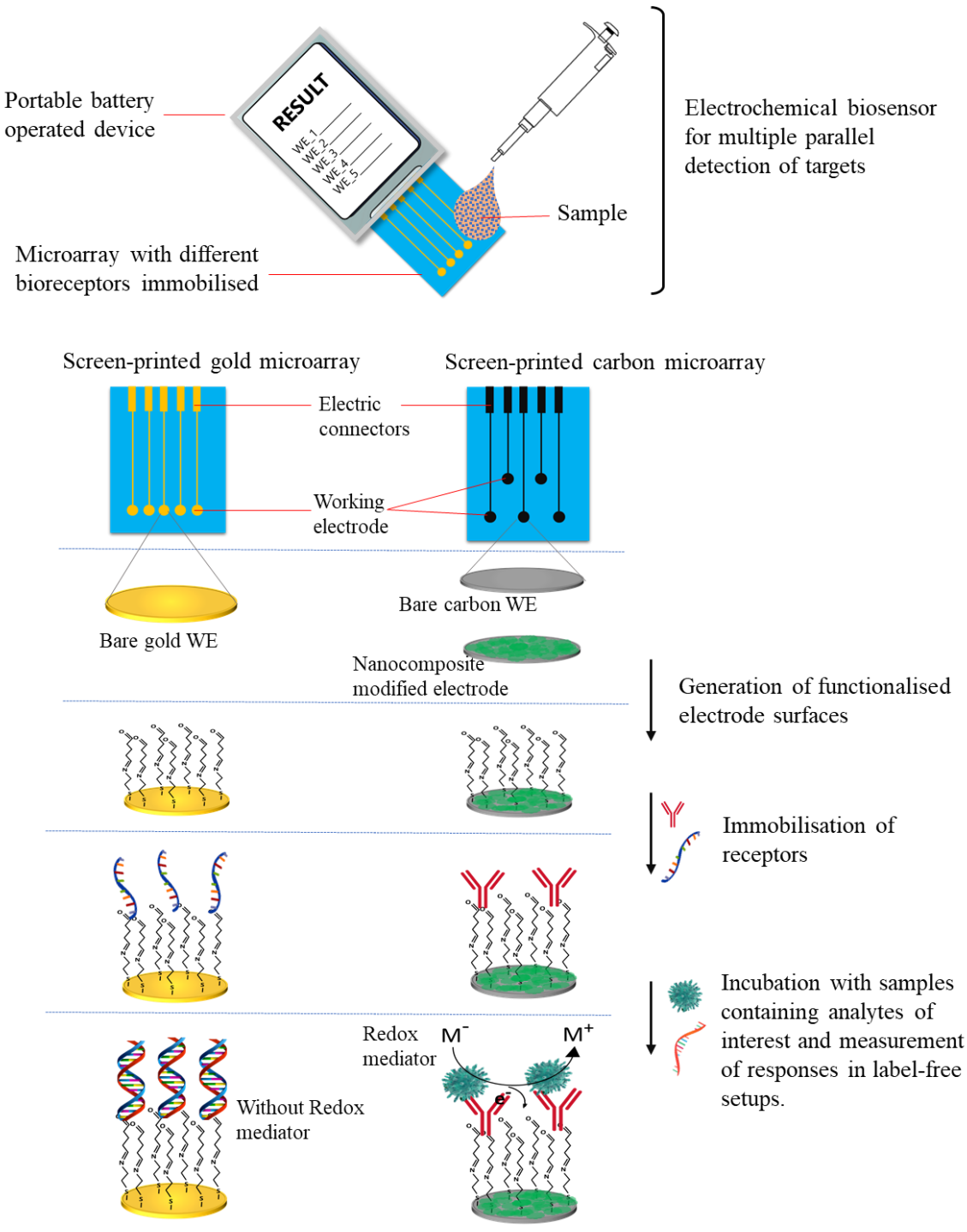

Figure 6. 1 Schematic of a label-free multiplexed immunosensor
A self-contained analytical system integration screen-printed microarray electrode with multiple capture biomolecules to target different analytes in a sample. Label-free detection of the analytes can be achieved either in the presence of a redox mediator (bottom right; eg. impedance biosensors) or direct detection of the binding affinity between molecules and the sensor surface (bottom left; eg. capacitive biosensors).

REFERENCES

Adams, R. N. (1958). Carbon Paste Electrodes - Analytical Chemistry. *Anal. Chem.* https://doi.org/10.1021/ac60141a600

Adhikari, B. R., Govindhan, M., Schraft, H., & Chen, A. (2016). Simultaneous and sensitive detection of acetaminophen and valacyclovir based on two dimensional graphene nanosheets. *Journal of Electroanalytical Chemistry*. https://doi.org/10.1016/j.jelechem.2016.09.023

Ahmad, Amreen, Verma, A. K., Krishna, S., Sharma, A., Singh, N., & Bharti, P. K. (2019). Plasmodium falciparum glutamate dehydrogenase is genetically conserved across eight malaria endemic states of India: Exploring new avenues of malaria elimination. *PLoS ONE*. https://doi.org/10.1371/journal.pone.0218210

Ahmad, Azrilawani, & Moore, E. (2012). Electrochemical immunosensor modified with self-assembled monolayer of 11-mercaptoundecanoic acid on gold electrodes for detection of benzo[a]pyrene in water. *Analyst*. https://doi.org/10.1039/c2an35236b

Alkire, S., Chatterjee, M., Conconi, A., Suman, S., & Vaz, A. (2014). Poverty in Rural and Urban Areas Direct comparisons using the global MPI 2014. *Oxford Poverty and Human Development Initiative*.

Amexo, M., Tolhurst, R., Barnish, G., & Bates, I. (2004). Malaria misdiagnosis: Effects on the poor and vulnerable. *Lancet*, Vol. 364, pp. 1896–1898. https://doi.org/10.1016/S0140-6736(04)17446-1

Andryukov, B. G., Besednova, N. N., Romashko, R. V., Zaporozhets, T. S., & Efimov, T. A. (2020). Label-free biosensors for laboratory-based diagnostics of infections: Current achievements and new trends. *Biosensors*. https://doi.org/10.3390/bios10020011

Arduini, F., Amine, A., Majorani, C., Di Giorgio, F., De Felicis, D., Cataldo, F., … Palleschi, G. (2010). High performance electrochemical sensor based on modified screen-printed electrodes with cost-effective dispersion of nanostructured carbon black. *Electrochemistry Communications*. https://doi.org/10.1016/j.elecom.2009.12.028

Arduini, F., Di Nardo, F., Amine, A., Micheli, L., Palleschi, G., & Moscone, D. (2012). Carbon Black-Modified Screen-Printed Electrodes as Electroanalytical Tools. *Electroanalysis*. https://doi.org/10.1002/elan.201100561

Arduini, F., Forchielli, M., Amine, A., Neagu, D., Cacciotti, I., Nanni, F., … Palleschi, G. (2014). Screen-printed biosensor modified with carbon black nanoparticles for the determination of paraoxon based on the inhibition of butyrylcholinesterase. *Microchimica Acta*. https://doi.org/10.1007/s00604-014-1370-y

Arduini, F., Micheli, L., Moscone, D., Palleschi, G., Piermarini, S., Ricci, F., & Volpe, G. (2016). Electrochemical biosensors based on nanomodified screen-printed electrodes: Recent applications in clinical analysis. *TrAC - Trends in Analytical Chemistry*. https://doi.org/10.1016/j.trac.2016.01.032

Arora, P., Hammes, G. G., & Oas, T. G. (2006). Folding mechanism of a multiple independently-folding domain protein: Double B domain of protein A. *Biochemistry*. https://doi.org/10.1021/bi060923s

Arora, P., Sindhu, A., Dilbaghi, N., & Chaudhury, A. (2011). Biosensors as innovative tools for the detection of food borne pathogens. *Biosensors and Bioelectronics*. https://doi.org/10.1016/j.bios.2011.06.002

Arribas, A., Martínez-Fernández, M., Moreno, M., Bermejo, E., Zapardiel, A., & Chicharro, M. (2013). Analysis of total polyphenols in wines by FIA with highly stable amperometric detection using carbon nanotube-modified electrodes. *Food Chemistry*, *136*(3–4), 1183–1192. https://doi.org/10.1016/j.foodchem.2012.09.027

Bahadir, E. B., & Sezgintürk, M. K. (2015). Applications of commercial biosensors in clinical, food, environmental, and biothreat/biowarfare analyses. *Analytical Biochemistry*, *478*(March), 107–120. https://doi.org/10.1016/j.ab.2015.03.011

Bandodkar, A. J., & Wang, J. (2014). Non-invasive wearable electrochemical sensors: A review. *Trends in Biotechnology*. https://doi.org/10.1016/j.tibtech.2014.04.005

Bard, A., Faulkner, L., Leddy, J., & Zoski, C. (1980). *Electrochemical methods: fundamentals and applications*. Retrieved from https://sci-hub.tw/http://fora.aa.ufl.edu/docs/47/20sept11/ucc_20sept11_abe5xxx.pdf

Bell, D, & Peeling, R. W. (2006). Evaluation of rapid diagnostic tests: malaria. *Nature Reviews Microbiology*, (September), S34–S40. https://doi.org/Doi 10.1038/Nrmico1524

Bell, David, Wongsrichanalai, C., & Barnwell, J. W. (2006). Ensuring quality and access for malaria diagnosis: how can it be achieved? *Nature Reviews. Microbiology*, *4*(9), 682–695. https://doi.org/10.1038/nrmicro1474

Belluzo, M., Ribone, M., & Lagier, C. (2008). Assembling Amperometric Biosensors for Clinical Diagnostics. *Sensors*. https://doi.org/10.3390/s8031366

Ben Rejeb, S., Tatoulian, M., Arefi Khonsari, F., Fischer Durand, N., Martel, A., Lawrence, J. F., … Le Goffic, F. (1998). Functionalization of nitrocellulose membranes using ammonia plasma for the covalent attachment of antibodies for use in membrane-based immunoassays. *Analytica Chimica Acta*. https://doi.org/10.1016/S0003-2670(98)00452-8

Blaschke, A. J., Hersh, A. L., Beekmann, S. E., Ince, D., Polgreen, P. M., & Hanson, K. E. (2015). Unmet diagnostic needs in infectious disease. *Diagnostic Microbiology and Infectious Disease*, *81*(1), 57–59. https://doi.org/10.1016/j.diagmicrobio.2014.10.005

Bogomolova, A., Komarova, E., Reber, K., Gerasimov, T., Yavuz, O., Bhatt, S., & Aldissi, M. (2009). Challenges of electrochemical impedance spectroscopy in protein biosensing. *Analytical Chemistry*. https://doi.org/10.1021/ac9002358

Boozer, C., Ladd, J., Chen, S., Yu, Q., Homola, J., & Jiang, S. (2005). DNA directed protein immobilization on mixed ssDNA/oligo(ethylene glycol) self-assembled monolayers for sensitive biosensors. *Analytical Chemistry*. https://doi.org/10.1021/ac048908l

Brent, A. J., Ahmed, I., Ndiritu, M., Lewa, P., Ngetsa, C., Lowe, B., … Scott, J. A. G. (2006). Incidence of clinically significant bacteraemia in children who present to hospital in Kenya: Community-based observational study. *Lancet*. https://doi.org/10.1016/S0140-6736(06)68180-4

Bristow, C. C., Adu-Sarkodie, Y., Ondondo, R., Bukusi, E. A., Dagnra, A., Oo, K. Y., … R.V., C. (2014). MULTI-SITE LABORATORY EVALUATION OF THE SD BIOLINE DUO HIV/SYPHILIS DUAL POINT-OF-CARE RAPID TEST. *Sexually Transmitted Diseases*.

Britton, S., Cheng, Q., & McCarthy, J. S. (2016). Novel molecular diagnostic tools for malaria elimination: A review of options from the point of view of high-throughput and applicability in resource limited settings. *Malaria Journal*, 1–8. https://doi.org/10.1186/s12936-016-1158-0

Brockman, S. (2012). Basics of Electrochemical Impedance Spectroscopy. *Application Note*.

Budai, D. (2010). Carbon Fiber-based Microelectrodes and Microbiosensors. In *Intelligent and Biosensors*. https://doi.org/10.5772/7158

Buerk, D, G. (1993). *Biosensors. Theory and applications*. Retrieved from https://scholar.google.com/scholar?hl=en&q=Buerk%2C+D.+G.+Biosensors.+Theory+and+Applications%3B+Technomic+Publishing+Co.%2C+Inc.%3A+Lancaster%2C+1993&btnG=&as_sdt=1%2C5&as_sdtp=

Cai, Z., Lou, G., Cai, T., Yang, J., & Wu, N. (2011). Development of a novel genotype-specific loop-mediated isothermal amplification technique for Hepatitis B virus genotypes B and C genotyping and quantification. *Journal of Clinical Virology*. https://doi.org/10.1016/j.jcv.2011.08.013

Caliendo, A. M., Gilbert, D. N., Ginocchio, C. C., Hanson, K. E., May, L., Quinn, T. C., … Jackson, A. F. (2013). Better Tests, Better Care: Improved Diagnostics for Infectious Diseases. *Clinical Infectious Diseases*, *57*(Suppl 3), 139–170. https://doi.org/10.1093/cid/cit578

Cançado, L. G., Takai, K., Enoki, T., Endo, M., Kim, Y. A., Mizusaki, H., … Pimenta, M. A. (2008). Measuring the degree of stacking order in graphite by Raman spectroscopy. *Carbon*. https://doi.org/10.1016/j.carbon.2007.11.015

Cao, X., Ye, Y., & Liu, S. (2011). Gold nanoparticle-based signal amplification for biosensing. *Analytical Biochemistry*. https://doi.org/10.1016/j.ab.2011.05.027

Castro-Sesquen, Y. E., Kim, C., Gilman, R. H., Sullivan, D. J., & Searson, P. C. (2016). Nanoparticle-Based Histidine-Rich Protein-2 Assay for the Detection of the Malaria Parasite Plasmodium falciparum. *American Journal of Tropical Medicine and Hygiene*, *95*(2), 354–357. https://doi.org/10.4269/ajtmh.15-0772

Cataldi, P., Athanassiou, A., & Bayer, I. (2018). Graphene Nanoplatelets-Based Advanced Materials and Recent Progress in Sustainable Applications. *Applied Sciences*. https://doi.org/10.3390/app8091438

Cerami, C., Frevert, U., Sinnis, P., Takacs, B., Clavijo, P., Santos, M. J., & Nussenzweig, V. (1992). The basolateral domain of the hepatocyte plasma membrane bears receptors for the circumsporozoite protein of plasmodium

falciparum sporozoites. *Cell*. https://doi.org/10.1016/0092-8674(92)90251-7

Chaubey, A., & Malhotra, B. D. (2002). Mediated biosensors. *Biosensors and Bioelectronics*, Vol. 17, pp. 441–456. https://doi.org/10.1016/S0956-5663(01)00313-X

Cho, Y. K., Kim, J., Lee, Y., Kim, Y. A., Namkoong, K., Lim, H., … Ko, C. (2006). Clinical evaluation of micro-scale chip-based PCR system for rapid detection of hepatitis B virus. *Biosensors and Bioelectronics*. https://doi.org/10.1016/j.bios.2005.10.005

Cinti, S., Arduini, F., Moscone, D., Palleschi, G., & Killard, A. J. (2014). Development of a hydrogen peroxide sensor based on screen-printed electrodes modified with inkjet-printed prussian blue nanoparticles. *Sensors (Switzerland)*. https://doi.org/10.3390/s140814222

Clausmeyer, J., Schuhmann, W., & Plumeré, N. (2014). Electrochemical patterning as a tool for fabricating biomolecule microarrays. *TrAC - Trends in Analytical Chemistry*. https://doi.org/10.1016/j.trac.2014.03.004

Compton, R. G., Laborda, E., & Ward, K. R. (2013). Understanding voltammetry: Simulation of electrode processes. In *Understanding Voltammetry: Simulation of Electrode Processes*. https://doi.org/10.1142/P910

Cordeiro, T. A. R., Gonçalves, M. V. C., Franco, D. L., Reis, A. B., Martins, H. R., & Ferreira, L. F. (2019). Label-free electrochemical impedance immunosensor based on modified screen-printed gold electrodes for the diagnosis of canine visceral leishmaniasis. *Talanta*. https://doi.org/10.1016/j.talanta.2018.11.087

Corgier, B. P., Marquette, C. A., & Blum, L. J. (2005). Diazonium-protein adducts for graphite electrode microarrays modification: direct and addressed electrochemical immobilization. *Journal of the American Chemical Society*. https://doi.org/10.1021/ja056946w

Cui, G., Jae Hyun Yoo, Joung Su Lee, Yoo, J., Jung Hee Uhm, Geun Sig Cha, & Nam, H. (2001). Effect of pre-treatment on the surface and electrochemical properties of screen-printed carbon paste electrodes. *Analyst*. https://doi.org/10.1039/b102934g

D'Orazio, P. (2003). Biosensors in clinical chemistry. *Clinica Chimica Acta*. https://doi.org/10.1016/S0009-8981(03)00241-9

Dai, Z., Yan, F., Chen, J., & Ju, H. (2003). Reagentless Amperometric Immunosensors Based on Direct Electrochemistry of Horseradish Peroxidase for Determination of Carcinoma Antigen-125. *Analytical Chemistry*. https://doi.org/10.1021/ac034213t

Daniels, J. S., & Pourmand, N. (2007). Label-Free Impedance Biosensors: Opportunities and Challenges. *Electroanalysis*. https://doi.org/10.1002/elan.200603855

Davis, J. J., Coleman, K. S., Azamian, B. R., Bagshaw, C. B., & Green, M. L. H. (2003). Chemical and biochemical sensing with modified single walled carbon nanotubes. *Chemistry - A European Journal*. https://doi.org/10.1002/chem.200304872

De Carvalho, C. C. C. R. (2011). Enzymatic and whole cell catalysis: Finding new strategies for old processes. *Biotechnology Advances*. https://doi.org/10.1016/j.biotechadv.2010.09.001

De Souza Castilho, M., Laube, T., Yamanaka, H., Alegret, S., & Pividori, M. I. (2011). Magneto immunoassays for plasmodium falciparum histidine-rich protein 2 related to malaria based on magnetic nanoparticles. *Analytical Chemistry*, *83*(14), 5570–5577. https://doi.org/10.1021/ac200573s

Deng, J., Liu, M., Lin, F., Zhang, Y., Liu, Y., & Yao, S. (2013). Self-assembled oligo(phenylene ethynylene)s/graphene nanocomposite with improved electrochemical performances for dopamine determination. *Analytica Chimica Acta*. https://doi.org/10.1016/j.aca.2012.12.051

Derda, R., Gitaka, J., Klapperich, C. M., Mace, C. R., Kumar, A. A., Lieberman, M., … Yager, P. (2015). Enabling the Development and Deployment of Next Generation Point-of-Care Diagnostics. *PLOS Neglected Tropical Diseases*, *9*(5), e0003676. https://doi.org/10.1371/journal.pntd.0003676

Devi, R., Thakur, M., & Pundir, C. S. (2011). Construction and application of an amperometric xanthine biosensor based on zinc oxide nanoparticles-polypyrrole composite film. *Biosensors and Bioelectronics*. https://doi.org/10.1016/j.bios.2011.01.014

Di Gennaro, P., Bruzzese, N., Anderlini, D., Aiossa, M., Papacchini, M., Campanella, L., & Bestetti, G. (2011). Development of microbial engineered whole-cell systems for environmental benzene determination. *Ecotoxicology and Environmental Safety*. https://doi.org/10.1016/j.ecoenv.2010.08.006

Diaconu, I., Cristea, C., Hârceagă, V., Marrazza, G., Berindan-Neagoe, I., & Săndulescu, R. (2013). Electrochemical immunosensors in breast and ovarian cancer. *Clinica Chimica Acta*. https://doi.org/10.1016/j.cca.2013.07.017

Dias, A. D., Kingsley, D. M., & Corr, D. T. (2014). Recent advances in bioprinting and applications for biosensing. *Biosensors*. https://doi.org/10.3390/bios4020111

Drain, P. K., Hyle, E. P., Noubary, F., Freedberg, K. A., Wilson, D., Bishai, W. R., … Bassett, I. V. (2014). Diagnostic point-of-care tests in resource-limited settings. *The Lancet Infectious Diseases*. https://doi.org/10.1016/S1473-3099(13)70250-0

Dreyer, W., Guhlke, C., & Müller, R. (2016). A new perspective on the electron transfer: Recovering the Butler-Volmer equation in non-equilibrium thermodynamics. *Physical Chemistry Chemical Physics*. https://doi.org/10.1039/c6cp04142f

Du, D., Yan, F., Liu, S., & Ju, H. (2003). Immunological assay for carbohydrate antigen 19-9 using an electrochemical immunosensor and antigen immobilization in titania sol-gel matrix. *Journal of Immunological Methods*. https://doi.org/10.1016/j.jim.2003.08.014

Easterbrook, P. J. (2016). Who to test and how to test for chronic hepatitis C infection – 2016 WHO testing guidance for low- and middle-income countries. *Journal of Hepatology*. https://doi.org/10.1016/j.jhep.2016.08.002

Easterbrook, P. J., Roberts, T., Sands, A., & Peeling, R. (2017). Diagnosis of viral

hepatitis. *Current Opinion in HIV and AIDS*. https://doi.org/10.1097/COH.0000000000000370

Ehsani, M., Chaichi, M. J., & Nezammeddin Hosseini, S. (2017). Comparison of CuO nanoparticle and CuO/MWCNT nanocomposite for amplification of chemiluminescence immunoassay for detection of the hepatitis B surface antigen in biological samples. *Sensors and Actuators, B: Chemical*. https://doi.org/10.1016/j.snb.2017.02.019

ElKaoutit, M. (2014). Application of Conducting Polymers in Electroanalysis. In *Aspects on Fundaments and Applications of Conducting Polymers*. https://doi.org/10.5772/26655

Elschner, A., Kirchmeyer, S., Lövenich, W., Merker, U., & Reuter, K. (2010). PEDOT: Principles and applications of an intrinsically conductive polyme. In *PEDOT: Principles and Applications of an Intrinsically Conductive Polymer*. https://doi.org/10.1201/b10318

Englebienne, P., Van Hoonacker, A., & Valsamis, J. (2000). Rapid homogeneous immunoassay for human ferritin in the Cobas Mira using colloidal gold as the reporter reagent. *Clinical Chemistry*.

European Parliament and Council. Directive 2008/98/EC of the European Parliament and of the Council of 19 November 2008 on waste and repealing certain directives (Waste framework. , LexUriServ. do § (2008).

Fan, Y., Liu, J. H., Yang, C. P., Yu, M., & Liu, P. (2011). Graphene-polyaniline composite film modified electrode for voltammetric determination of 4-aminophenol. *Sensors and Actuators, B: Chemical*. https://doi.org/10.1016/j.snb.2011.05.053

Faulkner, L., & Bard, A. (2002). *Electrochemical methods: fundamentals and applications*.

Felix, F. S., & Angnes, L. (2010). Fast and accurate analysis of drugs using amperometry associated with flow injection analysis. *Journal of Pharmaceutical Sciences*. https://doi.org/10.1002/jps.22192

Ferrari, A. C. (2007). Raman spectroscopy of graphene and graphite: Disorder, electron-phonon coupling, doping and nonadiabatic effects. *Solid State Communications*. https://doi.org/10.1016/j.ssc.2007.03.052

Filoti, D. I., Shire, S. J., Yadav, S., & Laue, T. M. (2015). Comparative Study of Analytical Techniques for Determining Protein Charge. *Journal of Pharmaceutical Sciences*. https://doi.org/10.1002/jps.24454

Fisher, A. C. (1996). Electrode Dynamics. In *New York: Oxford University Press*. Retrieved from https://books.google.com/books?id=KVCWQgAACAAJ&pgis=1

Fitzmaurice, C., Akinyemiju, T., Abera, S., Ahmed, M., Alam, N., Alemayohu, M. A., … Naghavi, M. (2017). The burden of primary liver cancer and underlying etiologies from 1990 to 2015 at the global, regional, and national level results from the global burden of disease study 2015. *JAMA Oncology*. https://doi.org/10.1001/jamaoncol.2017.3055

Fowler, J. M., Stuart, M. C., & Wong, D. K. Y. (2007). Self-assembled layer of thiolated protein G as an immunosensor scaffold. *Analytical Chemistry*. https://doi.org/10.1021/ac061175f

Gan, N., Yang, X., Xie, D., Wu, Y., & Wen, W. (2010). A disposable organophosphorus pesticides enzyme biosensor based on magnetic composite nano-particles modified screen printed carbon electrode. *Sensors*. https://doi.org/10.3390/s100100625

Gandhi, S., Suman, P., Kumar, A., Sharma, P., Capalash, N., & Raman Suri, C. (2015). Recent advances in immunosensor for narcotic drug detection. *BioImpacts*. https://doi.org/10.15171/bi.2015.30

Gao, Y. S., Xu, J. K., Lu, L. M., Wu, L. P., Zhang, K. X., Nie, T., … Wu, Y. (2014). Overoxidized polypyrrole/graphene nanocomposite with good electrochemical performance as novel electrode material for the detection of adenine and guanine. *Biosensors and Bioelectronics*. https://doi.org/10.1016/j.bios.2014.06.044

Gawali, D. H., & Wadhai, V. M. (2018). Technology Innovations, Challenges and Emerging Trends in Wearable Bio-Sensor Development. *2017 International Conference on Computing, Communication, Control and Automation, ICCUBEA 2017*. https://doi.org/10.1109/ICCUBEA.2017.8463742

Gerard, M., Chaubey, A., & Malhotra, B. D. (2002). Application of conducting polymers to biosensors. *Biosensors and Bioelectronics*. https://doi.org/10.1016/S0956-5663(01)00312-8

Gikunoo, E., Abera, A., & Woldesenbet, E. (2014). A novel carbon Nanofibers grown on glass microballoons immunosensor: A tool for early diagnosis of Malaria. *Sensors (Switzerland)*, *14*(8), 14686–14699. https://doi.org/10.3390/s140814686

Gilmartin, M. A. T., & Hart, J. P. (1995). Sensing with chemically and biologically modified carbon electrodes: A review. *Analyst*. https://doi.org/10.1039/AN9952001029

Gosser, D. (1993). *Cyclic voltammetry: simulation and analysis of reaction mechanisms*. Retrieved from https://sci-hub.tw/http://www.nehudlit.ru/books/detail6618.html

Govindhan, M., Lafleur, T., Adhikari, B. R., & Chen, A. (2015). Electrochemical Sensor Based on Carbon Nanotubes for the Simultaneous Detection of Phenolic Pollutants. *Electroanalysis*. https://doi.org/10.1002/elan.201400608

Grieshaber, D., MacKenzie, R., Voeroes, J., & Reimhult, E. (2008). Electrochemical biosensors-sensor principles and architectures. *Sensors*, *8*(3), 1400–1458. Retrieved from http://www.mdpi.com/1424-8220/8/3/1400/htm

Gubala, V., Harris, L. F., Ricco, A. J., Tan, M. X., & Williams, D. E. (2012). Point of Care Diagnostics: Status and Future. *Analytical Chemistry*, *84*(2), 487–515. https://doi.org/10.1021/ac2030199

Gupta, D. K., Dembele, L., Voorberg-van der Wel, A., Roma, G., Yip, A., Chuenchob, V., … Diagana, T. T. (2019). The Plasmodium liver-specific protein 2 (LISP2) is an early marker of liver stage development. *ELife*, *8*.

https://doi.org/10.7554/eLife.43362

Ha, J., Martin, S. M., Jeon, Y., In, J. Y., Brown, R. B., Nam, H., & Geun, S. C. (2005). A polymeric junction membrane for solid-state reference electrodes. *Analytica Chimica Acta*. https://doi.org/10.1016/j.aca.2005.06.011

Haab, B. B. (2003). Methods and applications of antibody microarrays in cancer research. *Proteomics*. https://doi.org/10.1002/pmic.200300595

Hallett, J. P., & Welton, T. (2011). Room-temperature ionic liquids: Solvents for synthesis and catalysis. 2. *Chemical Reviews*. https://doi.org/10.1021/cr1003248

Hemben, A., Ashley, J., & Tothill, I. (2017). Development of an Immunosensor for PfHRP 2 as a Biomarker for Malaria Detection. *Biosensors*, *7*(4), 28. https://doi.org/10.3390/bios7030028

Herring, A. J., Ballard, R. C., Pope, V., Adegbola, R. A., Changalucha, J., Fitzgerald, D. W., … Peeling, R. W. (2006). A multi-centre evaluation of nine rapid, point-of-care syphilis tests using archived sera. *Sexually Transmitted Infections*. https://doi.org/10.1136/sti.2006.022707

Hu, J., Wang, S., Wang, L., Li, F., Pingguan-Murphy, B., Lu, T. J., & Xu, F. (2014). Advances in paper-based point-of-care diagnostics. *Biosensors and Bioelectronics*, *54*, 585–597. https://doi.org/10.1016/j.bios.2013.10.075

Inci, F., Filippini, C., Baday, M., Ozen, M. O., Calamak, S., Durmus, N. G., … Demirci, U. (2015). Multitarget, quantitative nanoplasmonic electrical field-enhanced resonating device (NE 2 RD) for diagnostics . *Proceedings of the National Academy of Sciences*. https://doi.org/10.1073/pnas.1510824112

Ionescu, R. E. (2017). Biosensor Platforms for Rapid Detection of *E. coli* Bacteria. In Escherichia coli - *Recent Advances on Physiology, Pathogenesis and Biotechnological Applications*. https://doi.org/10.5772/67392

Ito, N., Saji, T., & Aoyagui, S. (1983). Electrochemical formation of stable ferrocene anion and the formal rate constant of the ferrocene0/- electrode. *Journal of Organometallic Chemistry*. https://doi.org/10.1016/0022-328X(83)85172-9

Jain, P., Chakma, B., Patra, S., & Goswami, P. (2014). Potential Biomarkers and Their Applications for Rapid and Reliable Detection of Malaria. *BioMed Research International*, *2014*, 1–20. https://doi.org/10.1155/2014/852645

Jain, R., Tiwari, D. C., & Karolia, P. (2014). Highly sensitive and selective polyaniline-zinc oxide nanocomposite sensor for betahistine hydrochloride in solubilized system. *Journal of Molecular Liquids*. https://doi.org/10.1016/j.molliq.2014.03.048

Jdanova, A. S., Poyard, S., Soldatkin, A. P., Jaffrezic-Renault, N., & Martelet, C. (1996). Conductometric urea sensor. Use of additional membranes for the improvement of its analytical characteristics. *Analytica Chimica Acta*. https://doi.org/10.1016/0003-2670(95)00548-X

Jiang, X., Li, D., Xu, X., Ying, Y., Li, Y., Ye, Z., & Wang, J. (2008). Immunosensors for detection of pesticide residues. *Biosensors and Bioelectronics*. https://doi.org/10.1016/j.bios.2008.01.035

Ju, H, Zhang, X., & Wang, J. (2011). *NanoBiosensing: principles, development and application*. Springer Science & Business Media.

Ju, Huangxian, Zhang, X., & Wang, J. (2011). *Signal Amplification for Nanobiosensing*. https://doi.org/10.1007/978-1-4419-9622-0_2

Justino, C. I. L., Freitas, A. C., Pereira, R., Duarte, A. C., & Rocha Santos, T. A. P. (2015). Recent developments in recognition elements for chemical sensors and biosensors. *TrAC - Trends in Analytical Chemistry*. https://doi.org/10.1016/j.trac.2015.03.006

Justino, C. I. L., Rocha-Santos, T. A. P., Cardoso, S., Duarte, A. C., & Cardosa, S. (2013). Strategies for enhancing the analytical performance of nanomaterial-based sensors. *TrAC - Trends in Analytical Chemistry*. https://doi.org/10.1016/j.trac.2013.02.004

Kang, X., Wang, J., Wu, H., Liu, J., Aksay, I. A., & Lin, Y. (2010). A graphene-based electrochemical sensor for sensitive detection of paracetamol. *Talanta*. https://doi.org/10.1016/j.talanta.2010.01.009

Kanyong, P., Hughes, G., Pemberton, R. M., Jackson, S. K., & Hart, J. P. (2016). Amperometric Screen-Printed Galactose Biosensor for Cell Toxicity Applications. *Analytical Letters*. https://doi.org/10.1080/00032719.2015.1070166

Kanyong, P., Rawlinson, S., & Davis, J. (2016a). A non-enzymatic sensor based on the redox of ferrocene carboxylic acid on ionic liquid film-modified screen-printed graphite electrode for the analysis of hydrogen peroxide residues in milk. *Journal of Electroanalytical Chemistry*. https://doi.org/10.1016/j.jelechem.2016.02.006

Kanyong, P., Rawlinson, S., & Davis, J. (2016b). A Voltammetric Sensor Based on Chemically Reduced Graphene Oxide-Modified Screen-Printed Carbon Electrode for the Simultaneous Analysis of Uric Acid, Ascorbic Acid and Dopamine. *Chemosensors*. https://doi.org/10.3390/chemosensors4040025

Kanyong, P., Rawlinson, S., & Davis, J. (2016c). Fabrication and electrochemical characterization of polydopamine redox polymer modified screen-printed carbon electrode for the detection of guanine. *Sensors and Actuators, B: Chemical*. https://doi.org/10.1016/j.snb.2016.04.099

Kanyong, P., Rawlinson, S., & Davis, J. (2016d). Gold nanoparticle modified screen-printed carbon arrays for the simultaneous electrochemical analysis of lead and copper in tap water. *Microchimica Acta*. https://doi.org/10.1007/s00604-016-1879-3

Kanyong, P., Rawlinson, S., & Davis, J. (2016e). Simultaneous electrochemical determination of dopamine and 5-hydroxyindoleacetic acid in urine using a screen-printed graphite electrode modified with gold nanoparticles. *Analytical and Bioanalytical Chemistry*. https://doi.org/10.1007/s00216-016-9351-0

Karolia, P., Tiwari, D. C., & Jain, R. (2015). Electrocatalytic sensing of omeprazole. *Ionics*. https://doi.org/10.1007/s11581-015-1394-2

Karunakaran, C., Pandiaraj, M., & Santharaman, P. (2015). Immunosensors. In

Biosensors and Bioelectronics. https://doi.org/10.1016/B978-0-12-803100-1.00004-9

Kellner, K., Posnicek, T., Ettenauer, J., Zuser, K., & Brandl, M. (2015). A new, low-cost potentiostat for environmental measurements with an easy-to-use PC interface. *Procedia Engineering*. https://doi.org/10.1016/j.proeng.2015.08.820

Kew, M. C. (2012). Hepatitis B Virus / Human Immunodeficiency Virus Co-Infection and Its Hepatocarcinogenic Potential in Sub-Saharan Black Africans. *Hepatitis Monthly*. https://doi.org/10.5812/hepatmon.7876

Khalafi, L., Rafiee, M., Shahbak, M., & Shirmohammadi, H. (2013). Kinetic study of the oxidation of catechols in the presence of N-methylaniline. *Journal of Chemistry*. https://doi.org/10.1155/2013/497515

Kim, D., Lee, S., & Piao, Y. (2017). Electrochemical determination of dopamine and acetaminophen using activated graphene-Nafion modified glassy carbon electrode. *Journal of Electroanalytical Chemistry*, *794*, 221–228. https://doi.org/10.1016/j.jelechem.2017.04.018

Kim, Y., Bong, S., Kang, Y., Yang, Y., Kumar, R., Seung, J., & Kim, H. (2010). Biosensors and Bioelectronics Electrochemical detection of dopamine in the presence of ascorbic acid using graphene modified electrodes. *Biosensors and Bioelectronics*, *25*(10), 2366–2369. https://doi.org/10.1016/j.bios.2010.02.031

Kirgoz, Ü. A., Timur, S., Odaci, D., Pérez, B., Alegret, S., & Merkoçi, A. (2007). Carbon nanotube composite as novel platform for microbial biosensor. *Electroanalysis*. https://doi.org/10.1002/elan.200603786

Kissinger, P. T., Preddy, C. R., Shoup, R. E., & Heineman, W. R. (2019). Fundamental Concepts of Analytical Electrochemistry. In *Laboratory Techniques in Electroanalytical Chemistry, Revised and Expanded* (pp. 11–50). https://doi.org/10.1201/9781315274263-2

Kobusingye, O. C., Hyder, A. A., Bishai, D., Hicks, E. R., Mock, C., & Joshipura, M. (2005). Emergency medical systems in low- and middle-income countries: recommendations for action. *Bulletin of the World Health Organization*. https://doi.org//S0042-96862005000800017

Koczula, K. M., & Gallotta, A. (2016). Lateral flow assays. *Essays In Biochemistry*. https://doi.org/10.1042/ebc20150012

Kost, G. (2002). *Principles & practice of point-of-care testing*. Retrieved from https://scholar.google.com/scholar_lookup?title=Principles+and+practice+of+point-of-care+testing&author=GJ+Kost&publication_year=2002&

Krampa, F. D., Aniweh, Y., Awandare, G. A., & Kanyong, P. (2017a). A disposable amperometric sensor based on high-performance PEDOT:PSS/Ionic liquid nanocomposite thin film-modified screen-printed electrode for the analysis of catechol in natural water samples. *Sensors (Switzerland)*, *17*(8), 1716. https://doi.org/10.3390/s17081716

Krampa, F. D., Aniweh, Y., Awandare, G., & Kanyong, P. (2017b). Recent Progress in the Development of Diagnostic Tests for Malaria. *Diagnostics*, *7*(3), 54. https://doi.org/10.3390/diagnostics7030054

Krampa, F. D., Aniweh, Y., Kanyong, P., & Awandare, G. A. (2018). Graphene nanoplatelet-based sensor for the detection of dopamine and N-acetyl-p-aminophenol in urine. *Arabian Journal of Chemistry*. https://doi.org/10.1016/j.arabjc.2018.10.006

Lai, G., Wu, J., Leng, C., Ju, H., & Yan, F. (2011). Disposable immunosensor array for ultrasensitive detection of tumor markers using glucose oxidase-functionalized silica nanosphere tags. *Biosensors and Bioelectronics*. https://doi.org/10.1016/j.bios.2011.02.032

Lamas-Ardisana, P. J., Queipo, P., Fanjul-Bolado, P., & Costa-García, A. (2008). Multiwalled carbon nanotube modified screen-printed electrodes for the detection of p-aminophenol: Optimisation and application in alkaline phosphatase-based assays. *Analytica Chimica Acta*. https://doi.org/10.1016/j.aca.2008.03.034

Lasia, A. (2014). Electrochemical impedance spectroscopy and its applications. In *Electrochemical Impedance Spectroscopy and its Applications*. https://doi.org/10.1007/978-1-4614-8933-7

Laviron, E., Roullier, L., & Degrand, C. (1980). A multilayer model for the study of space distributed redox modified electrodes. Part II. Theory and application of linear potential sweep voltammetry for a simple reaction. *Journal of Electroanalytical Chemistry*. https://doi.org/10.1016/S0022-0728(80)80003-9

Lee, H., Song, C., Hong, Y. S., Kim, M. S., Cho, H. R., Kang, T., … Kim, D. H. (2017). Wearable/disposable sweat-based glucose monitoring device with multistage transdermal drug delivery module. *Science Advances*. https://doi.org/10.1126/sciadv.1601314

Lee, S. Y., Lee, C. N., Mark, H., Meldrum, D. R., & Lin, C. W. (2007). Efficient, specific, compact hepatitis B diagnostic device: Optical detection of the hepatitis B virus by isothermal amplification. *Sensors and Actuators, B: Chemical*. https://doi.org/10.1016/j.snb.2007.05.015

Lee, T. M. H. (2008). Over-the-counter biosensors: Past, present, and future. *Sensors*. https://doi.org/10.3390/s8095535

Lee, W. G., Kim, Y. G., Chung, B. G., Demirci, U., & Khademhosseini, A. (2010). Nano/Microfluidics for diagnosis of infectious diseases in developing countries. *Advanced Drug Delivery Reviews*, *62*(4–5), 449–457. https://doi.org/10.1016/j.addr.2009.11.016

Lei, J., & Ju, H. (2012). Signal amplification using functional nanomaterials for biosensing. *Chemical Society Reviews*. https://doi.org/10.1039/c1cs15274b

Li, B., Sun, Z., Li, X., Li, X., Wang, H., Chen, W., … Mao, Y. (2017). Performance of pfHRP2 versus pLDH antigen rapid diagnostic tests for the detection of Plasmodium falciparum: a systematic review and meta-analysis. *Archives of Medical Science : AMS*, *13*(3), 541–549. https://doi.org/10.5114/aoms.2017.67279

Li, M., Bowen, A., Batz, N., Herold, R. M.-, KE, U., & 2009, U. (2009). *Lab on a Chip Technology, Part II: Fluid Control and Manipulation* (Herold Keith E & R. Avraham, Eds.). Caister Academic Press.

Li, Z., Cui, X., Zheng, J., Wang, Q., & Lin, Y. (2007). Effects of microstructure of carbon nanofibers for amperometric detection of hydrogen peroxide. *Analytica Chimica Acta*. https://doi.org/10.1016/j.aca.2007.06.046

Liebana, S., & Drago, G. A. (2016). Bioconjugation and stabilisation of biomolecules in biosensors. *Essays In Biochemistry*. https://doi.org/10.1042/ebc20150007

Lillehoj, P. B., Huang, M.-C., Truong, N., & Ho, C.-M. (2013). Rapid electrochemical detection on a mobile phone. *Lab on a Chip*, *13*(15), 2950. https://doi.org/10.1039/c3lc50306b

Limbut, W., Kanatharana, P., Mattiasson, B., Asawatreratanakul, P., & Thavarungkul, P. (2006). A comparative study of capacitive immunosensors based on self-assembled monolayers formed from thiourea, thioctic acid, and 3-mercaptopropionic acid. *Biosensors and Bioelectronics*. https://doi.org/10.1016/j.bios.2005.12.025

Lipman, N. S., Jackson, L. R., Trudel, L. J., & Weis-Garcia, F. (2005). Monoclonal versus polyclonal antibodies: Distinguishing characteristics, applications, and information resources. *ILAR Journal*. https://doi.org/10.1093/ilar.46.3.258

Liu, X., Lin, T. Y., & Lillehoj, P. B. (2014). Smartphones for Cell and Biomolecular Detection. *Annals of Biomedical Engineering*. https://doi.org/10.1007/s10439-014-1055-z

Liu, Y., Dong, X., & Chen, P. (2012). Biological and chemical sensors based on graphene materials. *Chemical Society Reviews*. https://doi.org/10.1039/c1cs15270j

Loget, G., Wood, J. B., Cho, K., Halpern, A. R., & Corn, R. M. (2013). Electrodeposition of polydopamine thin films for DNA patterning and microarrays. *Analytical Chemistry*. https://doi.org/10.1021/ac4022743

Lowe, C. R. (2008). Overview of Biosensor and Bioarray Technologies. In *Handbook of Biosensors and Biochips*. https://doi.org/10.1002/9780470061565.hbb003

Lu, L., Zhang, O., Xu, J., Wen, Y., Duan, X., Yu, H., … Nie, T. (2013). A facile one-step redox route for the synthesis of graphene/poly (3,4-ethylenedioxythiophene) nanocomposite and their applications in biosensing. *Sensors and Actuators, B: Chemical*. https://doi.org/10.1016/j.snb.2013.02.024

Luppa, P. B., Müller, C., Schlichtiger, A., & Schlebusch, H. (2011). Point-of-care testing (POCT): Current techniques and future perspectives. *TrAC - Trends in Analytical Chemistry*. https://doi.org/10.1016/j.trac.2011.01.019

Lynge, M. E., Van Der Westen, R., Postma, A., & Städler, B. (2011). Polydopamine - A nature-inspired polymer coating for biomedical science. *Nanoscale*. https://doi.org/10.1039/c1nr10969c

Mahato, K., Prasad, A., Maurya, P. K., & Chandra, P. (2016). Nanobiosensors: Next Generation Point-of-Care Biomedical Devices for Personalized Diagnosis. *Journal of Analytical & Bioanalytical Techniques*, *7*(2). https://doi.org/10.4172/2155-9872.1000e125

Makarychev-Mikhailov, S., Shvarev, A., & Bakker, E. (2008). New trends in ion-selective electrodes. In *Electrochemical Sensors, Biosensors and their*

Biomedical Applications. https://doi.org/10.1016/B978-012373738-0.50006-4

Mallesha, M., Manjunatha, R., Nethravathi, C., Suresh, G. S., Rajamathi, M., Melo, J. S., & Venkatesha, T. V. (2011). Functionalized-graphene modified graphite electrode for the selective determination of dopamine in presence of uric acid and ascorbic acid. *Bioelectrochemistry*, *81*(2), 104–108. https://doi.org/10.1016/j.bioelechem.2011.03.004

Manahan, S. (2010). Fundamentals of Analytical Chemistry. In *Fundamentals of Environmental Chemistry, Second Edition*. https://doi.org/10.1201/9781420056716.ch25

Mansur, H. S., Oréfice, R. L., Vasconcelos, W. L., Lobato, Z. P., & Machado, L. J. C. (2005). Biomaterial with chemically engineered surface for protein immobilization. *Journal of Materials Science: Materials in Medicine*. https://doi.org/10.1007/s10856-005-0632-y

Mao, H., Liang, J., Zhang, H., Pei, Q., Liu, D., Wu, S., … Song, X. M. (2015). Poly(ionic liquids) functionalized polypyrrole/graphene oxide nanosheets for electrochemical sensor to detect dopamine in the presence of ascorbic acid. *Biosensors and Bioelectronics*. https://doi.org/10.1016/j.bios.2015.03.059

Martín-Palma, R. J., Manso, M., Pérez-Rigueiro, J., García-Ruiz, J. P., & Martínez-Duart, J. M. (2004). Surface biofunctionalization of materials by amine groups. *Journal of Materials Research*. https://doi.org/10.1557/JMR.2004.0321

Mason, D. P., Kawamoto, F., Lin, K., Laoboonchai, A., Wongsrichanalai, C., D.P., M., … C., W. (2002). A comparison of two rapid field immunochromatographic tests to expert microscopy in the diagnosis of malaria. *Acta Tropica*. https://doi.org/10.1016/S0001-706X(02)00031-1

McGuinness, R. P., & Verdonk, E. (2009). Electrical impedance technology applied to cell-based assays. In *Label-Free Biosensors: Techniques and Applications* (p. 251). https://doi.org/10.1017/CBO9780511626531.013

McNaught, A., & McNaught, A. (1997). *Compendium of chemical terminology*. Retrieved from https://sci-hub.tw/http://www.old.iupac.org/publications/books/author/mcnaught.html

Meredith, P., & Sarna, T. (2006). The physical and chemical properties of eumelanin. *Pigment Cell Research*. https://doi.org/10.1111/j.1600-0749.2006.00345.x

Michopoulos, A., Kouloumpis, A., Gournis, D., & Prodromidis, M. I. (2014). Performance of layer-by-layer deposited low dimensional building blocks of graphene-prussian blue onto graphite screen-printed electrodes as sensors for hydrogen peroxide. *Electrochimica Acta*. https://doi.org/10.1016/j.electacta.2014.09.031

Mistry, K. K., Layek, K., Mahapatra, A., RoyChaudhuri, C., & Saha, H. (2014). A review on amperometric-type immunosensors based on screen-printed electrodes. *Analyst*. https://doi.org/10.1039/c3an02050a

Moczko, E., Istamboulie, G., Calas-Blanchard, C., Rouillon, R., & Noguer, T. (2012). Biosensor employing screen-printed PEDOT:PSS for sensitive detection of phenolic compounds in water. *Journal of Polymer Science, Part A: Polymer*

Chemistry. https://doi.org/10.1002/pola.26009

Morrin, A., Killard, A. J., & Smyth, M. R. (2003). Electrochemical characterization of commercial and home-made screen-printed carbon electrodes. *Analytical Letters*. https://doi.org/10.1081/AL-120023627

Morrison, D. W. G., Dokmeci, M. R., Demirci, U., & Khademhosseini, A. (2007). Clinical Applications of Micro- and Nanoscale Biosensors. In *Biomedical Nanostructures*. https://doi.org/10.1002/9780470185834.ch17

Moser, A. C., & Hage, D. S. (2008). Capillary electrophoresis-based immunoassays: Principles and quantitative applications. *Electrophoresis*. https://doi.org/10.1002/elps.200700871

Mueller, I., Galinski, M. R., Baird, J. K., Carlton, J. M., Kochar, D. K., Alonso, P. L., & del Portillo, H. A. (2009). Key gaps in the knowledge of Plasmodium vivax, a neglected human malaria parasite. *The Lancet Infectious Diseases*, *9*(9), 555–566. https://doi.org/10.1016/S1473-3099(09)70177-X

Nadjm, B., Amos, B., Mtove, G., Ostermann, J., Chonya, S., Wangai, H., … Reyburn, H. (2010). WHO guidelines for antimicrobial treatment in children admitted to hospital in an area of intense Plasmodium falciparum transmission: Prospective study. *BMJ (Online)*. https://doi.org/10.1136/bmj.c1350

Nagaraja, P., Vasantha, R. A., & Sunitha, K. R. (2001). A sensitive and selective spectrophotometric estimation of catechol derivatives in pharmaceutical preparations. *Talanta*. https://doi.org/10.1016/S0039-9140(01)00438-6

Naghavi, M., Abajobir, A. A., Abbafati, C., Abbas, K. M., Abd-Allah, F., Abera, S. F., … Murray, C. J. L. (2017). Global, regional, and national age-sex specifc mortality for 264 causes of death, 1980-2016: A systematic analysis for the Global Burden of Disease Study 2016. *The Lancet*. https://doi.org/10.1016/S0140-6736(17)32152-9

Nam, H.-W., Song, K. J., Ahn, H. J., Yang, Z., Chong, C.-K., Cho, P. Y., … Kim, T.-S. (2014). Probability of Antibody Formation against Circumsporozoite Protein of Plasmodium vivax among Korean Malaria Patients. *The Korean Journal of Parasitology*, *52*(2), 143–149. https://doi.org/10.3347/kjp.2014.52.2.143

Nambiar, S. R., Aneesh, P. K., & Rao, T. P. (2013). Ultrasensitive voltammetric determination of catechol at a gold atomic cluster/poly(3,4-ethylenedioxythiophene) nanocomposite electrode. *Analyst*. https://doi.org/10.1039/c3an00518f

Nassef, H. M., Bermudo Redondo, M. C., Ciclitira, P. J., Ellis, H. J., Fragoso, A., & O'Sullivan, C. K. (2008). Electrochemical immunosensor for detection of celiac disease toxic gliadin in foodstuff. *Analytical Chemistry*. https://doi.org/10.1021/ac801620j

Nematollahi, D., Afkhami, A., Mosaed, F., & Rafiee, M. (2004). Investigation of the electro-oxidation and oxidation of catechol in the presence of sulfanilic acid. *Research on Chemical Intermediates*. https://doi.org/10.1163/156856704323034030

Nematollahi, D., & Dehdashtian, S. (2008). Electrochemical oxidation of catechol in

the presence of indole: a facile and one-pot method for the synthesis of trisindolyl-o-benzoquinone. *Tetrahedron Letters*. https://doi.org/10.1016/j.tetlet.2007.11.151

Nematollahi, D., Shayani-Jam, H., Alimoradi, M., & Niroomand, S. (2009). Electrochemical oxidation of acetaminophen in aqueous solutions: Kinetic evaluation of hydrolysis, hydroxylation and dimerization processes. *Electrochimica Acta*. https://doi.org/10.1016/j.electacta.2009.07.077

Nemiroski, A., Christodouleas, D. C., Hennek, J. W., Kumar, A. A., Maxwell, E. J., Fernandez-Abedul, M. T., & Whitesides, G. M. (2014). Universal mobile electrochemical detector designed for use in resource-limited applications. *Proceedings of the National Academy of Sciences*. https://doi.org/10.1073/pnas.1405679111

Newman, J. D., & Turner, A. P. F. (2005). Home blood glucose biosensors: A commercial perspective. *Biosensors and Bioelectronics*. https://doi.org/10.1016/j.bios.2004.11.012

Ngamchuea, K., Eloul, S., Tschulik, K., & Compton, R. G. (2014). Planar diffusion to macro disc electrodes—what electrode size is required for the Cottrell and Randles-Sevcik equations to apply quantitatively? *Journal of Solid State Electrochemistry*. https://doi.org/10.1007/s10008-014-2664-z

Nielsen, K., Lin, M., Gall, D., & Jolley, M. (2000). Fluorescence polarization immunoassay: Detection of antibody to Brucella abortus. *Methods*. https://doi.org/10.1006/meth.2000.1038

Nkengasong, J. N., Nsubuga, P., Nwanyanwu, O., Gershy-Damet, G. M., Roscigno, G., Bulterys, M., … Birx, D. (2010). Laboratory systems and services are critical in global health: Time to end the neglect? *American Journal of Clinical Pathology*. https://doi.org/10.1309/AJCPMPSINQ9BRMU6

Orito, Y., Ishino, T., Iwanaga, S., Kaneko, I., Kato, T., Menard, R., … Yuda, M. (2013). Liver-specific protein 2: a Plasmodium protein exported to the hepatocyte cytoplasm and required for merozoite formation. *Molecular Microbiology*, *87*(1), 66–79. https://doi.org/10.1111/mmi.12083

Österholm, A. M., Shen, D. E., Gottfried, D. S., & Reynolds, J. R. (2016). Full Color Control and High-Resolution Patterning from Inkjet Printable Cyan/Magenta/Yellow Colored-to-Colorless Electrochromic Polymer Inks. *Advanced Materials Technologies*. https://doi.org/10.1002/admt.201600063

Oujji, N. Ben, Bakas, I., Istamboulié, G., Ait-Ichou, I., Ait-Addi, E., Rouillon, R., & Noguer, T. (2012). Acetylcholinesterase Immobilized on Magnetic Beads for Pesticides Detection: Application to Olive Oil Analysis. *Sensors (Switzerland)*. https://doi.org/10.3390/s120607893

Palanisamy, S., Karuppiah, C., Chen, S. M., Yang, C. Y., & Periakaruppan, P. (2014). Simultaneous and selective electrochemical determination of dihydroxybenzene isomers at a reduced graphene oxide and copper nanoparticles composite modified glassy carbon electrode. *Analytical Methods*. https://doi.org/10.1039/c4ay00433g

Parkinson, G., & Pejcic, B. (2005). Using Biosensors to Detect Emerging Infectious

Diseases. *Citeseer*, (July), 1–80. Retrieved from http://citeseerx.ist.psu.edu/viewdoc/download?doi=10.1.1.475.7819&rep=rep1&type=pdf

Parra, M. E., Evans, C. B., & Taylor, D. W. (1991). Identification of Plasmodium falciparum histidine-rich protein 2 in the plasma of humans with malaria. *Journal of Clinical Microbiology*, *29*(8), 1629–1634.

Patel, S., Nanda, R., Sahoo, S., & Mohapatra, E. (2016). Biosensors in health care: The milestones achieved in their development towards lab-on-chip-analysis. *Biochemistry Research International*. https://doi.org/10.1155/2016/3130469

Paul, B., Kumar, S., Tripathy, S., Vanjari, S. R. K., Singh, V., & Singh, S. G. (2016). A highly sensitive self assembled monolayer modified copper doped zinc oxide nanofiber interface for detection of Plasmodium falciparum histidine-rich protein-2: Targeted towards rapid, early diagnosis of malaria. *Biosensors and Bioelectronics*, *80*, 39–46. https://doi.org/10.1016/j.bios.2016.01.036

Paul, B., Panigrahi, A. K., Singh, V., & Singh, S. G. (2017). A multi-walled carbon nanotube-zinc oxide nanofiber based flexible chemiresistive biosensor for malaria biomarker detection. *Analyst*, *142*(12), 2128–2135. https://doi.org/10.1039/c7an00243b

Peeling, R. W., & Mabey, D. (2010). Point-of-care tests for diagnosing infections in the developing world. *Clinical Microbiology and Infection*. https://doi.org/10.1111/j.1469-0691.2010.03279.x

Pejcic, B., Marco, R. De, & Parkinson, G. (2006). The role of biosensors in the detection of emerging infectious diseases. *Analyst*. https://doi.org/10.1039/b603402k

Pereira, D. Y., Chiu, R. Y. T., Zhang, S. C. L., Wu, B. M., & Kamei, D. T. (2015). Single-step, paper-based concentration and detection of a malaria biomarker. *Analytica Chimica Acta*. https://doi.org/10.1016/j.aca.2015.04.040

Perkins, M. D., & Bell, D. R. (2008). Working without a blindfold: the critical role of diagnostics in malaria control. *Malaria Journal*, *7*(S1), S5. https://doi.org/10.1186/1475-2875-7-S1-S5

Perumal, V., & Hashim, U. (2014). Advances in biosensors: Principle, architecture and applications. *Journal of Applied Biomedicine*. https://doi.org/10.1016/j.jab.2013.02.001

Ping, J., Wang, Y., Fan, K., Wu, J., & Ying, Y. (2011). Direct electrochemical reduction of graphene oxide on ionic liquid doped screen-printed electrode and its electrochemical biosensing application. *Biosensors and Bioelectronics*. https://doi.org/10.1016/j.bios.2011.07.018

Pistonesi, M. F., Di Nezio, M. S., Centurión, M. E., Palomeque, M. E., Lista, A. G., & Fernández Band, B. S. (2006). Determination of phenol, resorcinol and hydroquinone in air samples by synchronous fluorescence using partial least-squares (PLS). *Talanta*. https://doi.org/10.1016/j.talanta.2005.12.050

Posthuma-Trumpie, G. A., Korf, J., & van Amerongen, A. (2009). Lateral flow (immuno)assay: its strengths, weaknesses, opportunities and threats. A literature

survey. *Analytical and Bioanalytical Chemistry*, *393*(2), 569–582. https://doi.org/10.1007/s00216-008-2287-2

Prakash, S., Chakrabarty, T., Singh, A. K., & Shahi, V. K. (2013). Polymer thin films embedded with metal nanoparticles for electrochemical biosensors applications. *Biosensors and Bioelectronics*. https://doi.org/10.1016/j.bios.2012.09.031

Preiss, U., Borukhovich, E., Alemayehu, N., Steinbach, I., & LaMantia, F. (2013). A permeation model for the electrochemical interface. *Modelling and Simulation in Materials Science and Engineering*. https://doi.org/10.1088/0965-0393/21/7/074006

Price, C. P. (2001). Regular review: Point of care testing. *BMJ*. https://doi.org/10.1136/bmj.322.7297.1285

Prieto-Simon, B., Campas, M., & Marty, J.-L. (2008). Biomolecule Immobilization in Biosensor Development: Tailored Strategies Based on Affinity Interactions. *Protein & Peptide Letters*. https://doi.org/10.2174/092986608785203791

Prodromidis, M. I. (2010). Impedimetric immunosensors—A review. *Electrochimica Acta*, *55*(14), 4227–4233. https://doi.org/10.1016/j.electacta.2009.01.081

Pudas, M., Halonen, N., Granat, P., & Vähäkangas, J. (2005). Gravure printing of conductive particulate polymer inks on flexible substrates. *Progress in Organic Coatings*. https://doi.org/10.1016/j.porgcoat.2005.07.008

Pulli, T., Höyhtyä, M., Söderlund, H., & Takkinen, K. (2005). One-step homogeneous immunoassay for small analytes. *Analytical Chemistry*. https://doi.org/10.1021/ac048379l

Raba, J., Fernández-baldo, M. a, Pereira, S. V, Messina, G. a, & Franco, A. (2013). Analytical biosensors for the pathogenic microorganisms determination. *Microbial Pathogens and Strategies for Combating Them: Science, Technology and Education*, 227–238.

Rackus, D. G., Shamsi, M. H., & Wheeler, A. R. (2015). Electrochemistry, biosensors and microfluidics: a convergence of fields. *Chemical Society Reviews*, *44*(15), 5320–5340. https://doi.org/10.1039/c4cs00369a

Ramírez-García, S., Alegret, S., Céspedes, F., & Forster, R. J. (2002). Carbon composite electrodes: Surface and electrochemical properties. *Analyst*, *127*(11), 1512–1519. https://doi.org/10.1039/b206201a

Randviir, E. P., Brownson, D. A. C., Gómez-Mingot, M., Kampouris, D. K., Iniesta, J., & Banks, C. E. (2012). Electrochemistry of Q-Graphene. *Nanoscale*. https://doi.org/10.1039/c2nr31823g

Randviir, E. P., Brownson, D. A. C., Metters, J. P., Kadara, R. O., & Banks, C. E. (2014). The fabrication, characterisation and electrochemical investigation of screen-printed graphene electrodes. *Physical Chemistry Chemical Physics*. https://doi.org/10.1039/c3cp55435j

Rani, S., Abdullah, W. F. H., Zain, Z. M., & Aqmar, N. Z. N. (2018). Integrated Circuit Design of 3 Electrode Sensing System Using Two-Stage Operational Amplifier. *IOP Conference Series: Materials Science and Engineering*. https://doi.org/10.1088/1757-899X/340/1/012017

Reyburn, H. (2010). New WHO guidelines for the treatment of malaria. *BMJ*, *340*(may28 1), c2637–c2637. https://doi.org/10.1136/bmj.c2637

Rodriguez-del Valle, M., Quakyi, I. A., Amuesi, J., Quaye, J. T., Nkrumah, F. K., & Taylor, D. W. (1991). Detection of antigens and antibodies in the urine of humans with Plasmodium falciparum malaria. *Journal of Clinical Microbiology*, *29*(6), 1236–1242.

Ronald, A. R., Quinn, T. C., Petti, C. A., Sande, M. A., & Polage, C. R. (2006). Laboratory Medicine in Africa: A Barrier to Effective Health Care. *Clinical Infectious Diseases*. https://doi.org/10.1086/499363

Rotariu, L., Zamfir, L. G., & Bala, C. (2010). Low potential thiocholine oxidation at carbon nanotube-ionic liquid gel sensor. *Sensors and Actuators, B: Chemical*. https://doi.org/10.1016/j.snb.2010.07.040

Roth, J. M., Korevaar, D. A., Leeflang, M. M. G., & Mens, P. F. (2016). Molecular malaria diagnostics: A systematic review and meta-analysis. *Critical Reviews in Clinical Laboratory Sciences*. https://doi.org/10.3109/10408363.2015.1084991

Ruecha, N., Rangkupan, R., Rodthongkum, N., & Chailapakul, O. (2014). Novel paper-based cholesterol biosensor using graphene/polyvinylpyrrolidone/polyaniline nanocomposite. *Biosensors and Bioelectronics*. https://doi.org/10.1016/j.bios.2013.08.018

Rusmini, F., Zhong, Z., & Feijen, J. (2007). Protein immobilization strategies for protein biochips. *Biomacromolecules*. https://doi.org/10.1021/bm061197b

Sadir, S., Prabhakaran, M. P., Wicaksono, D. H. B., & Ramakrishna, S. (2014). Fiber based enzyme-linked immunosorbent assay for C-reactive protein. *Sensors and Actuators, B: Chemical*. https://doi.org/10.1016/j.snb.2014.08.051

Sampath, R., & Ecker, D. J. (2004). *Novel biosensor for infectious disease diagnostics*. 181–185. Retrieved from https://books.google.com/books?hl=en&lr=&id=GSY0Tjq_M74C&oi=fnd&pg=PA181&dq=NOVEL+BIOSENSOR+FOR+INFECTIOUS+DISEASE+DIAGNOSTICS&ots=WbaLXSxcfR&sig=LUEFnD07SGd_wzLN2vazybleU5k

Saxena, V., & Malhotra, B. D. (2003). Prospects of conducting polymers in molecular electronics. *Current Applied Physics*. https://doi.org/10.1016/S1567-1739(02)00217-1

Scheiblauer, H., El-Nageh, M., Diaz, S., Nick, S., Zeichhardt, H., Grunert, H. P., & Prince, A. (2010). Performance evaluation of 70 hepatitis B virus (HBV) surface antigen (HBsAg) assays from around the world by a geographically diverse panel with an array of HBV genotypes and HBsAg subtypes. *Vox Sanguinis*. https://doi.org/10.1111/j.1423-0410.2009.01272.x

Scherf, A., Lopez-Rubio, J. J., & Riviere, L. (2008). Antigenic Variation in Plasmodium falciparum . *Annual Review of Microbiology*. https://doi.org/10.1146/annurev.micro.61.080706.093134

Schweitzer, A., Horn, J., Mikolajczyk, R. T., Krause, G., & Ott, J. J. (2015). Estimations of worldwide prevalence of chronic hepatitis B virus infection: A systematic review of data published between 1965 and 2013. *The Lancet*.

https://doi.org/10.1016/S0140-6736(15)61412-X

Scognamiglio, V. (2013). Nanotechnology in glucose monitoring: Advances and challenges in the last 10 years. *Biosensors and Bioelectronics*. https://doi.org/10.1016/j.bios.2013.02.043

Selimovic, A., & Martin, R. S. (2013). Encapsulated electrodes for microchip devices: Microarrays and platinized electrodes for signal enhancement. *Electrophoresis*. https://doi.org/10.1002/elps.201300163

Shahinpoor, M., & Kim, K. J. (2004). Ionic polymer-metal composites: III. Modeling and simulation as biomimetic sensors, actuators, transducers, and artificial muscles. *Smart Materials and Structures*. https://doi.org/10.1088/0964-1726/13/6/009

Sharma, M. K., Rao, V. K., Merwyn, S., Agarwal, G. S., Upadhyay, S., & Vijayaraghavan, R. (2011). A novel piezoelectric immunosensor for the detection of malarial Plasmodium falciparum histidine rich protein-2 antigen. *Talanta*, *85*(4), 1812–1817. https://doi.org/10.1016/j.talanta.2011.07.008

Sharma, Mukesh K., Agarwal, G. S., Rao, V. K., Upadhyay, S., Merwyn, S., Gopalan, N., … Prakash, S. (2010). Amperometric immunosensor based on gold nanoparticles/alumina sol-gel modified screen-printed electrodes for antibodies to Plasmodium falciparum histidine rich protein-2. *Analyst*, *135*(3), 608–614. https://doi.org/10.1039/b918880k

Sharma, Mukesh K., Rao, V. K., Agarwal, G. S., Rai, G. P., Gopalan, N., Prakash, S., … Vijayaraghavan, R. (2008). Highly sensitive amperometric immunosensor for detection of plasmodium falciparum histidine-rich protein 2 in serum of humans with malaria: Comparison with a commercial kit. *Journal of Clinical Microbiology*, *46*(11), 3759–3765. https://doi.org/10.1128/JCM.01022-08

Sharma, S., Zapatero-Rodríguez, J., Saxena, R., O'Kennedy, R., & Srivastava, S. (2018). Ultrasensitive direct impedimetric immunosensor for detection of serum HER2. *Biosensors and Bioelectronics*. https://doi.org/10.1016/j.bios.2018.01.056

Sheng, G., Xu, G., Xu, S., Wang, S., & Luo, X. (2015). Cost-effective preparation and sensing application of conducting polymer PEDOT/ionic liquid nanocomposite with excellent electrochemical properties. *RSC Advances*. https://doi.org/10.1039/c4ra15755a

Shinde, S. B., Fernandes, C. B., & Patravale, V. B. (2012). Recent trends in in-vitro nanodiagnostics for detection of pathogens. *Journal of Controlled Release*. https://doi.org/10.1016/j.jconrel.2011.11.033

Shirakawa, H., Louis, E. J., MacDiarmid, A. G., Chiang, C. K., & Heeger, A. J. (1977). Synthesis of electrically conducting organic polymers: Halogen derivatives of polyacetylene, (CH)x. *Journal of the Chemical Society, Chemical Communications*. https://doi.org/10.1039/C39770000578

Shourian, M., Ghourchian, H., & Boutorabi, M. (2015). Ultra-sensitive immunosensor for detection of hepatitis B surface antigen using multi-functionalized gold nanoparticles. *Analytica Chimica Acta*, *895*, 1–11. https://doi.org/10.1016/j.aca.2015.07.013

Shrivastava, S., Jadon, N., & Jain, R. (2016). Next-generation polymer nanocomposite-based electrochemical sensors and biosensors: A review. *TrAC - Trends in Analytical Chemistry*. https://doi.org/10.1016/j.trac.2016.04.005

Siangproh, W., Dungchai, W., Rattanarat, P., & Chailapakul, O. (2011). Nanoparticle-based electrochemical detection in conventional and miniaturized systems and their bioanalytical applications: A review. *Analytica Chimica Acta*. https://doi.org/10.1016/j.aca.2011.01.054

Sikarwar, B., Sharma, P. K., Srivastava, A., Agarwal, G. S., Boopathi, M., Singh, B., & Jaiswal, Y. K. (2014). Surface plasmon resonance characterization of monoclonal and polyclonal antibodies of malaria for biosensor applications. *Biosensors and Bioelectronics*, *60*, 201–209. https://doi.org/10.1016/j.bios.2014.04.025

Sin, M. L. Y., Mach, K. E., Wong, P. K., & Liao, J. C. (2014). Advances and challenges in biosensor-based diagnosis of infectious diseases. *Expert Review of Molecular Diagnostics*, *14*(2), 225–244. https://doi.org/10.1586/14737159.2014.888313

Singh, K., Solanki, P. R., Basu, T., & Malhotra, B. D. (2012). Polypyrrole/multiwalled carbon nanotubes-based biosensor for cholesterol estimation. *Polymers for Advanced Technologies*. https://doi.org/10.1002/pat.2020

Sinnis, P., Willnow, T. E., Briones, M. R. S., Herz, J., & Nussenzweig, V. (1996). Remnant lipoproteins inhibit malaria sporozoite invasion of hepatocytes. *The Journal of Experimental Medicine*, *184*(3), 945–954. https://doi.org/10.1084/jem.184.3.945

Spain, E., Kojima, R., Kaner, R. B., Wallace, G. G., O'Grady, J., Lacey, K., … Forster, R. J. (2011). High sensitivity DNA detection using gold nanoparticle functionalised polyaniline nanofibres. *Biosensors and Bioelectronics*. https://doi.org/10.1016/j.bios.2010.11.017

Srivastava, M., Das, A. K., Khanra, P., Uddin, M. E., Kim, N. H., & Lee, J. H. (2013). Characterizations of in situ grown ceria nanoparticles on reduced graphene oxide as a catalyst for the electrooxidation of hydrazine. *Journal of Materials Chemistry A*. https://doi.org/10.1039/c3ta11311f

Stephen, W. . (2004). Compendium of analytical nomenclature. *Endeavour*, *3*(3), 132. https://doi.org/10.1016/0160-9327(79)90104-2

Stradiotto, N. R., Yamanaka, H., & Zanoni, M. V. B. (2003). Electrochemical sensors: A powerful tool in analytical chemistry. *Journal of the Brazilian Chemical Society*. https://doi.org/10.1590/S0103-50532003000200003

Streeter, I., Wildgoose, G. G., Shao, L., & Compton, R. G. (2008). Cyclic voltammetry on electrode surfaces covered with porous layers: An analysis of electron transfer kinetics at single-walled carbon nanotube modified electrodes. *Sensors and Actuators, B: Chemical*. https://doi.org/10.1016/j.snb.2008.03.015

Subic, M., & Zoulim, F. (2018). How to improve access to therapy in hepatitis B patients. *Liver International*. https://doi.org/10.1111/liv.13640

Sun, Y. G., Cui, H., Li, Y. H., & Lin, X. Q. (2000). Determination of some catechol derivatives by a flow injection electrochemiluminescent inhibition method. *Talanta*. https://doi.org/10.1016/S0039-9140(00)00550-6

Suni, I. I. (2008). Impedance methods for electrochemical sensors using nanomaterials. *TrAC - Trends in Analytical Chemistry*. https://doi.org/10.1016/j.trac.2008.03.012

Tam, Y. J., Zeenathul, N. A., Rezaei, M. A., Mustafa, N. H., Azmi, M. L. M., Bahaman, A. R., … Rasedee, A. (2017). Wide dynamic range of surface-plasmon-resonance-based assay for hepatitis B surface antigen antibody optimal detection in comparison with ELISA. *Biotechnology and Applied Biochemistry*. https://doi.org/10.1002/bab.1528

Tan, F., Yan, F., & Ju, H. (2006). A designer ormosil gel for preparation of sensitive immunosensor for carcinoembryonic antigen based on simple direct electron transfer. *Electrochemistry Communications*. https://doi.org/10.1016/j.elecom.2006.08.026

Tan, F., Yan, F., & Ju, H. (2007). Sensitive reagentless electrochemical immunosensor based on an ormosil sol-gel membrane for human chorionic gonadotrophin. *Biosensors and Bioelectronics*. https://doi.org/10.1016/j.bios.2006.12.010

Tang, D. P., Yuan, R., Chai, Y. Q., Zhong, X., Liu, Y., Dai, J. Y., & Zhang, L. Y. (2004). Novel potentiometric immunosensor for hepatitis B surface antigen using a gold nanoparticle-based biomolecular immobilization method. *Analytical Biochemistry*. https://doi.org/10.1016/j.ab.2004.06.035

Taylor, L. H., Latham, S. M., & Mark, E. J. (2001). Risk factors for human disease emergence. *Philosophical Transactions of the Royal Society of London B: Biological Sciences*, *356*(1411), 983–989. Retrieved from http://rstb.royalsocietypublishing.org/content/royptb/356/1411/983.full.pdf

Terasawa, N., & Asaka, K. (2016). High-Performance PEDOT:PSS/Single-Walled Carbon Nanotube/Ionic Liquid Actuators Combining Electrostatic Double-Layer and Faradaic Capacitors. *Langmuir*. https://doi.org/10.1021/acs.langmuir.6b01148

Thakur, M. S., & Ragavan, K. V. (2013). Biosensors in food processing. *Journal of Food Science and Technology*. https://doi.org/10.1007/s13197-012-0783-z

The malERA Consultative Group on Diagnoses. (2011). A Research Agenda for Malaria Eradication: Diagnoses and Diagnostics. *PLoS Medicine*, *8*(1), e1000396. https://doi.org/10.1371/journal.pmed.1000396

Thévenot, D. R., Toth, K., Durst, R. A., & Wilson, G. S. (2001). Electrochemical biosensors: recommended definitions and classification. *Biosensors and Bioelectronics*, *16*(1), 121–131. Retrieved from http://www.sciencedirect.com/science/article/pii/S0956566301001154

Thevenot, D., Toth, K., Durst, R., Wilson, G., & Electrochemical, G. W. (2001). Electrochemical biosensors: recommended definitions and classification. *Biosensors and Bioelectronics*, *16*, 121–131. https://doi.org/10.1081/AL-100103209ï

Tripathi, V. S., Kandimalla, V. B., & Ju, H. (2006). Preparation of ormosil and its applications in the immobilizing biomolecules. *Sensors and Actuators, B: Chemical*. https://doi.org/10.1016/j.snb.2005.07.037

Trojanowicz, M., & Kołacińska, K. (2016). Recent advances in flow injection analysis. *Analyst*. https://doi.org/10.1039/c5an02522b

Trojanowicz, M., Szewczynska, M., & Wcislo, M. (2003). Electroanalytical flow measurements - Recent advances. *Electroanalysis*. https://doi.org/10.1002/elan.200390041

Turner, A. P. F., Karube, I., Wilson, G. S., & Worsfold, P. J. (1987). Biosensors: fundamentals and applications. *Analytica Chimica Acta*. https://doi.org/10.1016/s0003-2670(00)85361-1

Umezawa, Y., Umezawa, K., & Sato, H. (2007). Selectivity coefficients for ion-selective electrodes: Recommended methods for reporting KA,Bpot values (Technical Report). *Pure and Applied Chemistry*, *67*(3), 507–518. https://doi.org/10.1351/pac199567030507

UNITED STATES ENVIRONMENTAL PROTECTION AGENCY. (2012). *Proceedings of the Water Environment Federation*. https://doi.org/10.2175/193864705783867675

Uslu, B., & Ozkan, S. A. (2011). Electroanalytical Methods for the Determination of Pharmaceuticals: A Review of Recent Trends and Developments. *Analytical Letters*. https://doi.org/10.1080/00032719.2011.553010

Vigneshvar, S., Sudhakumari, C. C., Senthilkumaran, B., & Prakash, H. (2016). Recent Advances in Biosensor Technology for Potential Applications – An Overview. *Frontiers in Bioengineering and Biotechnology*. https://doi.org/10.3389/fbioe.2016.00011

Wang, D., Hu, W., Xiong, Y., Xu, Y., & Ming Li, C. (2015). Multifunctionalized reduced graphene oxide-doped polypyrrole/pyrrolepropylic acid nanocomposite impedimetric immunosensor to ultra-sensitively detect small molecular aflatoxin B1. *Biosensors and Bioelectronics*. https://doi.org/10.1016/j.bios.2014.06.070

Wang, H., Shen, G., & Yu, R. (2008). Aspects of recent development of immunosensors. In *Electrochemical Sensors, Biosensors and their Biomedical Applications*. https://doi.org/10.1016/B978-012373738-0.50011-8

Wang, Jo-Yu, & Ploehn, H. J. (1996). Dynamic mechanical analysis of the effect of water on glass bead-epoxy composites. *Journal of Applied Polymer Science*. https://doi.org/10.1002/(sici)1097-4628(19960110)59:2<345::aid-app19>3.3.co;2-d

Wang, Joseph. (2008). Electrochemical glucose biosensors. In *Electrochemical Sensors, Biosensors and their Biomedical Applications* (pp. 57–69). https://doi.org/10.1016/B978-012373738-0.50005-2

Wang, Li, Hua, E., Liang, M., Ma, C., Liu, Z., Sheng, S., … Feng, W. (2014). Graphene sheets, polyaniline and AuNPs based DNA sensor for electrochemical determination of BCR/ABL fusion gene with functional hairpin probe. *Biosensors and Bioelectronics*. https://doi.org/10.1016/j.bios.2013.07.049

Wang, Ling, Yang, R., Wang, H., Li, J., Qu, L., & Harrington, P. de B. (2015). High-selective and sensitive voltammetric sensor for butylated hydroxyanisole based on AuNPs-PVP-graphene nanocomposites. *Talanta*. https://doi.org/10.1016/j.talanta.2015.01.016

Wang, W., Xu, G., Cui, X. T., Sheng, G., & Luo, X. (2014). Enhanced catalytic and dopamine sensing properties of electrochemically reduced conducting polymer nanocomposite doped with pure graphene oxide. *Biosensors and Bioelectronics*. https://doi.org/10.1016/j.bios.2014.02.055

Wang, X. H., & Wang, S. (2008). Sensors and biosensors for the determination of small molecule biological toxins. *Sensors*. https://doi.org/10.3390/s8096045

Wang, X., Lu, X., & Chen, J. (2014). Development of biosensor technologies for analysis of environmental contaminants. *Trends in Environmental Analytical Chemistry*. https://doi.org/10.1016/j.teac.2014.04.001

Wang, Ying, Li, Y., Tang, L., Lu, J., & Li, J. (2009). Application of graphene-modified electrode for selective detection of dopamine. *Electrochemistry Communications*, *11*(4), 889–892. https://doi.org/10.1016/j.elecom.2009.02.013

Wang, You, Xu, H., Zhang, J., & Li, G. (2008). Electrochemical sensors for clinic analysis. *Sensors*. https://doi.org/10.3390/s8042043

Wei, M. Y., Wen, S. D., Yang, X. Q., & Guo, L. H. (2009). Development of redox-labeled electrochemical immunoassay for polycyclic aromatic hydrocarbons with controlled surface modification and catalytic voltammetric detection. *Biosensors and Bioelectronics*. https://doi.org/10.1016/j.bios.2009.02.031

Welle, A. M., & Jacobs, H. O. (2005). Printing of organic and inorganic nanomaterials using electrospray ionization and Coulomb-force-directed assembly. *Applied Physics Letters*. https://doi.org/10.1063/1.2149985

Wen, Y., Xu, J., Li, D., Liu, M., Kong, F., & He, H. (2012). A novel electrochemical biosensing platform based on poly(3,4-ethylenedioxythiophene):Poly(styrenesulfonate) composites. *Synthetic Metals*. https://doi.org/10.1016/j.synthmet.2012.03.004

WHO. (2016). WHO | Fact Sheet: World Malaria Report 2016. In *WHO*. Retrieved from http://www.who.int/malaria/media/world-malaria-report-2016/en/

WHO. (2017a). Global Hepatitis Report, 2017. In *World Health Organisation*. https://doi.org/10.1016/j.poly.2012.11.010

WHO. (2017b). Hepatitis B Fact sheet Updated. In *WHO*.

Wilson, M. S. (2005). Electrochemical immunosensors for the simultaneous detection of two tumor markers. *Analytical Chemistry*. https://doi.org/10.1021/ac0485278

World Health Organisation. (2016). Global health sector strategy on viral hepatitis 2016-2021. *Global Hepatitis Programme Department of HIV/AIDS*.

World Health Organization. (2011). *Increasing Access to Diagnostics Through Technology Transfer and Local Production*.

World Health Organization. (2015). World Malaria Report 2015. In *World Health*.

https://doi.org/ISBN 978 92 4 1564403

World Health Organization. (2018a). *The World malaria report 2018*. Retrieved from www.who.int/malaria%0Ahttps://apps.who.int/iris/bitstream/handle/10665/275867/9789241565653-eng.pdf?ua=1%0Ahttps://www.who.int/malaria/publications/world-malaria-report-2018/en/; consulté le 22/03/2019%0Ahttps://www.who.int/malaria/media/world-malaria-rep

World Health Organization. (2018b). WHO | World malaria report 2017. https://doi.org/http://www.who.int/malaria/publications/world-malaria-report-2017/report/en/

Wu, C., Tang, Y., Wan, C., Liu, H., & Wu, K. (2015). Enhanced-oxidation and highly-sensitive detection of acetaminophen, guanine and adenine using NMP-exfoliated graphene nanosheets-modified electrode. *Electrochimica Acta*. https://doi.org/10.1016/j.electacta.2015.03.088

Wu, L., Chen, J., Du, D., & Ju, H. (2006). Electrochemical immunoassay for CA125 based on cellulose acetate stabilized antigen/colloidal gold nanoparticles membrane. *Electrochimica Acta*. https://doi.org/10.1016/j.electacta.2005.06.011

Xiong, H., & Jin, B. (2011). The electrochemical behavior of AA and da on graphene oxide modified electrodes containing various content of oxygen functional groups. *Journal of Electroanalytical Chemistry*. https://doi.org/10.1016/j.jelechem.2011.06.034

Yang, D., Kroe-Barrett, R., Singh, S., & Laue, T. (2019). IgG Charge: Practical and Biological Implications. *Antibodies*. https://doi.org/10.3390/antib8010024

Yang, J., Cohen Stuart, M. A., & Kamperman, M. (2014). Jack of all trades: Versatile catechol crosslinking mechanisms. *Chemical Society Reviews*. https://doi.org/10.1039/c4cs00185k

Yang, L., Liu, D., Huang, J., & You, T. (2014). Simultaneous determination of dopamine, ascorbic acid and uric acid at electrochemically reduced graphene oxide modified electrode. *Sensors and Actuators, B: Chemical*. https://doi.org/10.1016/j.snb.2013.11.104

Yang, Z., Xie, Z., Liu, H., Yan, F., & Ju, H. (2008). Streptavidin-functionalized three-dimensional ordered nanoporous silica film for highly efficient chemiluminescent immunosensing. *Advanced Functional Materials*. https://doi.org/10.1002/adfm.200801022

Yanow, S. K. (2016). Molecular Diagnosis of Malaria in Low-Resource Settings. *Point of Care: The Journal of Near-Patient Testing & Technology*, *15*(1), 41–42. https://doi.org/10.1097/POC.0000000000000088

Yao, Y., Wen, Y., Xu, J., Zhang, L., & Duan, X. (2013). Application of commercial poly(3,4-ethylenedioxythiophene): Poly(styrene sulfonate) for electrochemical sensing of dopamine. *Journal of the Serbian Chemical Society*. https://doi.org/10.2298/JSC120927036Y

Yao, Y., Wen, Y., Zhang, L., Xu, J., Wang, Z., & Duan, X. (2013). A stable sandwich-type hydrogen peroxide sensor based on immobilizing horseradish

peroxidase to a silver nanoparticle monolayer supported by PEDOT:PSS-nafion composite electrode. *International Journal of Electrochemical Science*.

Yiğit, A., Yardim, Y., Çelebi, M., Levent, A., & Şentürk, Z. (2016). Graphene/Nafion composite film modified glassy carbon electrode for simultaneous determination of paracetamol, aspirin and caffeine in pharmaceutical formulations. *Talanta*. https://doi.org/10.1016/j.talanta.2016.05.046

Yoo, E. H., & Lee, S. Y. (2010). Glucose biosensors: An overview of use in clinical practice. *Sensors*. https://doi.org/10.3390/s100504558

Yu, Q., Wang, Q., Li, B., Lin, Q., & Duan, Y. (2015). Technological Development of Antibody Immobilization for Optical Immunoassays: Progress and Prospects. *Critical Reviews in Analytical Chemistry*. https://doi.org/10.1080/10408347.2014.881249

Zeng, X., Andrade, C. A. S., Oliveira, M. D. L., & Sun, X. L. (2012). Carbohydrate-protein interactions and their biosensing applications. *Analytical and Bioanalytical Chemistry*. https://doi.org/10.1007/s00216-011-5594-y

Zhan, L., Guo, S. Z., Song, F., Gong, Y., Xu, F., Boulware, D. R., … Bischof, J. C. (2017). The Role of Nanoparticle Design in Determining Analytical Performance of Lateral Flow Immunoassays. *Nano Letters*. https://doi.org/10.1021/acs.nanolett.7b02302

Zhang, F., Lin, L. X., Wang, G. W., Hu, R., Lin, C. J., & Chen, Y. (2012). A high-throughput electrochemical impedance spectroscopy evaluation of bioresponsibility of the titanium microelectrode array integrated with hydroxyapatite and silver. *Electrochimica Acta*. https://doi.org/10.1016/j.electacta.2012.08.033

Zhang, G. J., & Ning, Y. (2012). Silicon nanowire biosensor and its applications in disease diagnostics: A review. *Analytica Chimica Acta*, Vol. 749, pp. 1–15. https://doi.org/10.1016/j.aca.2012.08.035

Zhang, Z., Yan, J., Jin, H., & Yin, J. (2014). Tuning the reduction extent of electrochemically reduced graphene oxide electrode film to enhance its detection limit for voltammetric analysis. *Electrochimica Acta*. https://doi.org/10.1016/j.electacta.2014.06.159

Zhu, J., Liu, X., Wang, X., Huo, X., & Yan, R. (2015). Preparation of polyaniline-TiO2 nanotube composite for the development of electrochemical biosensors. *Sensors and Actuators, B: Chemical*. https://doi.org/10.1016/j.snb.2015.06.131

5.4 Appendixes: Publications

diagnostics

MDPI

Review

Recent Progress in the Development of Diagnostic Tests for Malaria

Francis D. Krampa [1,2], Yaw Aniweh [1], Gordon A. Awandare [1,2] and Prosper Kanyong [1,3,*]

1 West African Centre for Cell Biology of Infectious Pathogens (WACCBIP), University of Ghana, Legon, Accra, Ghana; fkrampa@gmail.com (F.D.K.); aniweh@gmail.com (Y.A.); gawandare@ug.edu.gh (G.A.A.)
2 Department of Biochemistry, Cell & Molecular Biology, University of Ghana, Legon, Accra, Ghana
3 Nanotechnology & Integrated Bioengineering Centre, Ulster University, Jordanstown BT37 0QB, UK
* Correspondence: p.kanyong@waccbip.org; Tel.: +233-(0)303-933-223

Received: 27 August 2017; Accepted: 14 September 2017; Published: 19 September 2017

Abstract: The impact of malaria on global health has continually prompted the need to develop effective diagnostic strategies. In malaria endemic regions, routine diagnosis is hampered by technical and infrastructural challenges to laboratories. These laboratories lack standard facilities, expertise or diagnostic supplies; thus, therapy is administered based on clinical or self-diagnosis. There is the need for accurate diagnosis of malaria due to the continuous increase in the cost of medication, and the emergence and spread of drug resistant strains. However, the widely utilized Giemsa-stained microscopy and immunochromatographic tests for malaria are liable to several drawbacks, including inadequate sensitivity and false-positive outcomes. Alternative methods that offer improvements in performance are either expensive, have longer turnaround time or require a level of expertise that makes them unsuitable for point-of-care (POC) applications. These gaps necessitate exploration of more efficient detection techniques with the potential of POC applications, especially in resource-limited settings. This minireview discusses some of the recent trends and new approaches that are seeking to improve the clinical diagnosis of malaria.

Keywords: rapid diagnostic tests (RDT); biosensing; lateral flow assays; *Plasmodium* spp.; multiplex biomarker detection; histidine-rich protein 2 (HRP2); lactate dehydrogenase (LDH); aldolase; point-of-care tests (POCT); disposal medical devices; infectious diseases

1. Introduction

The launch of several initiatives to eradicate malaria [1] has resulted in a global decline in morbidity and mortality [2]. Yet malaria remains a major global health problem, especially in tropical regions, and in 2015 an estimated 218 million cases with 395,000 deaths were recorded in Africa [3]. Among non-endemic regions such as European countries and the US, cases of imported malaria are on the increase [4]. One of the factors that has ensured the persistence of malaria has been the lack of analytical sensing tools that allow for early and accurate detection in asymptomatic individuals with low parasitemia levels in peripheral blood [5]. At present, the World Health Organization (WHO) recommends case management to be guided by detecting *Plasmodium* parasites or antigens in the peripheral blood of febrile patients and asymptomatic carriers. However, current techniques including microscopy and rapid diagnostic tests (RDTs) do not have satisfactory sensitivity for parasitemia. Alternative methods with superior performance are relatively expensive with low throughput; thus, rendering them unsuitable for routine use. Therefore, there is the need for the development of effective diagnostic strategies for field application, where diagnostic expertise in malaria is often lacking [6,7]. New technologies are focusing on developing point-of-care (POC) tests

ARTICLE IN PRESS

Arabian Journal of Chemistry (2018) xxx, xxx–xxx

King Saud University

Arabian Journal of Chemistry

www.ksu.edu.sa
www.sciencedirect.com

ORIGINAL ARTICLE

Polydopamine-functionalized graphene nanoplatelet smart conducting electrode for bio-sensing applications

Prosper Kanyong [a,b,*], Francis D. Krampa [a,c], Yaw Aniweh [a], Gordon A. Awandare [a,c]

[a] *West African Centre for Cell Biology of Infectious Pathogens (WACCBIP), University of Ghana, Legon, Accra, Ghana*
[b] *Department of Chemistry, Physical & Theoretical Chemistry Laboratory, University of Oxford, South Parks Road, Oxford OX1 3QZ, UK*
[c] *Department of Biochemistry, Cell & Molecular Biology, University of Ghana, Legon, Accra, Ghana*

Received 17 November 2017; accepted 1 January 2018

KEYWORDS

Polyethylene glycol;
Screen-printed electrodes;
Bio-sensing;
Mediated sensors;
Thin films;
Dopamine;
Organocatalysts

Abstract The development of a novel polydopamine (PDA)-functionalized graphene nanoplatelets (GNPs)-based disposable sensor is described. The sensor was fabricated by drop-coating PDA@GNPs in polyethylene glycol (PEG) and poly(3,4-ethylenedioxythiophene (PEDOT):poly(styrenesulfonate) (PSS) aqueous suspension onto the working area of a screen-printed electrode (SPE). The final sensor, designated as PDA@GNPs/PPP/SPE, was characterized by scanning electron microscopy (SEM), Raman spectroscopy, Faradaic electrochemical impedance spectroscopy (FEIS) and cyclic voltammetry (CV). Mediated detection of hydrogen peroxide (H_2O_2) via the redox properties of PDA was achieved. It showed excellent selectivity and sensitivity towards H_2O_2 with a limit of detection and sensitivity of 0.55 μM (S/N = 3) and 3.0 μA mM^{-1} cm^{-2}, respectively. Thereafter, glucose oxidase (GOx) was immobilized onto the electrode to develop GOx/PDA@GNPs/PPP/SPE sensor. The glucose biosensor exhibited a limit of detection of 0.25 μM (S/N = 3) and a sensitivity of 0.51 μA μM^{-1} cm^{-2}; thus, proving its potential suitability for bio-sensing applications.

* Corresponding author at: Department of Chemistry, Physical & Theoretical Chemistry Laboratory, University of Oxford, South Parks Road, Oxford OX1 3QZ, UK.
E-mail addresses: prosper.kanyong@chem.ox.ac.uk, p.kanyong@-waccbip.org (P. Kanyong).
Peer review under responsibility of King Saud University.

Production and hosting by Elsevier

1. Introduction

Graphene and its derivatives are widely used as surface modifiers for electrodes including glassy carbon and screen-printed electrodes during the preparation of electrochemical bio-(chemo) sensors (Kanyong et al., 2016a; Ratinac et al., 2011). Electrodeposition, drop-casting and physical adsorption are the most commonly employed methods for the modification

https://doi.org/10.1016/j.arabjc.2018.01.001
1878-5352 © 2018 Production and hosting by Elsevier B.V. on behalf of King Saud University.

Please cite this article in press as: Kanyong, P. et al., Polydopamine-functionalized graphene nanoplatelet smart conducting electrode for bio-sensing applications. Arabian Journal of Chemistry (2018), https://doi.org/10.1016/j.arabjc.2018.01.001

ARTICLE IN PRESS

Arabian Journal of Chemistry (2018) xxx, xxx–xxx

King Saud University

Arabian Journal of Chemistry

www.ksu.edu.sa
www.sciencedirect.com

ORIGINAL ARTICLE

Graphene nanoplatelet-based sensor for the detection of dopamine and *N*-acetyl-*p*-aminophenol in urine

Francis D. Krampa [a,b], Yaw Aniweh [a], Prosper Kanyong [a,c,*], Gordon A. Awandare [a,b]

[a] *West African Centre for Cell Biology of Infectious Pathogens (WACCBIP), University of Ghana, Legon, Accra, Ghana*
[b] *Department of Biochemistry, Cell & Molecular Biology, University of Ghana, Legon, Accra, Ghana*
[c] *Department of Chemistry, Physical & Theoretical Chemistry Laboratory, University of Oxford, South Parks Road, Oxford OX1 3QZ, UK*

Received 4 April 2018; accepted 23 October 2018

KEYWORDS

Dual sensor;
Nanocomposites;
Graphene;
Modified electrodes;
Simultaneous electrochemical analysis

Abstract This paper reports the development and application of a disposable sensor for the individual and simultaneous voltammetric determination of dopamine (DA) and *N*-acetyl-*p*-aminophenol (APAP). The sensor was fabricated by drop-coating graphene nanoplatelets (GNPs)-Nafion (Naf) nanocomposite onto the working area of a screen-printed electrode (SPE). The sensor, designated as GNPs-Naf/SPE, was characterized by scanning electron microscopy (SEM), Raman spectroscopy, electrochemical impedance spectroscopy (EIS) and cyclic voltammetry (CV). Differential pulse voltammetry (DPV) was used to simultaneously analyze DA and APAP in their binary mixtures. It showed excellent selectivity and sensitivity toward both compounds with limit of detection of 0.13 μM and 0.25 μM (S/N = 3) for DA and APAP, respectively. The performance of the sensor was evaluated by analyzing the compounds in human urine samples, and the recoveries were found to be well over 97.0%.

1. Introduction

Dopamine (DA) is a neurotransmitter among the catecholamines family and plays important functional roles in metabolic, renal, hormonal, cardiovascular and central nervous systems (Kurian et al., 2011). In the case of neurological disorders including, restless legs syndrome, Huntington's and Parkinson's diseases, schizophrenia, and attention deficit hyperactivity disorder, the concentration of DA in human bodily fluids have been found to be profoundly elevated; thus, DA is a vital

* Corresponding author at: Department of Chemistry, Physical & Theoretical Chemistry Laboratory, University of Oxford, South Parks Road, Oxford OX1 3QZ, UK.
E-mail addresses: p.kanyong@waccbip.org, prosper.kanyong@chem.ox.ac.uk (P. Kanyong).
Peer review under responsibility of King Saud University.

Production and hosting by Elsevier

https://doi.org/10.1016/j.arabjc.2018.10.006
1878-5352

Please cite this article in press as: Krampa, F.D. et al., Graphene nanoplatelet-based sensor for the detection of dopamine and *N*-acetyl-*p*-aminophenol in urine. Arabian Journal of Chemistry (2018), https://doi.org/10.1016/j.arabjc.2018.10.006

sensors

MDPI

Article

A Disposable Amperometric Sensor Based on High-Performance PEDOT:PSS/Ionic Liquid Nanocomposite Thin Film-Modified Screen-Printed Electrode for the Analysis of Catechol in Natural Water Samples

Francis D. Krampa [1,2], Yaw Aniweh [1], Gordon A. Awandare [1,2] and Prosper Kanyong [1,3,*]

1 West African Centre for Cell Biology of Infectious Pathogens (WACCBIP), University of Ghana, Legon, Accra, Ghana; fkrampa@gmail.com (F.D.K.); aniweh@gmail.com (Y.A.); gawandare@ug.edu.gh (G.A.A.)
2 Department of Biochemistry, Cell & Molecular Biology, University of Ghana, Legon, Accra, Ghana
3 Nanotechnology & Integrated Bioengineering Centre, Ulster University, Jordanstown BT37 0QB, UK
* Correspondence: p.kanyong@waccbip.org

Received: 8 June 2017; Accepted: 13 July 2017; Published: 26 July 2017

Abstract: A conducting polymer-based composite material of poly(3,4-ethylenedioxythiophene) (PEDOT): poly(4-styrenesulfonate) (PSS) doped with different percentages of a room temperature ionic liquid (IL), 1-ethyl-3-methylimidazolium tetrafluoroborate ([EMIM][BF_4]), was prepared and a very small amount of the composite (2.0 µL) was drop-coated on the working area of a screen-printed carbon electrode (SPCE). The SPCE, modified with PEDOT:PSS/IL composite thin-film, was characterized by cyclic voltammetry (CV), electrochemical impedance spectroscopy (EIS), scanning electron microscopy (SEM), profilometry and sessile contact angle measurements. The prepared PEDOT:PSS/IL composite thin-film exhibited a nano-porous microstructure and was found to be highly stable and conductive with enhanced electrocatalytic properties towards catechol, a priority pollutant. The linear working range for catechol was found to be 0.1 µM–330.0 µM with a sensitivity of 18.2 mA·mM·cm^{-2} and a calculated limit of detection (based on 3× the baseline noise) of 23.7 µM. When the PEDOT:PSS/IL/SPCE sensor was used in conjunction with amperometry in stirred solution for the analysis of natural water samples, the precision values obtained on spiked samples (20.0 µM catechol added) (n = 3) were 0.18% and 0.32%, respectively, with recovery values that were well over 99.0%.

Keywords: room temperature ionic liquids; PEDOT:PSS; disposable sensors; cyclic voltammetry; electrochemical impedance spectroscopy; screen-printed electrodes; conducting polymers; nanocomposites; hexacyanoferrate; sessile contact angle measurement

1. Introduction

Over the past 20 years, the development of sensitive and real-time analysis of phenolic compounds has received substantial scientific interest due to their high toxicity on the ecosystem, environment as well as human health [1]. Besides this, phenolic compounds as highly toxic organics has been extensively utilized in various industrial products including flavors, pharmaceuticals, antioxidants, agrochemicals, and polymerization inhibitors [1–4]. Among phenolic compounds, catechol, which is an ortho isomer of benzenediols, has been listed as a priority pollutant by both the European Union and the US Environmental Protection Agency [5,6] because it has a poor biodegradability and is extremely toxic to human health and the ecosystem [7,8]. Therefore, there is the need for the development

sensors

MDPI

Review

Recent Advances in the Development of Biosensors for Malaria Diagnosis

Francis D. Krampa [1,2,*], Yaw Aniweh [1], Prosper Kanyong [1,3] and Gordon A. Awandare [1,2]

1 West African Centre for Cell Biology of Infectious Pathogens (WACCBIP), University of Ghana, P.O. Box LG 25, Legon, Accra, Ghana; aniweh@gmail.com (Y.A.); p.kanyong@waccbip.org (P.K.); gawandare@ug.edu.gh (G.A.A.)

2 Department of Biochemistry, Cell & Molecular Biology, University of Ghana, P.O. Box LG 54, Legon, Accra, Ghana

3 Department of Chemistry, University of Oxford, South Parks Road, Oxford OX1 3QZ, UK

* Correspondence: fkrampa@gmail.com

Received: 7 October 2019; Accepted: 24 December 2019; Published: 1 February 2020

Abstract: The impact of malaria on global health has continually prompted the need to develop more effective diagnostic strategies that could overcome deficiencies in accurate and early detection. In this review, we examine the various biosensor-based methods for malaria diagnostic biomarkers, namely; *Plasmodium falciparum* histidine-rich protein 2 (PfHRP-2), parasite lactate dehydrogenase (pLDH), aldolase, glutamate dehydrogenase (GDH), and the biocrystal hemozoin. The models that demonstrate a potential for field application have been discussed, looking at the fabrication and analytical performance characteristics, including (but not exclusively limited to): response time, sensitivity, detection limit, linear range, and storage stability, which are first summarized in a tabular form and then described in detail. The conclusion summarizes the state-of-the-art technologies applied in the field, the current challenges and the emerging prospects for malaria biosensors.

Keywords: malaria biomarkers; biosensors; clinical diagnosis; medical devices; biosensing

1. Introduction

Malaria remains an important parasitic human disease globally, which is transmitted via the bite of female *Anopheles* mosquitoes. The greatest burden of the disease is in the tropical and subtropical regions of the world [1,2]. The disease causes high economic burden to the countries that are endemic, mostly, developing countries. The etiologic agent is an Apicomplexan protozoan of the genus *Plasmodium*. Six species of this genus, namely, *Plasmodium falciparum*, *Plasmodium malariae*, *Plasmodium knowlesi*, *Plasmodium ovale* (*P. ovale curtisi* and *P.ovale wallikeri*), *Plasmodium cynomolgi* and *Plasmodium vivax* are known to cause infection in humans. As the World Health Organization (WHO) sets the goal for malaria elimination by 2030 [3], the aim can only be achieved when all cases are accurately diagnosed and treated appropriately. Some of the endemic communities still lack access to routine testing in suspected cases. For example, in 2018, only 74% of patients suspected to have malaria, excluding undocumented cases, had access to diagnostic tests in public health facilities [2]. A total of 228 million cases were recorded worldwide during this period out of which 405,000 mortalities occurred [4].

Different control strategies have been effective, but limited by ineffective early diagnostic tools for detection, especially, at low parasitemia and surveillance in low-transmission settings. The ability to detect asymptomatic individuals will greatly impact on transmission dynamics, malaria control, and possibly towards elimination. Diagnostic testing may help health service providers to further investigate other aetiologies of febrile illnesses; prevent severe disease and probable death; reduce the presumptive use of antimalarial drugs and associated side-effects; and mitigate against the rapid